Calculation of cross sections and distributions for lepton flavor violating slepton pair production at e^-e^--collisions

Diplomarbeit
von
Andreas Redelbach

Institut für Theoretische Physik
der
Julius-Maximilians-Universität Würzburg

December 2000

Contents

Chapter 1

Introduction

It is common knowledge that the Standard Model of elementary particles has been tested with great accuracy. Nevertheless there are some problems that arise in the Standard Model (SM) that cannot be resolved within this framework. This is one of the reasons why there is a growing interest in theories that go beyond the SM. The basis of this work is supersymmetry (SUSY), one of the most attractive ways to extend the SM. Supersymmetric models predict the production of supersymmetric particles if the collider energies are roughly in the TeV-range.
One very interesting possibility in theories of SUSY is lepton flavor violation (LFV). Within the Standard Model, LFV is highly suppressed due to the smallness of $\frac{m_\nu}{v}$ [25], where m_ν denotes the largest neutrino Dirac mass and v the electroweak symmetry breaking scale. LFV is also suppressed if supersymmetry is unbroken; but supersymmetry has to be broken and the so-called soft SUSY-breaking terms can generate significant LFV. There is serious evidence that the atmospheric neutrino anomaly is due to neutrino oscillations, a lepton flavor violating phenomenon. In the low energy region, there are experimental bounds on lepton flavor violating processes, e.g. $\mu^- \to e^-\gamma$ and $\tau^- \to \mu^-\gamma$ that can occur via loop diagrams with supersymmetric particles in the loop.
In this work we study phenomenological aspects of LFV in electron-electron scattering at energies beyond LEP2, in the range of 200 GeV to 1000 GeV. Future linear colliders have the interesting possibility to run in an electron-electron mode, so that LFV in the accessible energy range could be examined. The electron-electron mode has the advantage that both beams can be highly polarized and that in general the level of background is lower than in electron-positron annihilation, so that rare processes can be studied more easily. If the possibilities of initial beam polarizations are exhausted, a further reduction of the background can be achieved.

The task of our work is to analyze special cases of lepton flavor violating processes that may arise in supersymmetric models in the case of electron-electron scattering at highest energies. For this case we derive results for the production of sleptons, the supersymmetric partners of leptons. These sleptons decay into a lepton of generation l, a lepton of generation l' and two neutralinos. All processes are calculated in terms of helicity amplitudes, so that one can examine polarization and helicity effects of incoming or outgoing leptons.
This work is devided into 9 chapters: After this short introduction we want to describe some basic ideas about the necessary theoretical framework. The third chapter deals with the peculiarities of the supersymmetric particles concerning their masses and mixings. As a next step we give explicit results for the helicity amplitudes for the production part, the decay part and the considered "$2 \to 4$"-processes. The fifth chapter contains analytic calculations concerning the phase space of the process. In this connection we derive analytical formulas for several interesting distributions. The sixth chapter shows the numerical results for the parameters in different supersymmetric scenarios. These results serve as numerical input parameters for the calculation of cross sections and distributions in the seventh chapter. In the analysis of the distributions we focus on the promising process $e^-e^- \to e^-\tau^-\tilde{\chi}_1^0\tilde{\chi}_1^0$ with the experimental signature $e^-\tau^- + \not{E}$. This type of process has the attractive feature that one can examine the τ^--helicities via its decay. Of course we can only make reasonable statements about the expectations whether this kind of process can be seen in future colliders, if we compare the calculated signal distributions with those of the background processes, what is done in the eighth chapter. In chapter 9 we conclude by summarizing the most important results.

Chapter 2

Theoretical framework

2.1 Motivation for Supersymmetry

Supersymmetry is a symmetry that relates fermions and bosons. The basic supersymmetry transformation turns a fermionic state into a bosonic state, and vice versa.
SUSY has the remarkable feature that it can solve the hierarchy problem of the SM in an elegant way. The hierarchy problem arises, because the squared masses of the scalar Higgs bosons are subject to quantum corrections Δm_H^2 leading to quadratically divergent contibutions [3]. Due to these loop-corrections, the squared Higgs mass is sensitive to the largest masses and/or ultraviolet cutoff in the theory that might be of the order of the Planck scale M_{Pl}. Therefore the "natural" squared mass of a fundamental Higgs scalar seems more likely to be of the order of M_{Pl}^2 than of the order of the electroweak scale in the range of $(100 \text{ GeV})^2$. Supersymmetry indeed provides a solution to the hierarchy problem, because it leads to systematic cancellations of the quadratic divergencies in fermionic and bosonic loop contributions to Δm_H^2.
Another convincing feature of SUSY is supersymmetric gauge coupling unification. Within the SM the running coupling constants do not meet at a high energy scale. But for the Minimal Supersymmetric Standard Model (MSSM) an unification of the three running coupling constants actually occurs at about 10^{16} GeV, if soft SUSY-breaking masses are roughly 1 TeV [22].
The fields of a supersymmetric theory form supermultiplets which contain both fermionic and bosonic degrees of freedom. In each supermultiplet the numbers of fermionic and bosonic degrees of freedom are equal. Moreover, as long as SUSY remains an unbroken symmetry, then both a boson and a

fermion of the same supermultiplet have the same mass. As no supersymmetric particles have been detected up to now, supersymmetry must be a broken symmetry. In order to retain the vanishing of the quadratic divergencies in scalar masses, SUSY must be broken in a "soft" way. If SUSY was broken in a more general way, supersymmetry would no longer solve the hierarchy problem mentioned above.
It is often assumed that soft SUSY-breaking occurs in a "hidden sector" containing only neutral fields with respect to the SM gauge group [5] which have very small couplings to the "visible sector" of the MSSM at the electroweak energy scale. Moreover one often assumes that soft terms of the MSSM are generated radiatively, so that soft SUSY-breaking can be mediated from the hidden sector to the visible one [3]. There are two main proposals when it comes to the mediating interactions, gravity mediated SUSY-breaking and gauge mediated SUSY-breaking.
In gravity mediated scenarios, it is supposed that the mediating interactions are of gravitational strength (see section 2.2 for more details).
In gauge mediated scenarios, soft SUSY-breaking terms originate from loop diagrams involving some messenger particles.
For the general case of a renormalizable supersymmetric theory, the possible soft SUSY-breaking terms in the Lagrangian are [3] (*h.c.*: Hermitian conjugate):

$$\begin{aligned}\mathcal{L}_{soft} &= -\frac{1}{2}\left(M_\lambda \lambda_a \lambda_a + h.c.\right) - \left(m_\phi^2\right)_{ij} \phi_i \phi_j^* \\ &\quad - \left(\frac{1}{2} b_{ij} \phi_i \phi_j + \frac{1}{6} A_{ijk} \phi_i \phi_j \phi_k + h.c.\right), \end{aligned} \tag{2.1}$$

Here M_λ are the masses for the supersymmmetric partners of the gauge bosons for each gauge group, $\left(m_\phi^2\right)_{ij}$ and b_{ij} stand for scalar squared mass terms, whereas A_{ijk} denotes $(scalar)^3$ couplings.

2.2 The Minimal Supersymmetric Standard Model

The Minimal Supersymmetric Standard Model (MSSM) is a minimal supersymmetric theory in the sense that one introduces one SUSY degree of freedom for every bosonic or fermionic degree of freedom of the Standard Model.

The MSSM shows the following features [5]:

- The MSSM is locally gauge invariant under the groups $SU(3)$ and $SU(2) \times U(1)$.
- The MSSM possesses the minimal structure for the Higgs sector of an anomaly free extension of the standard model with two hypercharge $Y = \pm 1/2$ doublets.
- The most general soft-SUSY breaking terms are included.
- R-parity is conserved. This multiplicative quantum number is defined as $R = (-1)^{3(B-L)+2S}$ (B: Baryon number, L: Lepton number, S: Spin) and yields an even value for the ordinary SM particles and an odd number for their superpartners.

The conservation of R-parity is related to $B - L$ invariance and implies important phenomenological consequences:

- If the initial state for any process consists of SM particles (with even R-parity), then SUSY particles can only be produced in even numbers.
- The lightest supersymmetric particle (LSP) has to be absolutely stable if R-parity is exactly conserved.
- Every supersymmetric particle heavier than the LSP must finally decay into a state with an odd number of LSPs.

From cosmological considerations the LSP should neither carry charge nor color. Therefore the LSP appears as a promising candidate for "cold" dark matter [3]. Throughout this work we refer to supersymmetric models that conserve R-parity.
At first we want to characterize the gauge eigenstates of the MSSM. Concerning the supermultiplet structure, one can distinguish between chiral supermultiplets that consist of two-component Weyl fermions and complex scalar fields, and gauge supermultiplets with spin-1/2 gauginos accompanied by spin-1 gauge bosons. Fields of the SUSY partners are always written with tildes on the SM counterpart.

In the MSSM case, one has the following chiral supermultiplets [3] for each family of quarks and leptons [3]:

Names	Spin 0	Spin 1/2	SM gauge group
Squarks, quarks	$\tilde{Q} = \left(\tilde{u}_L\ \tilde{d}_L\right)$	$Q = (u_L\ d_L)$	$\left(\mathbf{3}, \mathbf{2}, \frac{1}{6}\right)$
	$\tilde{u}_R^*$	$(u_R)^c$	$\left(\bar{\mathbf{3}}, \mathbf{1}, -\frac{2}{3}\right)$
	$\tilde{d}_R^*$	$(d_R)^c$	$\left(\bar{\mathbf{3}}, \mathbf{1}, \frac{1}{3}\right)$
Sleptons, leptons	$\tilde{L} = (\tilde{\nu_L}\ \tilde{e}_L)$	$L = (\nu_L\ e_L)$	$\left(\mathbf{1}, \mathbf{2}, -\frac{1}{2}\right)$
	$\tilde{e}_R^*$	$(e_R)^c$	$(\mathbf{1}, \mathbf{1}, 1)$
Higgs, Higgsinos	$h_2 = \left(h_2^+\ h_2^0\right)$	$\tilde{h}_2 = \left(\tilde{h}_2^+\ \tilde{h}_2^0\right)$	$\left(\mathbf{1}, \mathbf{2}, \frac{1}{2}\right)$
	$h_1 = \left(h_1^0\ h_1^-\right)$	$\tilde{h}_1 = \left(\tilde{h}_1^0\ \tilde{h}_1^-\right)$	$\left(\mathbf{1}, \mathbf{2}, -\frac{1}{2}\right)$

The (charge) conjugated fields of right-handed quarks, leptons and their superpartners appear in this table, because it is a standard convention that all chiral superfields are defined in terms of left-handed Weyl spinors [3]. Moreover it is common practise that the names of superpartners with spin-1/2 are obtained by adding "ino" to the Standard Model partner, whereas spin-0 supersymmetric particles start with "s" in front of their partners in the Standard Model.
The MSSM contains two Higgs supermultiplets with hypercharges $\pm\frac{1}{2}$. The Higgs chiral supermultiplet with $Y = +1/2$ has the Yukawa couplings that are necessary to give masses to up-type quarks. On the other hand, the $Y = -1/2$ supermultiplet has the Yukawa couplings to give masses to down-type quarks and charged leptons. The vacuum expectation value (VEV) v_2 of the $Y = +1/2$ Higgs field and the VEV v_1 of the $Y = -1/2$ Higgs field are connected to the known mass of the W boson and the weak coupling constant g:

$$v_1^2 + v_2^2 = v^2 = \frac{2m_W^2}{g^2} \tag{2.2}$$

The ratio of the Higgs VEVs at the electroweak scale,

$$\tan\beta = \frac{v_2}{v_1}, \tag{2.3}$$

is an important parameter in many supersymmetric scenarios.
The gauge supermultiplets of the MSSM can be described as follows [3]:

Names	Spin 1/2	Spin 1	$SU(3)_c$, $SU(2)_L$, $U(1)_Y$
Gluino, gluon	$\tilde{G}$	G	$(\mathbf{8}, \mathbf{1}, 0)$
Winos, W-bosons	$\tilde{W}^\pm\ \tilde{W}^0$	$W^\pm\ W^0$	$(\mathbf{1}, \mathbf{3}, 0)$
Bino, B-boson	$\tilde{B}^0$	B^0	$(\mathbf{1}, \mathbf{1}, 0)$

Due to soft SUSY-breaking (SSB) there are mixings of supersymmetric gauge states in the supersymmetric mass eigenstates. The mixing of the neutral gauginos and Higgsino states to the neutralinos as well as the mixing of charged slepton gauge eigenstates to the physical sleptons will be discussed in detail in chapter 3. Of course there is a mixing of squark gauge eigenstates that yield the squark mass eigenstates as well as a mixing of left-handed sneutrino gauge eigenstates that form the left-handed sneutrino mass eigenstates in the MSSM. Furthermore the mass eigenstates of the charged Higgsinos and gauginos are the charginos. In the case of the MSSM one can write down the possible soft SUSY-breaking terms in the following way [4]:

$$\begin{aligned}
-\mathcal{L}_{soft}^{MSSM} = & \frac{1}{2}\left(M_1\tilde{B}\tilde{B} + M_2\tilde{W}\tilde{W} + M_3\tilde{G}\tilde{G} + h.c.\right) \\
& + \left(m_{\tilde{Q}}^2\right)_{ij}\tilde{Q}_{Li}^\dagger\tilde{Q}_{Lj} + \left(m_{\tilde{u}}^2\right)_{ij}\tilde{u}_{Ri}^*\tilde{u}_{Rj} + \left(m_{\tilde{d}}^2\right)_{ij}\tilde{d}_{Ri}^*\tilde{d}_{Rj} \\
& + \left(m_{\tilde{L}}^2\right)_{ij}\tilde{L}_{Li}^\dagger\tilde{L}_{Lj} + \left(m_{\tilde{e}}^2\right)_{ij}\tilde{e}_{Ri}^*\tilde{e}_{Rj} \\
& + m_{h_1}^2 h_1^\dagger h_1 + m_{h_2}^2 h_2^\dagger h_2 + (B\mu h_1 h_2 + h.c.) \\
& + \Big(\left(A_u\right)_{ij} h_2\tilde{u}_{Ri}^*\tilde{Q}_{Lj} + \left(A_d\right)_{ij} h_1\tilde{d}_{Ri}^*\tilde{Q}_{Lj} \\
& + \left(A_e\right)_{ij} h_1\tilde{e}_{Ri}^*\tilde{L}_{Lj} + h.c.\Big)
\end{aligned} \tag{2.4}$$

The labels i and j are generation indices. The first line in (2.4) is for gaugino mass terms, the second line introduces squared mass terms for squarks, the third line shows squared mass terms for sleptons, whereas the fourth line displays the SUSY-breaking contributions to the Higgs potential. The last two lines introduce tri-linear couplings for up-type squarks, down-type squarks and charged sleptons, respectively. The matrices $\mathbf{A}$ are complex matrices in generation space with entries having dimension of mass.
Many unknown masses, phases and mixing angles arise with these soft SUSY-breaking terms. There are actually more than 100 new parameters in the MSSM Lagrangian that cannot be rotated away by redefining phases and flavor basis for the supermultiplets. As a result, some of these new phases and parameters can lead to unwanted large flavor-changing neutral currents (FCNC) and CP-violating effects. In order to evade such effects, one often assumes that the sfermion mass squared matrices are family-blind [3]:

$$\mathbf{m}_{\tilde{\mathbf{Q}}}^{\mathbf{2}} = m_{\tilde{Q}}^2\mathbf{1}; \quad \mathbf{m}_{\tilde{\mathbf{u}}}^{\mathbf{2}} = m_{\tilde{u}}^2\mathbf{1}; \quad \mathbf{m}_{\tilde{\mathbf{d}}}^{\mathbf{2}} = m_{\tilde{d}}^2\mathbf{1}; \quad \mathbf{m}_{\tilde{\mathbf{L}}}^{\mathbf{2}} = m_{\tilde{L}}^2\mathbf{1}; \quad \mathbf{m}_{\tilde{\mathbf{e}}}^{\mathbf{2}} = m_{\tilde{e}}^2\mathbf{1} \tag{2.5}$$

The mixing due to the tri-linear coupling matrices could also lead to unwanted large FCNC and CP-violating effects. In order to avoid this, one can make the further assumption that each A-matrix is proprtional to the corresponding Yukawa coupling matrix [3]:

$$\mathbf{A_u} = A_{u0}\mathbf{f_u}; \quad \mathbf{A_d} = A_{d0}\mathbf{f_d}; \quad \mathbf{A_e} = A_{e0}\mathbf{f_e} \tag{2.6}$$

This assumption ensures that only the sfermions of the third family, namely stops, sbottoms and staus, can have large $(scalar)^3$ couplings due to the large masses of their SM-partners. The Yukawa coupling matrices $\mathbf{f_u}$ and $\mathbf{f_d}$ are defined as

$$\mathbf{m_u} = \mathbf{f_u} v \sin\beta \tag{2.7}$$

$$\mathbf{m_d} = \mathbf{f_d} v \cos\beta \tag{2.8}$$

According to this definition, the Yukawa coupling matrices connect the masses of up-type fermions (i.e up-type quarks, neutrino-like leptons) to $v\sin\beta$ and the masses of down-type fermions (i.e. down-type quarks, charged leptons) to $v\cos\beta$.

2.3 The Minimal Supergravity Model

In gravity mediated SUSY-breaking, the hidden sector is connected to the MSSM sector at the electroweak scale through interactions of gravitational strength. One can assume that SUSY is broken in the hidden sector by a vacuum expectation value $\langle F\rangle$ of a complex scalar auxiliary field that does not propagate. Then the very rough approximation

$$m_{soft} \sim \frac{\langle F\rangle}{M_{Pl}} \tag{2.9}$$

should give the order of the soft SUSY-breaking mass terms [3]. It should be noted that the dimension of F is mass squared. m_{soft} vanishes in the limit of unbroken SUSY ($\langle F\rangle \to 0$) and also in the limit of no gravity ($M_{Pl} \to \infty$ or $G_{Newton} \to 0$). In an effective field theory the interaction between the two sectors is a result of a supergravity Lagrangian with non-renormalizable terms that are suppressed by powers of the Planck scale, because the gravitational coupling is proportional to $1/M_{Pl}$. One might worry if this non-renormalizability is reasonable. But it is due to the fact that even a renormalizable model will lose this property at least at the Planck scale where the non-renormalizable effects of gravity are included [23]. In practise one introduces a cutoff at the Planck scale.
The non-renormalizable part of a supergravity Lagrangian [3] looks like

$$-\mathcal{L}_{nr} = \frac{1}{M_{Pl}} F_X \sum_a \frac{1}{2}\left(c_a\lambda_a\lambda_a + h.c.\right) + \frac{1}{M_{Pl}^2} F_X F_X^* k_{ij}\phi_i\phi_j^*$$

$$+\frac{1}{M_{Pl}}F_X\left(\frac{1}{6}f'_{ijk}\phi_i\phi_j\phi_k+\frac{1}{2}\mu'_{ij}\phi_i\phi_j\right)+c.c. \tag{2.10}$$

Here F_X is the auxiliary field for a chiral supermultiplet X in the hidden sector, ϕ_i stands for scalar fields in the MSSM and λ_a denotes the gaugino fields of the MSSM. It can be shown that $\mathcal{L}_{nr}$ is part of a nonrenormalizable supersymmetric Lagrangian, although the terms of $\mathcal{L}_{nr}$ are not supersymmetric by themselves [3]. If one assumes that $\sqrt{\langle F_X\rangle}\sim 10^{10}$ GeV, then $\mathcal{L}_{nr}$ yields a soft SUSY-breaking Lagrangian of the form (2.1) with dimensionless couplings c_a, k_{ij}, f'_{ijk} and mass-dimension coupling μ'_{ij}.
In the special case of a "minimal" form for the normalization of kinetic terms and gauge interactions in the full, nonrenormalizable Lagrangian of supergravity there is a common dimensionless $c_a = c$ for the three gauginos and the same $k_{ij} = k\delta_{ij}$ for all scalars. Moreover the coupling characterized by f'_{ijk} is proportional to the Yukawa couplings, $f'_{ijk} = \kappa f_{ijk}$ and the mass-dimension coupling is proportional to μ_{ij}, $\mu'_{ij} = \varrho\mu_{ij}$ with universal and dimensionless constants κ and ϱ. Then the soft terms of the MSSM can be written in terms of four parameters [3]:

$$m_{1/2}=c\frac{<F_X>}{M_{Pl}},\quad m_0^2=k\frac{|<F>|^2}{M_{Pl}^2},\quad A_0=\kappa\frac{<F_X>}{M_{Pl}},\quad B_0=\varrho\frac{<F_X>}{M_{Pl}} \tag{2.11}$$

With the help of these four parameters, the soft SUSY-breaking parameters at the Planck scale $M_{Pl} = 2.4\cdot 10^{18}$ GeV can be written as follows [3]:

$$M_3 = M_2 = M_1 = m_{1/2}; \tag{2.12}$$
$$\mathbf{m^2_{\tilde{Q}}} = \mathbf{m^2_{\tilde{u}}} = \mathbf{m^2_{\tilde{d}}} = \mathbf{m^2_{\tilde{L}}} = \mathbf{m^2_{\tilde{e}}} = m_0^2\mathbf{1}; \quad m^2_{h_1} = m^2_{h_2} = m_0^2; \tag{2.13}$$
$$\mathbf{A_u} = A_0\mathbf{f_u}; \quad \mathbf{A_d} = A_0\mathbf{f_d}; \quad \mathbf{A_e} = A_0\mathbf{f_e}; \tag{2.14}$$
$$b = B_0\mu \tag{2.15}$$

In this framework both the squared scalar masses and the A-parameters are flavor diagonal and universal [5]. This kind of universality relations evades unwanted FCNCs and CP-violating effects (tree-level FCNC's are automatically absent [5]). The mentioned forms of SSB parameters are boundary conditions for the renormalization group equations (RGEs) at the Planck scale. The RGE evolution of these soft parameters down to the electroweak scale then gives us the mass spectrum of the MSSM in terms of five basic parameters, namely $m_{1/2}, m_0^2, A_0, B_0, \mu$ (plus the gauge and Yukawa couplings of the MSSM). The model described above is often called the Minimal Supergravity (mSUGRA) scenario for the soft SUSY-breaking terms.
For the mSUGRA scenarios of this work we refer to the new parameters $\tan\beta$

and sign(μ) (sign of SUSY Higgs-mixing term) instead of B_0 and μ. One can introduce these new parameters by removing μ and B_0 in favor of m_Z and $\tan\beta$, but the sign of μ is not fixed in that procedure [5].

2.4 MSSM with right-handed neutrinos

In order to illustrate the effects of right-handed neutrinos in the MSSM, it will suffice to first explain their effects in an extended SM framework. The generalization to the MSSM with right-handed neutrinos is then straightforward.

If one considers the possibility that the neutrinos could have small masses then LFV arises quite naturally under some general assumptions. An interesting model that can explain the generation of small neutrino masses is the see-saw mechanism [14]. This mechanism essentially relates the smallness of the Dirac neutrino masses to the existence of very heavy right-handed Majorana neutrinos. This kind of explanation of the neutrino mass hierarchy is not restricted to theories beyond the SM. The see-saw mechanism can be incorporated into the SM description if one includes right-handed neutrinos. The relevant lepton mass terms in a Lagrangian without R-parity violation considering both right-handed Majorana and Dirac neutrinos are given by [13]:

$$\begin{aligned}\mathcal{L} &= -\overline{e_{Ri}}\,(m_l)_{ij}\,e_{Lj} - \overline{e_{Li}}\left(m_l^\dagger\right)_{ij} e_{Rj} \\ &\quad - \left(\overline{\nu_{Li}}\;\; \overline{(\nu_{Ri})^c}\right) \underbrace{\begin{pmatrix} 0_{ij} & (m_D)_{ji} \\ (m_D)_{ij} & (M_R)_{ij} \end{pmatrix}}_{M_\nu} \begin{pmatrix} \nu_{Lj} \\ \nu_{Rj} \end{pmatrix} \qquad (2.16)\end{aligned}$$

Here the labels i and j are lepton generation indices and charge conjugation is denoted by the "c" superscript. Apart from the respective fermion fields this Lagrangian contains the charged lepton mass matrix m_l, the Dirac neutrino mass matrix m_D and the Majorana mass matrix M_R for right-handed neutrinos. The lepton mass matrix and the Dirac neutrino mass matrix are directly connected to the Yukawa coupling matrices f_e and f_ν [13]:

$$(m_l)_{ij} = (f_e)_{ij}\, v\cos\beta \qquad (2.17)$$

$$(m_D)_{ij} = (f_\nu)_{ij}\, v\sin\beta \qquad (2.18)$$

In general these relations between fermion masses, Higgs VEV and β hold for the running fermion masses rather than the physical pole masses. But

in the case of leptons the running masses at the electroweak scale equal the pole masses up to tiny corrections [13].
The important point that enables the see-saw mechanism to generate the desired mass scales is that a right-handed neutrino is an electroweak singlet so that its mass is not protected by the electroweak symmetry and could even be of the order of the Planck scale. Focusing on one neutrino generation at first, the neutrinos form mass eigenstates denoted by ν_1 and ν_2 that are related to the gauge eigenstates through the unitary matrix U_ν[14]:

$$\begin{pmatrix} \nu_1 \\ \nu_2 \end{pmatrix} = \underbrace{\begin{pmatrix} \cos\theta^\nu & -\sin\theta^\nu \\ \sin\theta^\nu & \cos\theta^\nu \end{pmatrix}}_{U_\nu} \begin{pmatrix} \nu_L \\ \nu_R \end{pmatrix} \tag{2.19}$$

For one generation of neutrinos U_ν can be parametrized by the neutrino mixing angle θ^ν and diagonalizes the neutrino mass matrix M_ν (for $i = j = 1$) given above [14],

$$(U_\nu)^T M_\nu U_\nu = diag\,(m_1, m_2)\,. \tag{2.20}$$

In order to see how the see-saw mechanism works, one can at first consider the limit $m_D << M_R$. In this limit the neutrino mixing angle is very small,

$$\theta^\nu \simeq -\frac{m_D}{M_R} \tag{2.21}$$

and the mass eigenvalues are given as

$$m_1 \simeq -\frac{m_D^2}{M_R}, \qquad m_2 \simeq M_R. \tag{2.22}$$

This then yields a very light mass eigenstate ν_1 that predominantly consists of ν_L and a heavy eigenstate mainly composed of ν_R.
We work in a basis where the charged lepton Yukawa coupling $\mathbf{f_e}$ is diagonal. The assumptions that the Majorana mass terms are much larger than the neutrino Dirac matrix elements in conjunction with the requirement that the Majorana mass matrix is in diagonal form lead to the following equation for the Dirac neutrino masses of generation i [13]:

$$m_{\nu_i} = \frac{(f_{\nu_i} v \sin\beta)^2}{M_{R_i}} \tag{2.23}$$

The soft-SUSY breaking terms involving sleptons read as follows [13]:

$$\begin{aligned}
-\mathcal{L}_{soft} &= \left(m_{\tilde{L}}^2\right)_{ij} \tilde{L}_{Li}^{\dagger}\tilde{L}_{Lj} + \left(m_{\tilde{e}}^2\right)_{ij} \tilde{e}_{Ri}^{*}\tilde{e}_{Rj} + \left(m_{\tilde{\nu}}^2\right)_{ij} \tilde{\nu}_{Ri}^{*}\tilde{\nu}_{Rj} \\
&\quad + \Big((A_e)_{ij}\, h_1 \tilde{e}_{Ri}^{*}\tilde{L}_{Lj} + (A_\nu)_{ij}\, h_2 \tilde{\nu}_{Ri}^{*}\tilde{L}_{Lj} \\
&\quad + \frac{1}{2} (b_R)_{ij}\, \tilde{\nu}_{Ri}^{*}\tilde{\nu}_{Rj}^{*} + h.c. \Big) \qquad (2.24)
\end{aligned}$$

As already mentioned, one can impose mSUGRA conditions on the soft SUSY-breaking terms, so that the SSB terms are universal at the gravitational scale [13]:

$$\left(m_{\tilde{L}}^2\right)_{ij} = \left(m_{\tilde{e}}^2\right)_{ij} = \left(m_{\tilde{\nu}}^2\right)_{ij} = m_0^2 \delta_{ij} \qquad (2.25)$$

$$(A_\nu)_{ij} = (f_\nu)_{ij}\, A_0, (A_e)_{ij} = (f_e)_{ij}\, A_0 \qquad (2.26)$$

$$(b_R)_{ij} = (M_R)_{ij}\, B_0 \qquad (2.27)$$

2.5 SUSY $SU(5)$ Grand Unified Theory with right-handed neutrinos

The $SU(5)$ group representation for a Grand Unified Theory (GUT) predicts a symmetry between quarks and leptons at a very high energy scale M_{GUT}. This symmetry has to be broken at lower energies in order to be consistent with the vast differences between quarks and leptons.

Before considering the effects of a supersymmetric version of $SU(5)$ GUT with right-handed neutrinos in more detail, let us first give some basic ideas of $SU(5)$ in general: $SU(5)$ is the smallest unitary group into which all interaction gauge groups i.e. color group $SU(3)_c$, weak isospin group of left-handed particles $SU(2)_L$ and the gauge group of weak hypercharge $U(1)_Y$ can be embedded [22]. The color group $SU(3)_c$ is "blind" against the electroweak interaction and the leptons do not carry any color. Therefore the subgroups $SU(3)_c$ and $SU(2)_L \times U(1)_Y$ of $SU(5)$ must commute with each other. In the 5×5 matrix representation of $SU(5)$-generators one can relate the first three rows and columns to $SU(3)_c$ and the last two rows and columns to $SU(2)_L \times U(1)_Y$. The fermion fields of the first (i=1) quark and lepton generation form the following left-handed $SU(2)$ doublets and singlets [22]:

$$\begin{pmatrix} \nu_e \\ e \end{pmatrix}_L, \begin{pmatrix} u \\ d \end{pmatrix}_L, e_L^c, u_L^c, d_L^c$$

In this context the superscript "c" denotes the charge conjugated field. In order to get the analogous fields for the second (i=2) quark and lepton generation, one simply has to set

$$e \to \mu, u \to c, d \to s.$$

The third (i=3) generation fields of quarks and leptons are obtained by the substitutions

$$e \to \tau, u \to t, d \to b.$$

With these notations one can write down $SU(5)$ multiplets (here for the first generation) [13]:

- SU(5) anti-quintuplet:

$$\overline{\phi}_{i=1} = (d_1^c, d_2^c, d_3^c, e, -\nu_e)_L \tag{2.28}$$

  The color quantum numbers are denoted by the indices 1,2,3.

- SU(5) decuplet in antisymmetric representation:

$$\psi_{i=1} = \frac{1}{\sqrt{2}} \begin{pmatrix} 0 & u_3^c & -u_2^c & u_1 & d_1 \\ -u_3^c & 0 & u_1^c & u_2 & d_2 \\ u_2^c & -u_1^c & 0 & u_3 & d_3 \\ -u_1 & -u_2 & -u_3 & 0 & -e^c \\ -d_1 & -d_2 & -d_3 & e^c & 0 \end{pmatrix}_L \tag{2.29}$$

In the minimal $SU(5)$ GUT model, the charged lepton Yukawa coupling constants equal the down-type quark Yukawa coupling constants at the GUT-scale [13]. From a group theoretical point of view the aforementioned decuplet representation is decomposed into $SU(3)$- and $SU(2)$-parts as [22]

$$\mathbf{10} = (\bar{\mathbf{3}}, \mathbf{1}) + (\mathbf{3}, \mathbf{2}) + (\mathbf{1}, \mathbf{1}), \tag{2.30}$$

with:

- $(\bar{\mathbf{3}}, \mathbf{1})$: Color anti-triplet, isospin singlet
- $(\mathbf{3}, \mathbf{2})$: Color triplet, isospin doublet
- $(\mathbf{1}, \mathbf{1})$: Total singlet

In a 5×5 matrix representation of the $SU(5)$-decuplet, the $SU(3)$ and $SU(2)$ parts can be included in the following way:

$$\mathbf{10} = \begin{pmatrix} (\bar{\mathbf{3}}, \mathbf{1}) & (\mathbf{3}, \mathbf{2}) \\ (\mathbf{3}, \mathbf{2})^T & (\mathbf{1}, \mathbf{1}) \end{pmatrix} \tag{2.31}$$

$SU(5)$ can spontaneously break down to $SU(3)_c \times SU(2)_L \times U(1)_Y$ and give masses to SU(5) gauge fields X_i and Y_i. But gluons, W- and B-bosons still remain massless in this first symmetry breaking mechanism. In a second step a modified version of the Higgs mechanism of the Glashow-Salam-Weinberg theory is used to break $SU(2)_L \times U(1)_Y$ down to $U(1)_{EM}$ [22]. For the first symmetry breaking mechanism the Higgs fields transform as the adjoint 24-dimensional representation of $SU(5)$, whereas the Higgs fields transform as the fundamental (5-dimensional) representation of $SU(5)$ for the second spontaneous symmetry breaking, so that for the second case $h^5 = (h_1, h_2, h_3, h_4, h_5)$. But this second spontaneous symmetry breaking shall only affect the h_4, h_5-components that are connected to the $SU(2)$ symmetry. The other Higgs field components $h^{col} = h_1, h_2, h_3$ must not be broken, so that color symmetry remains unbroken and gluons remain massless.
For a supersymmetric extension of the fermion part of $SU(5)$, one has to use the chiral superfields instead of just the fermionic fields. The Higgs doublets can be embedded in the fundamental $\mathbf{5}$ (for h) and $\bar{\mathbf{5}}$ (for h^c) representations of $SU(5)$.
We explicitly extend the SUSY $SU(5)$ GUT to the SUSY $SU(5)$ GUT model with right-handed neutrinos by including the right-handed neutrino fields in a singlet representation.
The soft SUSY-breaking involving sleptons are

$$\begin{aligned} -\mathcal{L}_{soft} &= \left(m^2_{\psi}\right)_{ij} \tilde{\psi}^{\dagger}_i \tilde{\psi}_j + \left(m^2_{\bar{\phi}}\right)_{ij} \tilde{\bar{\phi}}^{\dagger}_i \tilde{\bar{\phi}}_j + \left(m^2_{\tilde{\nu}}\right)_{ij} \tilde{\nu}^*_{Ri} \tilde{\nu}_{Rj} \\ &\quad + \left(\frac{1}{4} (A_u)_{ij} \tilde{\psi}_i \tilde{\psi}_j h + \sqrt{2} (A_d)_{ij} \tilde{\psi}_i \tilde{\bar{\phi}}_j h^c + \right. \\ &\quad \left. (A_\nu)_{ij} \tilde{\nu}^*_{Ri} \tilde{\bar{\phi}}_j h + h.c. \right). \end{aligned} \tag{2.32}$$

In order to avoid clutter, we only show the family indices in this soft SUSY-breaking Lagrangian. In the mSUGRA framework, these soft-SUSY breaking terms have universal structures at the Planck scale [13],

$$\left(m^2_{\psi}\right)_{ij} = \left(m^2_{\bar{\phi}}\right)_{ij} = (m^2_{\tilde{\nu}})_{ij} = m_0^2 \delta_{ij}, \tag{2.33}$$

$$(A_u)_{ij} = (f_u)_{ij} A_0, (A_d)_{ij} = (f_d)_{ij} A_0, (A_\nu)_{ij} = (f_\nu)_{ij} A_0. \tag{2.34}$$

Chapter 3

Masses and mixings

3.1 Neutralinos

In the MSSM the neutralino mass matrix depends basically on 4 SUSY parameters, namely M_1, M_2, β and μ. But it should be noted that it is common practice to require that all three gaugino mass parameters are equal at the GUT-scale [3]. Then the gaugino masses at the electroweak scale can be expressed in terms of one of them. The relation between the masses of the gaugino connected to $U(1)$ and the gaugino related to $SU(2)$ reads [3]

$$M_1 = \frac{5g^{'2}}{3g^2} M_2 \tag{3.1}$$

with the gauge couplings $g^{'}$ for $U(1)$ and g for $SU(2)$. Under this assumption there are only three free parameters for the neutralino mass matrix. The neutralino mass matrix has a symmetric form and reads in the $\tilde{B}, \tilde{W}, \tilde{h}_1^0, \tilde{h}_2^0$ basis [2]:

$$Y' = \begin{pmatrix} M_1 & 0 & -m_Z s_{\theta_W} c_\beta & m_Z s_{\theta_W} s_\beta \\ 0 & M_2 & m_Z c_{\theta_W} c_\beta & -m_Z c_{\theta_W} s_\beta \\ -m_Z s_{\theta_W} c_\beta & m_Z c_{\theta_W} c_\beta & 0 & -\mu \\ m_Z s_{\theta_W} s_\beta & -m_Z c_{\theta_W} s_\beta & -\mu & 0 \end{pmatrix} \tag{3.2}$$

$$\text{with } s_\alpha \equiv \sin\alpha \text{ and } c_\alpha \equiv \cos\alpha \tag{3.3}$$

The weak mixing angle is denoted by θ_W. But the vertex factors are later written in the photino-zino-neutral Higgsino-basis, where the neutralinos are described by the two-component Weyl-spinors

$$\tilde{\psi}^0 = \begin{pmatrix} -i\lambda_\gamma & -i\lambda_Z & \psi^0_{\tilde{h}_1} & \psi^0_{\tilde{h}_2} \end{pmatrix} \tag{3.4}$$

as an eigenstate basis.
The neutralino mass terms in the Lagrangian are [3]

$$-\frac{1}{2}\left(\tilde{\psi}^0\right)^T Y'\tilde{\psi}^0 + h.c. \; . \tag{3.5}$$

Then the aforementioned neutralino mass matrix Y' is transformed to the $\tilde{\gamma}, \tilde{Z}, \tilde{h}_1^0, \tilde{h}_2^0$-basis through

$$Y = O_N^T Y' O_N \tag{3.6}$$

with the orthogonal matrix [2]

$$O_N = \begin{pmatrix} \cos\theta_W & -\sin\theta_W & 0 & 0 \\ \sin\theta_W & \cos\theta_W & 0 & 0 \\ 0 & 0 & 1 & 0 \\ 0 & 0 & 0 & 1 \end{pmatrix}. \tag{3.7}$$

By choosing a special point in the SUSY parameter space the matrix Y is fixed and has to be diagonalized by a unitary matrix N which can be chosen such that $N^* Y N^{-1}$ leads to a diagonal matrix Y_D with the real, increasing and positive neutralino masses [2],

$$N^* Y N^{-1} = Y_D = diag\left(m_{\tilde{\chi}_1^0}, m_{\tilde{\chi}_2^0}, m_{\tilde{\chi}_3^0}, m_{\tilde{\chi}_4^0}\right). \tag{3.8}$$

The neutralino diagonalization matrix N can be obtained by squaring (3.8),

$$N Y^\dagger Y N^{-1} = Y_D^2. \tag{3.9}$$

With the help of N, the four neutralino mass eigenstates are defined by

$$\tilde{\chi}_i^0 = N_{ij}\tilde{\psi}_j^0 \;\; (i, j : 1, \ldots 4). \tag{3.10}$$

3.2 Charged sleptons in the MSSM

The charged slepton mass squared matrix $M_{\tilde{l}}^2$ determines masses and mixings of these scalar particles. The general charged scalar lepton mass squared matrix is conveniently written as

$$M_{\tilde{l}}^2 = \begin{pmatrix} m_L^2 & m_{LR}^{2T} \\ m_{LR}^2 & m_R^2 \end{pmatrix}. \tag{3.11}$$

This 6×6 matrix consists of 3×3 submatrices, namely m_L^2 that contains the squared masses of the left-handed slepton sector, m_{LR}^2 with squared masses of the left-right slepton sector and m_R^2 with squared masses of the right-handed part. The matrix $M_{\tilde{l}}^2$ is in a lepton flavor conserving form, if these submatrices contain only diagonal elements. In this case the entries corresponding to a generation g of leptons are obtained in the following way [5]:

$$\begin{aligned}
\left(m_L^2\right)_g &= \left(m_{\tilde{l}_L}^2\right)_g + m_g^2 + m_Z^2 cos2\beta \left(T_{3L} + \sin^2\theta_W\right) &(3.12)\\
\left(m_R^2\right)_g &= \left(m_{\tilde{l}_R}^2\right)_g + m_g^2 - m_Z^2 cos2\beta \sin^2\theta_W &(3.13)\\
\left(m_{LR}^2\right)_g &= m_g \left(A_g - \mu\tan\beta\right) &(3.14)
\end{aligned}$$

Throughout this study we work in the massless electron and muon limit, whereas the tau-lepton is considered massless only from an kinematical point of view and the mass of tau is taken into account for vertex factors and matrix elements. As a consequence of negligible electron and muon masses, off-diagonal elements that arise from m_{LR}^2 are only of relevance here for the third generation i.e. stau part. In this notation T_{3L} stands for the third component of the weak isospin, namely $-1/2$ for the charged left-handed leptons, m_g^2 is just the squared lepton mass of generation g, whereas $\left(m_{\tilde{l}_{L,R}}^2\right)_g$ stands for the left- and right-handed slepton SSB masses connected to generation g. The charged slepton mass squared matrix without lepton flavor violation thus takes the explicit form

$$M_{\tilde{l},0}^2 = \begin{pmatrix} (m_L^2)_e & 0 & 0 & 0 & 0 & 0 \\ 0 & (m_L^2)_\mu & 0 & 0 & 0 & 0 \\ 0 & 0 & (m_L^2)_\tau & 0 & 0 & (m_{LR}^2)_\tau \\ 0 & 0 & 0 & (m_R^2)_e & 0 & 0 \\ 0 & 0 & 0 & 0 & (m_R^2)_\mu & 0 \\ 0 & 0 & (m_{LR}^2)_\tau & 0 & 0 & (m_R^2)_\tau \end{pmatrix}. \tag{3.15}$$

Diagonalization of $M_{\tilde{l},0}^2$ leads to the squared scalar lepton masses

$$\left(m_L^2\right)_e, \left(m_L^2\right)_\mu, m_{\tilde{\tau}_1}^2, \left(m_R^2\right)_e, \left(m_R^2\right)_\mu, m_{\tilde{\tau}_2}^2 \text{ with}$$

$$m_{\tilde{\tau}_1}^2 = \frac{1}{2}\left(\left(m_L^2\right)_\tau + \left(m_R^2\right)_\tau - \sqrt{\left((m_L^2)_\tau - (m_R^2)_\tau\right)^2 + 4\left(m_{LR}^2\right)_\tau^2}\right) \tag{3.16}$$

$$m_{\tilde{\tau}_2}^2 = \frac{1}{2}\left(\left(m_L^2\right)_\tau + \left(m_R^2\right)_\tau + \sqrt{\left((m_L^2)_\tau - (m_R^2)_\tau\right)^2 + 4\left(m_{LR}^2\right)_\tau^2}\right) \tag{3.17}$$

The mass values $\tilde{\tau}_{1,2}$ are the eigenvalues connected to the stau 2×2 submatrix of $M_{\tilde{l},0}^2$. The angle $\theta_{\tilde{\tau}}$ for left-/right-stau mixing is determined by [4]

$$\tan\left(2\theta_{\tilde{\tau}}\right) = \frac{2\left(m_{LR}^2\right)_\tau}{\left(m_L^2\right)_\tau - \left(m_R^2\right)_\tau}. \tag{3.18}$$

3.3 LFV in the MSSM

Technically speaking, LFV is induced if the mass matrices of leptons and their scalar superpartners are not diagonalized in the same basis.
Without further assumptions, the lepton flavor violating entries in the mass squared matrix of charged sleptons are not fixed. One can introduce flavor mixing by multiplying the aforementioned flavor diagonal mass squared matrix with an unitary 6×6 matrix. In the case of slepton mixing in the left-handed and/or right-handed (index L, R) slepton sector, the necessary flavor mixing matrix can be parametrized by an appropriate 3×3 orthogonal flavor mixing matrix V_i (with $i : L, R$). The charged slepton mass squared matrix with lepton flavor mixing is then obtained in the following way:

$$M_{\tilde{l}}^2 \quad = \quad \begin{pmatrix} V_L & 0 \\ 0 & V_R \end{pmatrix} M_{\tilde{l},0}^2 \begin{pmatrix} V_L^T & 0 \\ 0 & V_R^T \end{pmatrix} \tag{3.19}$$

If one diagonalizes $M_{\tilde{l}}^2$ one gets the same mass eigenvalues for the six charged sleptons as mentioned above. This diagonalization to the matrix $M_{\tilde{l},D}^2$ is in general done by a unitary matrix U such that [4]

$$M_{\tilde{l},D}^2 = U M_{\tilde{l}}^2 U^\dagger. \tag{3.20}$$

U can be chosen orthogonal for a real $M_{\tilde{l}}^2$. The six charged slepton mass eigenstates can in general be written as

$$\tilde{l}_i = U_{ig} \left(\tilde{l}_L\right)_g + U_{ig+3} \left(\tilde{l}_R\right)_g \quad (i : 1 \ldots 6, g : 1 \ldots 3) \tag{3.21}$$

in terms of the gauge eigenstates. Equation (3.21) holds for other R-parity conserving SUSY models, too.

3.3.1 Slepton mixing between selectrons and smuons

Slepton mixing between selectrons and smuons can be introduced by the orthogonal matrix ($i : L, R$)

$$V_i^{12} = \begin{pmatrix} \cos\phi_i^{12} & -\sin\phi_i^{12} & 0 \\ \sin\phi_i^{12} & \cos\phi_i^{12} & 0 \\ 0 & 0 & 1 \end{pmatrix}. \tag{3.22}$$

Apart from the flavor mixing angles ϕ_L^{12} and ϕ_R^{12}, the mass differences between the sleptons involved are important parameters for lepton flavor violating processes. We define the mass differences between smuons and selectrons of the left-handed and right-handed slepton sector as follows:

$$
\begin{aligned}
(m_L)_\mu &= (m_L)_e + \Delta_L^{12} && (3.23)\\
(m_R)_\mu &= (m_R)_e + \Delta_R^{12} && (3.24)
\end{aligned}
$$

Due to (3.19), the charged slepton mass squared matrix reads in this case

$$
\left(M_{\tilde{l}}^2\right)^{12} = \begin{pmatrix} a_L^{12} & b_L^{12} & 0 & 0 & 0 & 0 \\ b_L^{12} & c_L^{12} & 0 & 0 & 0 & 0 \\ 0 & 0 & (m_L^2)_\tau & 0 & 0 & (m_{LR}^2)_\tau \\ 0 & 0 & 0 & a_R^{12} & b_R^{12} & 0 \\ 0 & 0 & 0 & b_R^{12} & c_R^{12} & 0 \\ 0 & 0 & (m_{LR}^2)_\tau & 0 & 0 & (m_R^2)_\tau \end{pmatrix}. \tag{3.25}
$$

The matrix $\left(M_{\tilde{l}}^2\right)^{12}$ is defined by the following abbreviations:

$$
\begin{aligned}
a_i^{12} &= \left(m_i^2\right)_e \cos^2\phi_i^{12} + \left((m_i)_e + \Delta_i^{12}\right)^2 \sin^2\phi_i^{12} && (3.26)\\
b_i^{12} &= \left(m_i^2\right)_e \cos\phi_i^{12} \sin\phi_i^{12} - \left((m_i)_e + \Delta_i^{12}\right)^2 \cos\phi_i^{12} \sin\phi_i^{12} && (3.27)\\
c_i^{12} &= \left((m_i)_e + \Delta_i^{12}\right)^2 \cos^2\phi_i^{12} + \left(m_i^2\right)_e \sin^2\phi_i^{12} && (3.28)
\end{aligned}
$$

The orthogonal slepton diagonalization matrix takes the form

$$
\begin{aligned}
U^{12} &= \begin{pmatrix} 1 & 0 & 0 & 0 & 0 & 0 \\ 0 & 1 & 0 & 0 & 0 & 0 \\ 0 & 0 & \cos\theta_{\tilde{\tau}} & 0 & 0 & \sin\theta_{\tilde{\tau}} \\ 0 & 0 & 0 & 1 & 0 & 0 \\ 0 & 0 & 0 & 0 & 1 & 0 \\ 0 & 0 & -\sin\theta_{\tilde{\tau}} & 0 & 0 & \cos\theta_{\tilde{\tau}} \end{pmatrix} \begin{pmatrix} (V_L^{12})^T & 0 \\ 0 & (V_R^{12})^T \end{pmatrix} \\
&= \begin{pmatrix} c_{\phi_L^{12}} & s_{\phi_L^{12}} & 0 & 0 & 0 & 0 \\ -s_{\phi_L^{12}} & c_{\phi_L^{12}} & 0 & 0 & 0 & 0 \\ 0 & 0 & c_{\theta_{\tilde{\tau}}} & 0 & 0 & s_{\theta_{\tilde{\tau}}} \\ 0 & 0 & 0 & c_{\phi_R^{12}} & s_{\phi_R^{12}} & 0 \\ 0 & 0 & 0 & -s_{\phi_R^{12}} & c_{\phi_R^{12}} & 0 \\ 0 & 0 & -s_{\theta_{\tilde{\tau}}} & 0 & 0 & c_{\theta_{\tilde{\tau}}} \end{pmatrix}. && (3.29)
\end{aligned}
$$

In this case stau left-right mixing does not couple to the flavor mixing. If we introduce flavor mixing only in one slepton sector, there still is no LFV in the other sector due to the decoupling of left-right mixing and flavor mixing. In order to separate the necessary parameters in a reasonable way, we will later examine the special cases of:

- Lepton flavor mixing of selectrons and smuons in the left-handed slepton sector: The independent parameters are ϕ_L^{12} and Δ_L^{12} and the respective slepton diagonalization matrix U can be obtained from the more general form of U^{12} in (3.29) by setting $\phi_R^{12} = 0$.

- Lepton flavor mixing between selectrons and smuons in the right-handed slepton sector: The independent parameters are in this case ϕ_R^{12} and Δ_R^{12}. The specific slepton diagonalization matrix U can be obtained from the more general form of U^{12} in (3.29) by setting $\phi_L^{12} = 0$.

3.3.2 Slepton mixing between selectrons and staus

We can introduce slepton mixing between selectrons and staus with an orthogonal mixing matrix ($i : L, R$)

$$V_i^{13} = \begin{pmatrix} \cos\phi_i^{13} & 0 & -\sin\phi_i^{13} \\ 0 & 1 & 0 \\ \sin\phi_i^{13} & 0 & \cos\phi_i^{13} \end{pmatrix}. \tag{3.30}$$

Apart from the flavor mixing angles ϕ_L^{13} and ϕ_R^{13}, the mass differences between the sleptons concerned are important parameters for lepton flavor violating processes. We define the mass differences between staus and selectrons of the left-handed and right-handed slepton sector as follows:

$$(m_L)_\tau = (m_L)_e + \Delta_L^{13} \tag{3.31}$$
$$(m_R)_\tau = (m_R)_e + \Delta_R^{13}, \tag{3.32}$$

With the help of the orthogonal transformation (3.19), we obtain the following slepton mass squared matrix that includes both left-handed and right-handed flavor mixing angles and the mass differences:

$$\left(M_{\tilde{l}}^2\right)^{13} = \begin{pmatrix} a_L^{13} & 0 & b_L^{13} & d_{LR}^{13} & 0 & e_{LR}^{13} \\ 0 & (m_L^2)_\mu & 0 & 0 & 0 & 0 \\ b_L^{13} & 0 & c_L^{13} & f_{LR}^{13} & 0 & g_{LR}^{13} \\ d_{LR}^{13} & 0 & f_{LR}^{13} & a_R^{13} & 0 & b_R^{13} \\ 0 & 0 & 0 & 0 & (m_R^2)_\mu & 0 \\ e_{LR}^{13} & 0 & g_{LR}^{13} & b_R^{13} & 0 & c_R^{13} \end{pmatrix} \tag{3.33}$$

The symbols in $\left(M^2_{\tilde{l}}\right)^{13}$ denote the following matrix elements:

$$\begin{aligned}
a_i^{13} &= \left(m_i^2\right)_e \cos^2\phi_i^{13} + \left((m_i)_e + \Delta_i^{13}\right)^2 \sin^2\phi_i^{13} && (3.34)\\
b_i^{13} &= \left(m_i^2\right)_e \cos\phi_i^{13}\sin\phi_i^{13} - \left((m_i)_e + \Delta_i^{13}\right)^2 \cos\phi_i^{13}\sin\phi_i^{13} && (3.35)\\
c_i^{13} &= \left((m_i)_e + \Delta_i^{13}\right)^2 \cos^2\phi_i^{13} + \left(m_i^2\right)_e \sin^2\phi_i^{13} && (3.36)\\
d_{LR}^{13} &= \left(m_{LR}^2\right)_\tau \sin\phi_L^{13}\sin\phi_R^{13} && (3.37)\\
e_{LR}^{13} &= -\left(m_{LR}^2\right)_\tau \cos\phi_R^{13}\sin\phi_L^{13} && (3.38)\\
f_{LR}^{13} &= -\left(m_{LR}^2\right)_\tau \cos\phi_L^{13}\sin\phi_R^{13} && (3.39)\\
g_{LR}^{13} &= \left(m_{LR}^2\right)_\tau \cos\phi_L^{13}\cos\phi_R^{13} && (3.40)
\end{aligned}$$

In this case the slepton diagonalization matrix U takes the form

$$\begin{aligned}
U^{13} &= \begin{pmatrix} 1 & 0 & 0 & 0 & 0 & 0 \\ 0 & 1 & 0 & 0 & 0 & 0 \\ 0 & 0 & \cos\theta_{\tilde{\tau}} & 0 & 0 & \sin\theta_{\tilde{\tau}} \\ 0 & 0 & 0 & 1 & 0 & 0 \\ 0 & 0 & 0 & 0 & 1 & 0 \\ 0 & 0 & -\sin\theta_{\tilde{\tau}} & 0 & 0 & \cos\theta_{\tilde{\tau}} \end{pmatrix} \begin{pmatrix} (V_L^{13})^T & 0 \\ 0 & (V_R^{13})^T \end{pmatrix} \\
&= \begin{pmatrix} c_{\phi_L^{13}} & 0 & s_{\phi_L^{13}} & 0 & 0 & 0 \\ 0 & 1 & 0 & 0 & 0 & 0 \\ -c_{\theta_{\tilde{\tau}}} s_{\phi_L^{13}} & 0 & c_{\theta_{\tilde{\tau}}} c_{\phi_L^{13}} & -s_{\theta_{\tilde{\tau}}} s_{\phi_R^{13}} & 0 & s_{\theta_{\tilde{\tau}}} c_{\phi_R^{13}} \\ 0 & 0 & 0 & c_{\phi_R^{13}} & 0 & s_{\phi_R^{13}} \\ 0 & 0 & 0 & 0 & 1 & 0 \\ s_{\theta_{\tilde{\tau}}} s_{\phi_L^{13}} & 0 & -s_{\theta_{\tilde{\tau}}} c_{\phi_L^{13}} & -c_{\theta_{\tilde{\tau}}} s_{\phi_R^{13}} & 0 & c_{\theta_{\tilde{\tau}}} c_{\phi_R^{13}} \end{pmatrix}. \qquad (3.41)
\end{aligned}$$

Here the stau left-right mixing is coupled to the flavor mixing. This leads to the effect that once we introduce a flavor mixing angle in one slepton sector, non-vanishing $\theta_{\tilde{\tau}}$ generates lepton flavor violating matrix elements in the left-right sector.

In order to separate the necessary parameters in a reasonable way, we will later examine the special cases of:

- Lepton flavor mixing between slectrons and staus in the left-handed slepton sector: The independent parameters are ϕ_L^{13} and Δ_L^{13} and the respective slepton diagonalization matrix U can be obtained from the more general form of U^{13} in (3.41) by setting $\phi_R^{13} = 0$.

- Lepton flavor mixing between selectrons and staus in the right-handed slepton sector: The independent parameters are in this case ϕ_R^{13} and Δ_R^{13}. The specific slepton diagonalization matrix U can be obtained from the more general form of U^{13} in (3.41) by setting $\phi_L^{13} = 0$.

3.4 LFV in the MSSM with right-handed neutrinos

The universal relations of (2.25, 2.26, 2.27) have to be altered at scales different from M_{Pl} because of quantum corrections. One can evolve the RGEs for the soft SUSY-breaking terms at a one loop level in order to get these parameters at the electroweak scale. For that purpose one can take into account solutions for the RGEs in the leading logarithmic approximation where the Yukawa couplings are subject to corrections, whereas the common SSB parameters i.e. m_0^2, A_0 are not modified. This leads to the following corrections concerning the entries in the slepton mass squared matrix of the MSSM [13]:

$$\left(\delta m_L^2\right)_{ij} \simeq -\frac{1}{8\pi^2}\left(3m_0^2 + A_0^2\right) V_{ik}^{MNS*} \left(f_{\nu_k}\right)^2 V_{jk}^{MNS} \ln\left(\frac{M_{GUT}}{M_{R_k}}\right) \tag{3.42}$$

$$\left(\delta m_R^2\right)_{ij} \simeq 0 \tag{3.43}$$

$$\left(\delta A\right)_{ij} \simeq -\frac{3A_0}{8\pi^2} f_{e_i} V_{ik}^{MNS*} V_{jk}^{MNS} \left(f_{\nu_k}\right)^2 \ln\left(\frac{M_{GUT}}{M_{R_k}}\right) \tag{3.44}$$

The first of these equations gives the off-diagonal corrections of the elements in the left-handed 3×3 slepton mass squared matrix, the following relation holds for actually vanishing corrections of the right-handed slepton mass squared matrix elements and the third approximation describes corrections of the entries in the left-right mixing part of the charged slepton mass squared matrix.

It should be mentioned that for our numerical calculations of the corrections (3.42, 3.43, 3.44) we actually started from the GUT-scale instead of the Planck-scale for basically two reasons: First we want to stick as closely as possible to the mSUGRA papers [10], [11], [12] and their input parameters. In the scenario input papers the MSSM parameters were obtained using the mSUGRA parameters at the GUT-scale, too. Second the right-handed (s)neutrinos are only included into the MSSM with no further underlying theory beyond the GUT scale.

Off-diagonal ($i \neq j$) entries or equivalently lepton flavor violating elements are induced by the loop-effects of neutrino Yukawa couplings f_ν.

The corrections come from the following two one-loop diagrams with right-handed neutrinos/sneutrinos describing radiative corrections for Dirac neutrino masses [13]:

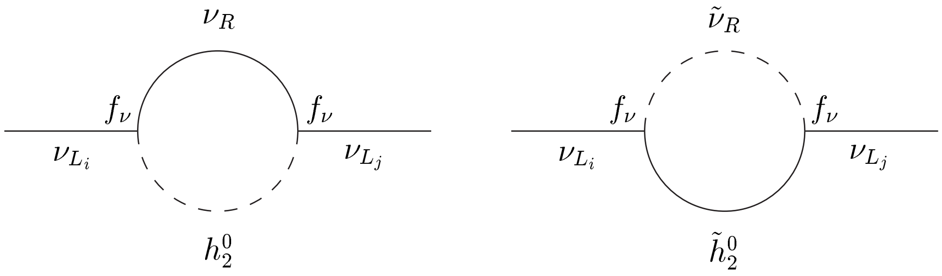

The right diagram is the supersymmetric version of the left one and i, j stand for lepton flavor indices. For energy scales below M_R, the right-handed neutrinos are decoupled from the left-handed ones. The neutrino mixing matrix V^{MNS} i.e. Maki-Nakagama-Sakata matrix is the leptonic analog of the Kobayashi-Maskawa matrix for the quarks. The light neutrino mass matrix m_ν is diagonalized by V^{MNS} [24],

$$\left(V^{MNS}\right)^T m_\nu V^{MNS} = diag\left(m_{\nu_1}, m_{\nu_2}, m_{\nu_3}\right). \tag{3.45}$$

This relation is equivalent to V^{MNS} transforming neutrino mass eigenstates ν_{M_i} into neutrino flavor eigenstates ν_{F_α}:

$$\nu_{F_\alpha} = \left(V^{MNS}\right)_{\alpha i} \nu_{M_i} \tag{3.46}$$

The MNS-matrix itself can be parametrized in the same way as the Kobayashi-Maskawa matrix in the quark sector, namely by three mixing angles and in principle one CP-violating phase that is not taken into accout here [13]:

$$V^{MNS} = \begin{pmatrix} c_{\theta_{13}^\nu} c_{\theta_{12}^\nu} & c_{\theta_{13}^\nu} s_{\theta_{12}^\nu} & s_{\theta_{13}^\nu} \\ -c_{\theta_{23}^\nu} s_{\theta_{12}^\nu} - s_{\theta_{23}^\nu} s_{\theta_{13}^\nu} c_{\theta_{12}^\nu} & c_{\theta_{23}^\nu} c_{\theta_{12}^\nu} - s_{\theta_{23}^\nu} s_{\theta_{13}^\nu} s_{\theta_{12}^\nu} & s_{\theta_{23}^\nu} c_{\theta_{13}^\nu} \\ s_{\theta_{23}^\nu} s_{\theta_{12}^\nu} - c_{\theta_{23}^\nu} s_{\theta_{13}^\nu} c_{\theta_{12}^\nu} & -s_{\theta_{23}^\nu} c_{\theta_{12}^\nu} - c_{\theta_{23}^\nu} s_{\theta_{13}^\nu} s_{\theta_{12}^\nu} & c_{\theta_{23}^\nu} c_{\theta_{13}^\nu} \end{pmatrix} \tag{3.47}$$

Numerical values for neutrino mixing parameters From the recent results on the atmospheric neutrino problem it seems to be more and more justified that it is a result of $\nu_\mu - \nu_\tau$ oscillations. Therefore the difference of squared masses $\Delta m_{32}^2 = m_3^2 - m_2^2$ and the mixing angle $\sin^2 2\theta_{23}$ can be approximated by the experimental results for atmospheric neutrinos [26]:

$$\Delta m^2_{atm} \simeq \Delta m^2_{32} \simeq \left(10^{-3} - 10^{-2}\right) (\mathrm{eV})^2 \tag{3.48}$$
$$\sin^2 2\theta_{atm} \simeq \sin^2 2\theta^\nu_{23} > 0.8 \tag{3.49}$$

The mixing angle connected to $\nu_e - \nu_\tau$ oscillations is limited by results from reactor and accelerator experiments [14]

$$\sin^2 \theta^\nu_{13} \leq (0.047 - 0.02). \tag{3.50}$$

The solar neutrino problem seems to be solved by $\nu_e - \nu_\mu$ oscillations, so that the respective mixing parameters Δm^2_{sun} and $\sin^2 2\theta_{sun}$ can be approximated by

$$\Delta m^2_{sun} \simeq \Delta m^2_{12} \tag{3.51}$$
$$\sin^2 2\theta_{sun} \simeq \sin^2 2\theta^\nu_{12} \tag{3.52}$$

But unfortunately there are several possible parameter regions for Δm^2_{sun} and $\sin^2 2\theta_{sun}$. We refer to the so-called large mixing angle MSW solutions with approximately bimaximal mixing, the parameter region that is preferred right now. The large mixing angle MSW solutions correspond to the following parameter region [27]:

$$\Delta m^2_{sun} = \left(8 \cdot 10^{-6} - 3 \cdot 10^{-4}\right) (\mathrm{eV})^2 \qquad \sin^2 2\theta_{sun} > 0.5 \tag{3.53}$$

As a choice of numerical input values concerning the neutrino mixing angles and masses, we took:

$$\begin{array}{ccc} \theta^\nu_{12} = \dfrac{\pi}{4}, & \theta^\nu_{13} = 0.05, & \theta^\nu_{23} = \dfrac{\pi}{4} \\ m_{\nu_1} = 0 \text{ eV}, & m_{\nu_2} = 0.003 \text{ eV}, & m_{\nu_3} = 0.07 \text{ eV} \end{array} \tag{3.54}$$

3.5 LFV in $SU(5)$ SUSY GUT with right-handed neutrinos

If one considers $SU(5)$ SUSY GUT with right-handed neutrinos, LFV is radiatively induced both to left-handed and right-handed sleptons. The universal structure of the soft-SUSY breaking terms no longer holds if one takes into account one-loop corrections of the SSB terms. For a leading logarithmic approximation the evolution of the RGEs from the Planck scale down to the electroweak scale yields the following corrections of the elements in the slepton mass squared matrix of the MSSM [13]:

$$\left(\delta m_L^2\right)_{ij} \simeq -\frac{1}{8\pi^2}\left(3m_0^2+A_0^2\right)\left(f_{\nu_k}\right)^2 V_{ik}^{MNS*}V_{jk}^{MNS}\ln\frac{M_{Pl}}{M_{R_k}} \quad (3.55)$$

$$\left(\delta m_R^2\right)_{ij} \simeq -\frac{3}{8\pi^2}\left(3m_0^2+A_0^2\right)\left(f_{u_3}\right)^2 V_{3i}^{KM}V_{3j}^{KM*}\ln\frac{M_{Pl}}{M_{GUT}} \quad (3.56)$$

$$\begin{aligned}(\delta A)_{ij} \simeq & -\frac{3}{8\pi^2}A_0\Bigg(f_{e_i}V_{ik}^{MNS*}V_{jk}^{MNS}\left(f_{\nu_k}\right)^2\ln\frac{M_{Pl}}{M_{R_k}}+ \\ & 3f_{e_j}V_{3j}^{KM*}V_{3i}^{KM}\left(f_{u_3}\right)^2\ln\frac{M_{Pl}}{M_{GUT}}\Bigg)\end{aligned} \quad (3.57)$$

Off-diagonal ($i \neq j$) entries or equivalently lepton flavor violating elements are induced both by the loop-effects of the neutrino Yukawa coupling f_ν and the top-quark Yukawa coupling f_{u_3}. The corrections in the right-handed slepton sector arise from the following two one-loop diagrams describing radiative corrections to the right-handed lepton masses [13]:

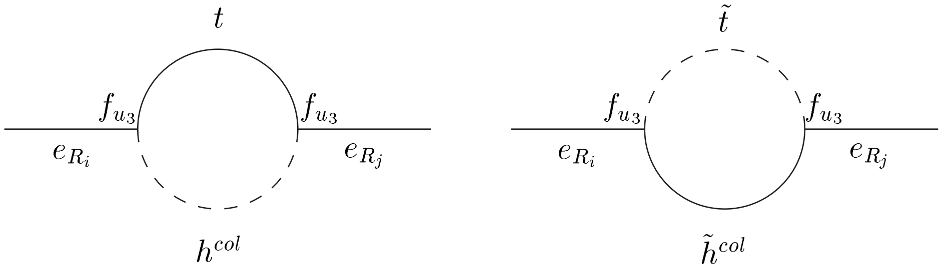

The right one of these diagrams is again the supersymmetric version of the left one and i, j denote lepton flavor indices. It is important to note that the $SU(3)$ color-Higgs components are decoupled from leptons and quarks for energies below the GUT-scale. This is the reason for the leading logarithmic corrections due to these diagrams running between the Planck scale and the GUT-scale. There is an additional contribution to the corrections of the left-right matrix elements, too.

The radiative correction in the left-handed sector is due to the one-loop diagrams with right-handed neutrinos/sneutrinos as already displayed in the previous section. But now we start the corrections due to the right-handed (s)neutrinos already from the Planck scale down to the right-handed (s)neutrino mass scale, because the underlying GUT theory is valid for this energy region. It should be clear that the corresponding contributions from the other quarks can be neglected compared to the large top Yukawa coupling

$$f_{u_3} = \frac{m_t}{v \sin\beta}. \tag{3.58}$$

For the running top quark mass at the electroweak scale we take [13]
$m_t(m_Z) \simeq 175$ GeV.
The Kobayashi-Maskawa matrix V^{KM} can be parametrized using three mixing angles and neglecting the CP-violating phase [21]:

$$V^{KM} = \begin{pmatrix} c_{\theta^q_{12}} c_{\theta^q_{13}} & s_{\theta^q_{12}} c_{\theta^q_{13}} & s_{\theta^q_{13}} \\ -s_{\theta^q_{12}} c_{\theta^q_{23}} - c_{\theta^q_{12}} s_{\theta^q_{23}} s_{\theta^q_{13}} & c_{\theta^q_{12}} c_{\theta^q_{23}} - s_{\theta^q_{12}} s_{\theta^q_{23}} s_{\theta^q_{13}} & s_{\theta^q_{23}} c_{\theta^q_{13}} \\ s_{\theta^q_{12}} s_{\theta^q_{23}} - c_{\theta^q_{12}} c_{\theta^q_{23}} s_{\theta^q_{13}} & -c_{\theta^q_{12}} s_{\theta^q_{23}} - s_{\theta^q_{12}} c_{\theta^q_{23}} s_{\theta^q_{13}} & c_{\theta^q_{23}} c_{\theta^q_{13}} \end{pmatrix} \tag{3.59}$$

The necessary mixing angles are extracted from experiments and are given as [21]:

$$\begin{aligned} \sin\theta^q_{12} &= 0.221 \pm 0.03 \\ \sin\theta^q_{13} &= 0.0035 \pm 0.0015 \\ \sin\theta^q_{23} &= 0.040 \pm 0.008 \end{aligned} \tag{3.60}$$

Chapter 4

Amplitudes

4.1 Vertex factors and propagators

In order to write down the amplitudes for the production of two sleptons in electron-electron collisions at highest energies and their following decays, one has to specify the relevant vertex factors at first. In our case each vertex is a neutralino-lepton-slepton vertex which is basically different if the slepton is right-handed or left-handed.
Of course the Majorana character of the neutralinos plays an important role for the vertex factors and amplitudes. As there is no distinction between particle and antiparticle for a Majorana fermion, the direction of a Majorana fermion line i.e. the flow of some quantum number connected to this line is arbitrary. After choosing the particular direction of the arrows the Feynman rules come into play. It should be emphasized that it is important to keep track of the spinor indices α, β which have to be contracted (see form of amplitudes for details).

Vertex factors The desired vertex that connects a lepton l_g^- of generation g, a neutralino mass eigenstate j and a slepton $\tilde{l}_\alpha^-$ is given for the configuration of the arrows as in the following figure [2]:

$$i\left(A_{(L)\alpha g} + A_{(R)\alpha g} + \left(B_{(L)\alpha g} + B_{(R)\alpha g}\right)\gamma_5\right)_{\lambda\kappa}$$

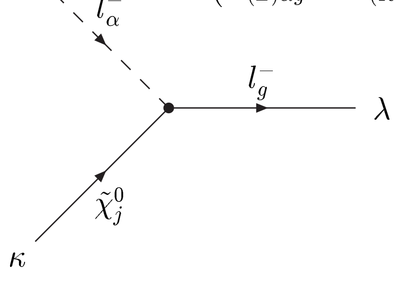

The vertex factors for the other arrow configurations can be obtained by the rules for this kind of vertex as described in [1]:

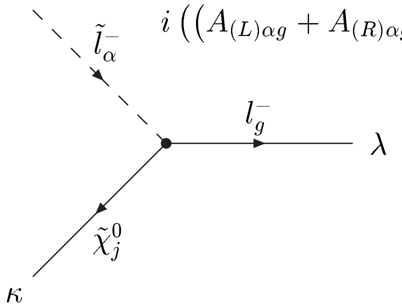

$$i\left(\left(A_{(L)\alpha g}+A_{(R)\alpha g}+\left(B_{(L)\alpha g}+B_{(R)\alpha g}\right)\gamma_5\right)C\right)_{\lambda\kappa}$$

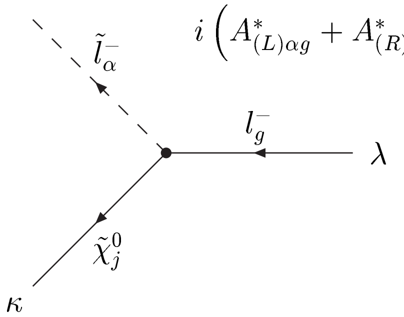

$$i\left(A^*_{(L)\alpha g}+A^*_{(R)\alpha g}-\left(B^*_{(L)\alpha g}+B^*_{(R)\alpha g}\right)\gamma_5\right)_{\kappa\lambda}$$

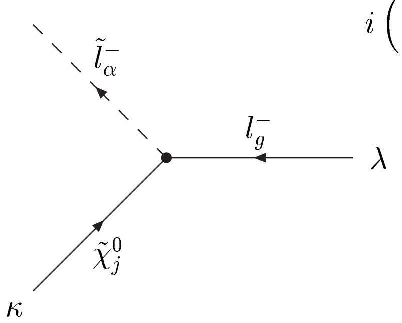

$$\begin{aligned} i\Big(&-\left(A^*_{(L)\alpha g}+A^*_{(R)\alpha g}\right)C^{-1} \\ &+\left(B^*_{(L)\alpha g}+B^*_{(R)\alpha g}\right)C^{-1}\gamma_5\Big)_{\kappa\lambda} \end{aligned}$$

It is important to mention that we work in the mass eigenstate basis for the sleptons, so that in general we have to sum over the contributions of left-handed and right-handed sleptons.

The factors connected to left-handed sleptons, $A_{(L)\alpha g}$ and $B_{(L)\alpha g}$ are compact notations [2] for

$$
\begin{aligned}
A_{(L)\alpha g} &= \left(-\frac{1}{\sqrt{2}} \frac{g m_g}{2 m_W \cos\beta} N^*_{j3} + \frac{e}{\sqrt{2}} N_{j1} \right. \\
&\quad \left. + \frac{1}{\sqrt{2}} \frac{g}{\cos\theta_W} \left(\frac{1}{2} - \sin^2\theta_W \right) N_{j2} \right) U_{\alpha g}, \qquad (4.1) \\
B_{(L)\alpha g} &= \left(\frac{1}{\sqrt{2}} \frac{g m_g}{2 m_W \cos\beta} N^*_{j3} + \frac{e}{\sqrt{2}} N_{j1} \right. \\
&\quad \left. + \frac{1}{\sqrt{2}} \frac{g}{\cos\theta_W} \left(\frac{1}{2} - \sin^2\theta_W \right) N_{j2} \right) U_{\alpha g}. \qquad (4.2)
\end{aligned}
$$

Already at this point one can say that for our purposes a term in the vertex factor proportional to the lepton mass of the first or the second generation can be neglected. The factors related to right-handed sleptons, $A_{(R)\alpha g}$ and $B_{(R)\alpha g}$ stand [2] for

$$
\begin{aligned}
A_{(R)\alpha g} &= \left(-\frac{1}{\sqrt{2}} \frac{g m_g}{2 m_W \cos\beta} N_{j3} - \frac{e}{\sqrt{2}} N^*_{j1} + \frac{1}{\sqrt{2}} \frac{g \sin^2\theta_W}{\cos\theta_W} N^*_{j2} \right) U_{\alpha(g+3)}, \quad (4.3) \\
B_{(R)\alpha g} &= \left(-\frac{1}{\sqrt{2}} \frac{g m_g}{2 m_W \cos\beta} N_{j3} + \frac{e}{\sqrt{2}} N^*_{j1} - \frac{1}{\sqrt{2}} \frac{g \sin^2\theta_W}{\cos\theta_W} N^*_{j2} \right) U_{\alpha(g+3)}. \quad (4.4)
\end{aligned}
$$

One should keep in mind that the A- and B-factors are implicitly j-dependent.

Propagators Apart from the vertex factors, we have to specify the propagator terms, too. There are several possible Majorana fermion propagator types [1] in the Breit-Wigner form:

(a) 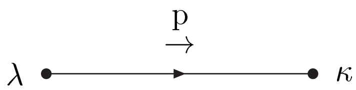

$\left(\frac{i(\not{p}+m)}{p^2-m^2+i\epsilon} \right)_{\kappa\lambda}$

(b) 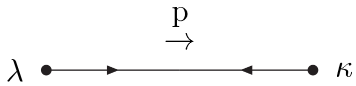

$\left(\frac{iC^{-1}(\not{p}+m)}{p^2-m^2+i\epsilon} \right)_{\kappa\lambda}$

(c) 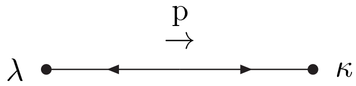

$\left(\frac{-i(\not{p}+m)C}{p^2-m^2+i\epsilon} \right)_{\kappa\lambda}$

The momentum flow is indicated to be from left to right. The charge conjugation matrix C appears in "fermion-number violating" propagators with clashing arrows.

The charge conjugation matrix C fulfills some characteristic rules [1]:

$$
\begin{aligned}
C^{\dagger} &= C^{-1} && (4.5)\\
C^{T} &= -C && (4.6)\\
C^{-1} i\gamma_5 C &= i\gamma_5^T && (4.7)\\
C^{-1}\gamma_\mu\gamma_5 C &= \gamma_5^T\gamma_\mu^T && (4.8)\\
C^{-1}\gamma_\mu C &= -\gamma_\mu^T && (4.9)\\
C^{-1}\sigma_{\mu\nu} C &= -\sigma_{\mu\nu}^T && (4.10)
\end{aligned}
$$

Moreover we need the expression for the Breit-Wigner propagator of a scalar particle of mass m and total width Γ:

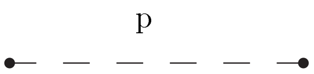

$$\frac{i}{p^2 - m^2 + im\Gamma}$$

4.2 Production amplitude

We give the results in the form of helicity amplitudes both for production and decay. For the production amplitude the following two types of Feynman diagrams corresponding to t- and u-channel are to be taken into account:

$a :$

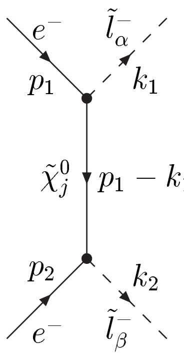

$b :$

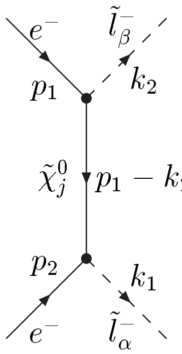

The form of the amplitudes can be derived using Feynman rules and taking care about the above mentioned Majorana peculiarities. The form of the amplitude shall be shown for a diagram of type a:

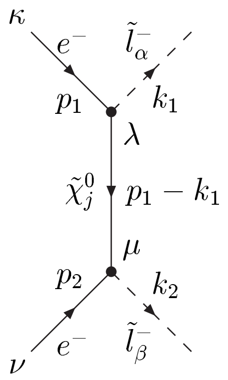

$$i\left(A^*_{(L)\alpha 1}+A^*_{(R)\alpha 1}-\left(B^*_{(L)\alpha 1}+B^*_{(R)\alpha 1}\right)\gamma_5\right)_{\lambda\kappa}u\left(p_1\right)_\kappa$$

$$\left(i\frac{\not{p}_1-\not{k}_1+m_j}{(p_1-k_1)^2-m_j^2}\right)_{\mu\lambda}$$

$$\begin{aligned} i\Big(&-\left(A^*_{(L)\beta 1}+A^*_{(R)\beta 1}\right)C^{-1} \\ &+\left(B^*_{(L)\beta 1}+B^*_{(R)\beta 1}\right)C^{-1}\gamma_5\Big)_{\mu\nu}u\left(p_2\right)_\nu \end{aligned}$$

Connecting the given terms results in:

$$\begin{aligned} \mathcal{M}^a \;=\; &-\Bigg(\Bigg(\Big(-\left(A^*_{(L)\beta 1}+A^*_{(R)\beta 1}\right)C^{-1} \\ &+\left(B^*_{(L)\beta 1}+B^*_{(R)\beta 1}\right)C^{-1}\gamma_5\Big)_{\mu\nu}u\left(p_2\right)\Bigg)_\nu\Bigg)^T\left(\frac{\not{p}_1-\not{k}_1+m_j}{\left(p_1-k_1\right)^2-m_j^2}\right)_{\mu\lambda} \\ &\Big(\left(A^*_{(L)\alpha 1}+A^*_{(R)\alpha 1}-\left(B^*_{(L)\alpha 1}+B^*_{(R)\alpha 1}\right)\gamma_5\right)_{\lambda\kappa}u\left(p_1\right)_\kappa\Big) \end{aligned} \tag{4.11}$$

Now that the spinor indices are contracted the right way, one can make use [1] of

$$u^T\left(p_2\right)=\overline{v}\left(p_2\right)C^T, \tag{4.12}$$

so that the form of this amplitude is

$$\begin{aligned} \mathcal{M}^a \;=\; &-\frac{1}{\left(p_1-k_1\right)^2-m_j^2}\overline{v}\left(p_2\right)\left(-\left(A^*_{(L)\beta 1}+A^*_{(R)\beta 1}\right)\right. \\ &\left.+\left(B^*_{(L)\beta 1}+B^*_{(R)\beta 1}\right)\gamma_5\right)\left(\not{p}_1-\not{k}_1+m_j\right) \\ &\times\left(A^*_{(L)\alpha 1}+A^*_{(R)\alpha 1}-\left(B^*_{(L)\alpha 1}+B^*_{(R)\alpha 1}\right)\gamma_5\right)u\left(p_1\right). \end{aligned} \tag{4.13}$$

In order to keep expressions shorter, it is useful to introduce

$$A_{\alpha,1} \;=\; -\left(A^*_{(L)\alpha 1}+A^*_{(R)\alpha 1}\right), \tag{4.14}$$

$$B_{\alpha,1} \;=\; B^*_{(L)\alpha 1}+B^*_{(R)\alpha 1}. \tag{4.15}$$

These abbreviations make it possible to write down the amplitude $\mathcal{M}^a$ as follows:

$$\begin{aligned} \mathcal{M}^a \;=\; &-\frac{1}{\left(p_1-k_1\right)^2-m_j^2}\overline{v}(p_2)\left(A_{\beta,1}+B_{\beta,1}\gamma_5\right) \\ &\times\left(\not{p}_1-\not{k}_1+m_j\right)\left(-A_{\alpha,1}-B_{\alpha,1}\gamma_5\right)u\left(p_1\right) \end{aligned} \tag{4.16}$$

The amplitude for the second type of production diagram, the crossed version of the first one, can be written in a similar way:

$$\begin{aligned}\mathcal{M}^b &= -\frac{1}{(p_1-k_2)^2-m_j^2}\overline{v}(p_2)\left(A_{\alpha,1}+B_{\alpha,1}\gamma_5\right)\\ &\quad\times\left(\not{p}_1-\not{k}_2+m_j\right)\left(-A_{\beta,1}-B_{\beta,1}\gamma_5\right)u\left(p_1\right)\end{aligned}\tag{4.17}$$

Of course the labels α and β as well as the four-momenta k_1 and k_2 are exchanged between the two expressions. Instead of exchanging the outgoing sleptons, we could also exchange the incoming leptons i.e. fermions which would give us an extra minus sign between the crossed and uncrossed diagrams. In order to check that the relative plus sign between the diagrams $\mathcal{M}^a$ and $\mathcal{M}^b$ is consistent with the extra minus sign for exchanging the incoming leptons, we have a look at the transpose of $\mathcal{M}^b$:

$$\begin{aligned}\left(\mathcal{M}^b\right)^T &= \mathcal{M}^b=-\frac{1}{(p_1-k_2)^2-m_j^2}u^T\left(p_1\right)\left(-A_{\beta,1}-B_{\beta,1}\gamma_5\right)^T\\ &\quad\times\left(\not{p}_1-\not{k}_2+m_j\right)^T\left(A_{\alpha,1}+B_{\alpha,1}\gamma_5\right)^T\bar{v}^T\left(p_2\right)\end{aligned}\tag{4.18}$$

In order to be able to compare this result with $\mathcal{M}^a$, we need the following relations:

$$(p_1-k_2)^2 = (p_2-k_1)^2\tag{4.19}$$

$$\not{p}_1-\not{k}_2 = \not{k}_1-\not{p}_2\tag{4.20}$$

$$\bar{v}^T\left(p_2\right) = C^{-1}u\left(p_2\right)\tag{4.21}$$

$$\gamma_5^T = \gamma_5 \qquad \text{(in Weyl representation (4.27))}\tag{4.22}$$

$$\left(\not{k}_1-\not{p}_2+m_j\right)^T = C^{-1}\left(\not{p}_2-\not{k}_1+m_j\right)C\tag{4.23}$$

This leads to

$$\begin{aligned}\mathcal{M}^b &= -\frac{1}{(p_2-k_1)^2-m_j^2}u^T\left(p_1\right)\left(-A_{\beta,1}-B_{\beta,1}\gamma_5\right)C^{-1}\\ &\quad\times\left(\not{p}_2-\not{k}_1+m_j\right)C\left(A_{\alpha,1}+B_{\alpha,1}\gamma_5\right)C^{-1}u\left(p_2\right).\end{aligned}\tag{4.24}$$

In the Weyl representation (4.27) γ_5 and C^{-1} commute, and with the relation

$$-\bar{v}\left(p_1\right)=u^T\left(p_1\right)C^{-1}\tag{4.25}$$

we obtain

$$\begin{aligned}\mathcal{M}^b &= \frac{1}{(p_2-k_1)^2-m_j^2}\bar{v}(p_1)\left(A_{\beta,1}+B_{\beta,1}\gamma_5\right)\left(\not{p}_2-\not{k}_1+m_j\right)\\ &\quad\times\left(-A_{\alpha,1}-B_{\alpha,1}\gamma_5\right)u\left(p_2\right).\end{aligned}\tag{4.26}$$

Therefore we can obtain the amplitude $\mathcal{M}^b$ from $\mathcal{M}^a$ (4.16) by the exchange of the incoming lepton momenta $p_1 \leftrightarrow p_2$ if we insert an relative minus sign between both diagrams which is consistent with the Pauli principle.

Calculation of helicity amplitudes for production With this input the helicity amplitudes can be calculated for the possible helicity combinations of the incoming electrons. For that purpose we chose the Dirac γ-matrices in the Weyl representation [6], with the three Pauli matrices denoted by σ^i:

$$\gamma^0 = \begin{pmatrix} 0 & 1 \\ 1 & 0 \end{pmatrix}, \gamma^i = \begin{pmatrix} 0 & \sigma^i \\ -\sigma^i & 0 \end{pmatrix}, \gamma_5 = \begin{pmatrix} -1 & 0 \\ 0 & 1 \end{pmatrix} \tag{4.27}$$

$$C = -i\gamma^2\gamma^0 \tag{4.28}$$

In this representation we used properly normalized fermion helicity spinors of the following form [6]:

$$u(\vec{p}, h_1) = \begin{pmatrix} \sqrt{E - 2h_1|\vec{p}|}\chi(\vec{p}, h_1) \\ \sqrt{E + 2h_1|\vec{p}|}\chi(\vec{p}, h_1) \end{pmatrix}, \tag{4.29}$$

$$v(\vec{p}, h_2) = \begin{pmatrix} -2h_2\sqrt{E + 2h_2|\vec{p}|}\chi(\vec{p}, -h_2) \\ 2h_2\sqrt{E - 2h_2|\vec{p}|}\chi(\vec{p}, -h_2) \end{pmatrix} \tag{4.30}$$

In this notation E stands for the energy of each electron with momentum $\vec{p}$ and $-\vec{p}$ and helicities h_1 and h_2, respectively. For the electron going in z-direction the relevant Pauli spinor $\chi(+z, h)$ is given as [6]

$$\chi\left(+z, +\frac{1}{2}\right) = \begin{pmatrix} 1 \\ 0 \end{pmatrix}, \chi\left(+z, -\frac{1}{2}\right) = \begin{pmatrix} 0 \\ 1 \end{pmatrix}. \tag{4.31}$$

For the other electron moving in -z-direction the Pauli spinors read [6]

$$\chi\left(-z, +\frac{1}{2}\right) = \begin{pmatrix} 0 \\ i \end{pmatrix}, \chi\left(-z, -\frac{1}{2}\right) = \begin{pmatrix} i \\ 0 \end{pmatrix}. \tag{4.32}$$

These Pauli spinors are inserted into the helicity spinors and using the aforementioned Weyl representation of the γ matrices one can calculate the helicity amplitudes for the possible helicity combinations h_1 and h_2 of the incoming electrons.
A general form for the helicity amplitudes for a process with the amplitude

$$\mathcal{M}_{h_1,h_2} = \bar{v}_{h_2} Q u_{h_1} \tag{4.33}$$

is examined in [6]. This type of amplitude typically arises in fermion-antifermion annihilation into bosons. The 4×4 matrix Q depends on the final bosons. In our case these bosons are scalar particles and we do not have to worry about possible boson spin effects. The results in [6] are given for an amplitude of the form (4.33) with the γ matrices in the Weyl representation and the mentioned conventions for the helicity spinors of the incoming fermions. In the limit of negligible masses of the incoming particles i.e. $m \to 0$, the possible helicity amplitudes have the form

$$\mathcal{M}_{+\frac{1}{2},+\frac{1}{2}} = 2iEQ_{33} \tag{4.34}$$
$$\mathcal{M}_{-\frac{1}{2},+\frac{1}{2}} = 2iEQ_{32} \tag{4.35}$$
$$\mathcal{M}_{+\frac{1}{2},-\frac{1}{2}} = 2iEQ_{23} \tag{4.36}$$
$$\mathcal{M}_{-\frac{1}{2},-\frac{1}{2}} = 2iEQ_{22}. \tag{4.37}$$

These equations give the desired helicity amplitudes as soon as one inserts the explicit form of the elements of the matrix Q.
For that purpose one has to determine the form of the matrices $\not{q}$ and $\not{q}\gamma_5$ for a general four-momentum $q = (q_0, \vec{q})$. Matrices of this type appear in the matrix Q for the production amplitudes $\mathcal{M}^a$ and $\mathcal{M}^b$ apart from the 4×4 identity matrix. In the Weyl representation (4.27) the matrices $\not{q}$ and $\not{q}\gamma_5$ have the form

$$\not{q} = q_\mu \gamma^\mu = \begin{pmatrix} 0 & 0 & q_0 - q_3 & -q_1 + iq_2 \\ 0 & 0 & -q_1 - iq_2 & q_0 + q_3 \\ q_0 + q_3 & q_1 - iq_2 & 0 & 0 \\ q_1 + iq_2 & q_0 - q_3 & 0 & 0 \end{pmatrix} \tag{4.38}$$

$$\not{q}\gamma_5 = \begin{pmatrix} 0 & 0 & q_0 - q_3 & -q_1 + iq_2 \\ 0 & 0 & -q_1 - iq_2 & q_0 + q_3 \\ -q_0 - q_3 & -q_1 + iq_2 & 0 & 0 \\ -q_1 - iq_2 & -q_0 + q_3 & 0 & 0 \end{pmatrix} \tag{4.39}$$

We do not have to compute $\gamma_5\not{q}\gamma_5$, because

$$\gamma_5\not{q}\gamma_5 = \gamma_5 q_\mu \gamma^\mu \gamma_5 = -\gamma_5\gamma_5 q_\mu \gamma_\mu = -\not{q}. \tag{4.40}$$

Now the necessary elements of the matrix Q connected to the amplitude $\mathcal{M}^a$ can be determined in a straightforward way.
Neglecting terms proportional to the electron mass, the results for $\mathcal{M}^a_{\alpha,\beta,h_1,h_2}$ are

$$\begin{aligned} \mathcal{M}^a_{\alpha,\beta,-\frac{1}{2},+\frac{1}{2}} = & \sum_j \frac{-2iE}{(p_1 - k_1)^2 - m_j^2} \left(-A_{\beta,1}A_{\alpha,1} + B_{\beta,1}B_{\alpha,1}\right. \\ & \left. + A_{\beta,1}B_{\alpha,1} - B_{\beta,1}A_{\alpha,1}\right) \left(-(k_1)_x + i(k_1)_y\right), \end{aligned} \tag{4.41}$$

$$\mathcal{M}^a_{\alpha,\beta,+\frac{1}{2},-\frac{1}{2}} = \sum_j \frac{-2iE}{(p_1-k_1)^2 - m_j^2} \left(-A_{\beta,1}A_{\alpha,1} + B_{\beta,1}B_{\alpha,1} \right.$$
$$\left. -A_{\beta,1}B_{\alpha,1} + B_{\beta,1}A_{\alpha,1}\right)\left((k_1)_x + i\,(k_1)_y\right), \tag{4.42}$$
$$\mathcal{M}^a_{\alpha,\beta,+\frac{1}{2},+\frac{1}{2}} = \sum_j \frac{-2iE}{(p_1-k_1)^2 - m_j^2} \left(-A_{\beta,1}A_{\alpha,1} - B_{\beta,1}B_{\alpha,1} \right.$$
$$\left. -A_{\beta,1}B_{\alpha,1} - B_{\beta,1}A_{\alpha,1}\right) m_j, \tag{4.43}$$
$$\mathcal{M}^a_{\alpha,\beta,-\frac{1}{2},-\frac{1}{2}} = \sum_j \frac{-2iE}{(p_1-k_1)^2 - m_j^2} \left(-A_{\beta,1}A_{\alpha,1} - B_{\beta,1}B_{\alpha,1} \right.$$
$$\left. +A_{\beta,1}B_{\alpha,1} + B_{\beta,1}A_{\alpha,1}\right) m_j. \tag{4.44}$$

As the t- and u-channel neutralinos are just virtual particles, one has to sum over all neutralino labels j. It should be clear from the definition of $\mathcal{M}^a$ and $\mathcal{M}^b$ that the helicity amplitudes for the $\mathcal{M}^b_{\alpha,\beta,h_1,h_2}$ diagrams can be obtained from the respective $\mathcal{M}^a$ diagram by exchanging α and β as well as k_1 and k_2:

$$\mathcal{M}^b_{\alpha,\beta,h_1,h_2}(k_1) = \mathcal{M}^a_{\beta,\alpha,h_1,h_2}(k_2) \tag{4.45}$$

It is important to note that in the case of spherical coordinates there is no azimuthal angle dependence in the absolute squared amplitudes, because the azimuthal angle dependence actually drops out: For the absolute squared amplitudes, the terms with k_1 in the numerator yield $\left|\vec{k}_1\right|^2 \sin^2\theta$ and the propagator terms are only dependent on the absolute value $\left|\vec{k}_1\right|$ and $\cos\angle\left(\vec{p}_1, \vec{k}_1\right)$. Therefore there is no loss of generality when we choose the process to be in the xz-plane when it comes to the amplitudes, so that $(k_1)_y = 0$ and $(k_2)_y = 0$. For this choice of the production plane the four-momenta k_1 and k_2 are given as

$$k_1 = \begin{pmatrix} \sqrt{k_1^2 + \left|\vec{k}_1\right|^2} \\ \left|\vec{k}_1\right| \sin\theta \\ 0 \\ \left|\vec{k}_1\right| \cos\theta \end{pmatrix}, \qquad k_2 = \begin{pmatrix} \sqrt{k_2^2 + \left|\vec{k}_1\right|^2} \\ -\left|\vec{k}_1\right| \sin\theta \\ 0 \\ -\left|\vec{k}_1\right| \cos\theta \end{pmatrix}. \tag{4.46}$$

The momentum conservation rule $\vec{k}_2 = -\vec{k}_1$ in the CMS system has already been included.

As a last point concerning the results for the helicity amplitudes for production it is necessary to write them in such a way that one can see the dependencies of the different amplitudes on constants and parameters. For that purpose we have to insert the explicit form of the vertex factors in the introduced compact notations. Then the helicity amplitudes for $\mathcal{M}^a$ are:

$$\begin{aligned}
\mathcal{M}^a_{\alpha,\beta,-\frac{1}{2},+\frac{1}{2}} &= \sum_j \frac{i\sqrt{s}}{(p_1-k_1)^2-m_j^2}\left(eN_{j1}-gN_{j2}\sin\theta_W\tan\theta_W\right) \\
&\quad\times\left(2eN^*_{j1}+g\cos 2\theta_W\sec\theta_W N^*_{j2}\right)U^*_{\beta 4}U^*_{\alpha 1}\left|\vec{k}_1\right|\sin\theta \qquad (4.47)\\
\mathcal{M}^a_{\alpha,\beta,+\frac{1}{2},-\frac{1}{2}} &= \sum_j \frac{-i\sqrt{s}}{(p_1-k_1)^2-m_j^2}\left(eN_{j1}-gN_{j2}\sin\theta_W\tan\theta_W\right) \\
&\quad\times\left(2eN^*_{j1}+g\cos 2\theta_W\sec\theta_W N^*_{j2}\right)U^*_{\beta 1}U^*_{\alpha 4}\left|\vec{k}_1\right|\sin\theta \qquad (4.48)\\
\mathcal{M}^a_{\alpha,\beta,+\frac{1}{2},+\frac{1}{2}} &= \sum_j \frac{2i\sqrt{s}}{(p_1-k_1)^2-m_j^2}\left(eN_{j1}-gN_{j2}\sin\theta_W\tan\theta_W\right)^2 \\
&\quad\times U^*_{\beta 4}U^*_{\alpha 4}m_j \qquad (4.49)\\
\mathcal{M}^a_{\alpha,\beta,-\frac{1}{2},-\frac{1}{2}} &= \sum_j \frac{i\sqrt{s}}{(p_1-k_1)^2-m_j^2}\left(\frac{1}{2}\right)\left(2eN^*_{j1}+g\cos 2\theta_W\sec\theta_W N^*_{j2}\right)^2 \\
&\quad\times U^*_{\beta 1}U^*_{\alpha 1}m_j \qquad (4.50)
\end{aligned}$$

The Mandelstam variable s stands for the squared beam energy,

$$s=(p_1+p_2)^2 \qquad (4.51)$$

The final results for the crossed diagrams $\mathcal{M}^b$ can be obtained from those above with the relation (4.45):

$$\begin{aligned}
\mathcal{M}^b_{\alpha,\beta,-\frac{1}{2},+\frac{1}{2}} &= \sum_j \frac{-i\sqrt{s}}{(p_1-k_2)^2-m_j^2}\left(eN_{j1}-gN_{j2}\sin\theta_W\tan\theta_W\right) \\
&\quad\times\left(2eN^*_{j1}+g\cos 2\theta_W\sec\theta_W N^*_{j2}\right)U^*_{\alpha 4}U^*_{\beta 1}\left|\vec{k}_1\right|\sin\theta \qquad (4.52)\\
\mathcal{M}^b_{\alpha,\beta,+\frac{1}{2},-\frac{1}{2}} &= \sum_j \frac{i\sqrt{s}}{(p_1-k_2)^2-m_j^2}\left(eN_{j1}-gN_{j2}\sin\theta_W\tan\theta_W\right) \\
&\quad\times\left(2eN^*_{j1}+g\cos 2\theta_W\sec\theta_W N^*_{j2}\right)U^*_{\alpha 1}U^*_{\beta 4}\left|\vec{k}_1\right|\sin\theta \qquad (4.53)\\
\mathcal{M}^b_{\alpha,\beta,+\frac{1}{2},+\frac{1}{2}} &= \sum_j \frac{2i\sqrt{s}}{(p_1-k_2)^2-m_j^2}\left(eN_{j1}-gN_{j2}\sin\theta_W\tan\theta_W\right)^2 \\
&\quad\times U^*_{\alpha 4}U^*_{\beta 4}m_j \qquad (4.54)\\
\mathcal{M}^b_{\alpha,\beta,-\frac{1}{2},-\frac{1}{2}} &= \sum_j \frac{i\sqrt{s}}{(p_1-k_2)^2-m_j^2}\left(\frac{1}{2}\right)\left(2eN^*_{j1}+g\cos 2\theta_W\sec\theta_W N^*_{j2}\right)^2 \\
&\quad\times U^*_{\alpha 1}U^*_{\beta 1}m_j \qquad (4.55)
\end{aligned}$$

The explicit forms of the production helicity amplitudes show that incoming "massless" electrons with opposite helicities couple both to the left-handed and right-handed slepton sector. On the other hand two incoming electrons of positive/negative helicity are coupled to the right-/left-handed slepton sector exclusively. These relations are due to the fact that we have treated the incoming electrons as massless, so that no left-right mixing terms (proportional to the mass of the electron) can occur in the production process.
For the four-vectors k_1 and k_2 of the form (4.46), the Mandelstam t- and u-variables in the propagator factors can be written as:

$$\begin{aligned} t = (p_1 - k_1)^2 &= -\sqrt{s}\sqrt{k_1^2 + \frac{1}{4s}\lambda\left(s, k_1^2, k_2^2\right)} \\ &\quad + k_1^2 + \frac{1}{2}\sqrt{\lambda\left(s, k_1^2, k_2^2\right)}\cos\theta \end{aligned} \tag{4.56}$$

$$\begin{aligned} u = (p_1 - k_2)^2 &= -\sqrt{s}\sqrt{k_2^2 + \frac{1}{4s}\lambda\left(s, k_1^2, k_2^2\right)} \\ &\quad + k_2^2 - \frac{1}{2}\sqrt{\lambda\left(s, k_1^2, k_2^2\right)}\cos\theta \end{aligned} \tag{4.57}$$

In order to obtain the correct kinematic λ factors, relation (5.21)

$$\left|\vec{k_1}\right| = \left|\vec{k_2}\right| = \frac{1}{2\sqrt{s}}\sqrt{\lambda\left(s, k_1^2, k_2^2\right)},$$

has been used.
The amplitude related to electron helicities h_1 and h_2 and the production of slepton $\tilde{l}_\alpha^-$ and slepton $\tilde{l}_\beta^-$ is the sum of $\mathcal{M}^a_{\alpha,\beta,h_1,h_2}$ and $\mathcal{M}^b_{\alpha,\beta,h_1,h_2}$.

4.3 Decay amplitude

The subsequent decays of the produced sleptons are described in the respective decay frames of these sleptons. In these frames the respective decaying scalar particle is at rest and the two decay products, namely a lepton and a neutralino are being produced in opposite directions and with opposite-sign momenta. The direction of their motion can be chosen to be the z-axis in the respective decay frame.
But first the form of the decay amplitudes has to be determined. For that

purpose the following vertex is considered [2]:

$$i\left(A_{(L)\alpha l}+A_{(R)\alpha l}+\left(B_{(L)\alpha l}+B_{(R)\alpha l}\right)\gamma_5\right)_{\lambda\kappa}$$

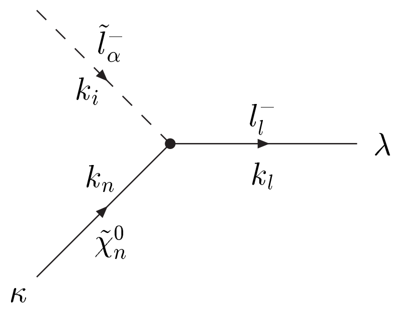

Now the amplitude for this diagram can be written as

$$\begin{aligned}\mathcal{M} &= \overline{u}\left(k_l\right)_\lambda\left(A_{(L)\alpha l}+A_{(R)\alpha l}+\left(B_{(L)\alpha l}+B_{(R)\alpha l}\right)\gamma_5\right)_{\lambda\kappa} v\left(k_n\right)_\kappa \\ &= \overline{u}\left(k_l\right)\left(A_{(L)\alpha l}+A_{(R)\alpha l}+\left(B_{(L)\alpha l}+B_{(R)\alpha l}\right)\gamma_5\right) v\left(k_n\right) \qquad (4.58)\end{aligned}$$

which is a general result for the decay amplitude. In order to get the helicity amplitudes one can make use of the above mentioned characteristics of the rest frame of the decaying slepton labeled by $(*)$. The decay products moving in opposite directions must have the same helicities, otherwise angular momentum conservation for the decaying spin-0 particle would be violated. For the decay helicity amplitude calculation we use the spinors in the Weyl representation. For this calculation we can choose the final fermions to move in the $\pm$ z-direction in the $(*)$-reference frame, because the decay of a scalar particle is spherically symmetric in $(*)$.
Finally we obtain

$$\mathcal{M}^{gen}_{\alpha,l,n,-\frac{1}{2},+\frac{1}{2}} = 0\,, \qquad (4.59)$$

$$\mathcal{M}^{gen}_{\alpha,l,n,+\frac{1}{2},-\frac{1}{2}} = 0\,, \qquad (4.60)$$

$$\begin{aligned}\mathcal{M}^{gen}_{\alpha,l,n,+\frac{1}{2},+\frac{1}{2}} &= i\sqrt{E_l{}^*+\left|\vec{k}_l{}^*\right|}\sqrt{E_n{}^*+\left|\vec{k}_n{}^*\right|} \\ &\quad\times\left(A_{(L)\alpha l}+A_{(R)\alpha l}-B_{(L)\alpha l}-B_{(R)\alpha l}\right) \\ &\quad -i\sqrt{E_l{}^*-\left|\vec{k}_l^*\right|}\sqrt{E_n{}^*-\left|\vec{k}_n{}^*\right|} \\ &\quad\times\left(A_{(L)\alpha l}+A_{(R)\alpha l}+B_{(L)\alpha l}+B_{(R)\alpha l}\right), \qquad (4.61)\end{aligned}$$

$$
\begin{aligned}
\mathcal{M}^{gen}_{\alpha,l,n,-\frac{1}{2},-\frac{1}{2}} &= -i\sqrt{E_l{}^* - |\vec{k}_l{}^*|}\sqrt{E_n{}^* - |\vec{k}_n{}^*|} \\
&\quad \times \left(A_{(L)\alpha l} + A_{(R)\alpha l} - B_{(L)\alpha l} - B_{(R)\alpha l}\right) \\
&\quad + i\sqrt{E_l{}^* + |\vec{k}_l{}^*|}\sqrt{E_n{}^* + |\vec{k}_n{}^*|} \\
&\quad \times \left(A_{(L)\alpha l} + A_{(R)\alpha l} + B_{(L)\alpha l} + B_{(R)\alpha l}\right), \qquad (4.62)
\end{aligned}
$$

for the helicity combinations connected to the decay amplitude of slepton α into lepton l and neutralino n in the sleptonic decay frame $(*)$. Here the first helicity index $\pm\frac{1}{2}$ refers to the lepton and the second helicity index stands for the helicity of the neutralino. If we use the following kinematic relations,

$$
E_l{}^* = \sqrt{m_l{}^2 + |\vec{k}_l{}^*|^2}, E_n{}^* = \sqrt{k_i^2} - \sqrt{m_l^2 + |\vec{k}_l{}^*|^2}, |\vec{k}_n{}^*| = |\vec{k}_l{}^*|, \qquad (4.63)
$$

the given results are only dependent on the kinematic variables $|\vec{k}_l{}^*|$ and k_i^2.

Decay into τ and $\tilde{\chi}^0$ A modification of this form of helicity amplitudes will be applied for the decay amplitudes $M_{\alpha,\tau,n}$ describing the decay of slepton $\tilde{l}^-_\alpha$ into tau and neutralino $\tilde{\chi}^0_n$. In the actual calculations we assume that the τ^--mass can be neglected kinematically, but not in the vertex factors and matrix elements. The energy-momentum relation for an outgoing τ^- lepton of relative high energy,

$$
|\vec{k}_\tau| = E_\tau\sqrt{1 - \frac{m_\tau^2}{E_\tau^2}} \simeq E_\tau\left(1 - \frac{m_\tau^2}{2E_\tau^2}\right), \qquad (4.64)
$$

suggests this kinematic approximation to us.
Going back to the explicit form of the vertex factors for the non-vanishing decay helicity amplitudes then yields:

$$
\begin{aligned}
\mathcal{M}_{\alpha,\tau,n,+\frac{1}{2},+\frac{1}{2}} &= -i\sqrt{|\vec{k}_\tau{}^*|}\sqrt[4]{k_i^2}\Bigg(g\frac{m_\tau}{m_W}N^*_{n3}\sec\beta U_{\alpha3} \\
&\quad + 2U_{\alpha6}\left(eN^*_{n1} - gN^*_{n2}\sin\theta_W\tan\theta_W\right)\Bigg) \qquad (4.65) \\
\mathcal{M}_{\alpha,\tau,n,-\frac{1}{2},-\frac{1}{2}} &= i\sqrt{|\vec{k}_\tau{}^*|}\sqrt[4]{k_i^2} \\
&\quad \times\Bigg(2eN_{n1}U_{\alpha3} + g\Bigg(-\frac{m_\tau}{m_W}\sec\beta N_{n3}U_{\alpha6} \\
&\quad + N_{n2}U_{\alpha3}\left(\sec\theta_W - 2\sin\theta_W\tan\theta_W\right)\Bigg)\Bigg) \qquad (4.66)
\end{aligned}
$$

Using the kinematic expression (5.30)

$$\left|\vec{k}_\tau{}^*\right| = \frac{1}{2\sqrt{k_i^2}}\sqrt{\lambda\left(k_i^2, m_\tau^2 \simeq 0, m_n^2\right)}$$

for the momentum of the τ^--lepton in the sleptonic decay frame, one can write the decay helicity amplitudes in the following way:

$$\begin{aligned}
\mathcal{M}_{\alpha,\tau,n,+\frac{1}{2},+\frac{1}{2}}\left(k_i^2\right) &= -i\sqrt[4]{\lambda\left(k_i^2, 0, m_n^2\right)}\frac{1}{\sqrt{2}}\left(g\frac{m_\tau}{m_W}N_{n3}^* \sec\beta U_{\alpha 3}\right. \\
&\quad \left. +2U_{\alpha 6}\left(eN_{n1}^* - gN_{n2}^* \sin\theta_W \tan\theta_W\right)\right) \qquad (4.67) \\
\mathcal{M}_{\alpha,\tau,n,-\frac{1}{2}-\frac{1}{2}}\left(k_i^2\right) &= i\sqrt[4]{\lambda\left(k_i^2, 0, m_n^2\right)}\left(\sqrt{2}eN_{n1}U_{\alpha 3}\right. \\
&\quad +g\left(-\frac{1}{\sqrt{2}}\frac{m_\tau}{m_W}\sec\beta N_{n3}U_{\alpha 6} + N_{n2}U_{\alpha 3}\right. \\
&\quad \left.\left.\times\left(\frac{1}{\sqrt{2}}\sec\theta_W - \sqrt{2}\sin\theta_W \tan\theta_W\right)\right)\right) \qquad (4.68)
\end{aligned}$$

The helicity decay mode with positive helicities (4.67) has a coupling to the right-handed slepton sector through $U_{\alpha 6}$ and a coupling to the left-handed slepton sector through $U_{\alpha 3}$. The coupling to the left-handed sector is proportional to $\frac{m_\tau}{m_W}\sec\beta$ and is approximately suppressed as $\frac{m_\tau}{m_W}$ for $\sec\beta \simeq 1$. But we are especially interested in decays with the lightest neutralinos (i.e. $n = 1$) outgoing. For typical SUSY parameters the neutralino matrix elements N_{11} and N_{12} are larger than N_{13} which again reduces the contribution of the left-handed slepton sector proportional to m_τ.
For the helicity decay mode with negative helicities (4.68), coupling strengths to the slepton sectors are reversed: Here the coupling to the left-handed slepton sector is not suppressed by a mass scale $\frac{m_\tau}{m_W}$, whereas the coupling to the right-handed slepton part is proportional to $\frac{m_\tau}{m_W}\sec\beta N_{n3}$.

Decay into "light" lepton and $\tilde{\chi}^0$ If the outgoing lepton is a lighter lepton l' of the first or second generation, one can neglect its mass completely and thus gets the simpler results for the decay amplitude:

$$\begin{aligned}
\mathcal{M}_{\alpha,l',n,+\frac{1}{2},+\frac{1}{2}} &= 2i\sqrt{\left|\vec{k}_{l'}{}^*\right|}\sqrt[4]{k_i^2}U_{\alpha(l'+3)} \\
&\quad \times\left(-eN_{n1}^* + gN_{n2}^* \sin\theta_W \tan\theta_W\right) \qquad (4.69)
\end{aligned}$$

$$
\begin{aligned}
\mathcal{M}_{\alpha,l',n,-\frac{1}{2},-\frac{1}{2}} &= 2i\sqrt{\left|\vec{k}_{l'}{}^{*}\right|}\sqrt[4]{k_i^2}U_{\alpha l'} \\
&\times\left(eN_{n1}+gN_{n2}\left(\frac{1}{2}\sec\theta_W-\sin\theta_W\tan\theta_W\right)\right) \qquad (4.70)
\end{aligned}
$$

Making use of (5.30) yields

$$
\left|\vec{k}_{l'}{}^{*}\right| = \frac{1}{2\sqrt{k_i^2}}\sqrt{\lambda\left(k_i^2, m_{l'}^2 \simeq 0, m_n^2\right)}.
$$

This results in the following amplitudes for the sleptonic decay into a "massless" lepton l' and neutralino n:

$$
\begin{aligned}
\mathcal{M}_{\alpha,l',n,+\frac{1}{2},+\frac{1}{2}}\left(k_i^2\right) &= i\sqrt[4]{\lambda\left(k_i^2,0,m_n^2\right)}\sqrt{2}U_{\alpha(l'+3)} \\
&\times\left(-eN_{n1}^{*}+gN_{n2}^{*}\sin\theta_W\tan\theta_W\right) \qquad (4.71) \\
\mathcal{M}_{\alpha,l',n,-\frac{1}{2},-\frac{1}{2}}\left(k_i^2\right) &= i\sqrt[4]{\lambda\left(k_i^2,0,m_n^2\right)}U_{\alpha l'}\sqrt{2}\Bigg(eN_{n1} \\
&+gN_{n2}\left(\frac{1}{2}\sec\theta_W-\sin\theta_W\tan\theta_W\right)\Bigg) \qquad (4.72)
\end{aligned}
$$

If we have a look at the helicity decay mode for positive helicities (4.71), we see that there is only a contribution from the right-handed slepton sector through $U_{\alpha(l'+3)}$. The possible coupling to the left-handed sector proportional to the respective lepton mass vanishes if we work in the limit of "massless" leptons of the first two generations.
On the other side the helicity decay mode connected to negative helicities (4.72) couples to the left-handed slepton sector through $U_{\alpha l'}$.
It should be mentioned that the helicity of a massless particle is a Lorentz-invariant quantity, whereas the helicity of a massive particle is reference frame-dependent. As a consequence of this fact, helicity amplitudes for massless particles (in our case the leptons) are Lorentz-invariant, but helicity amplitudes for massive particles (in our case neutralinos) are not Lorentz-invariant. We are, however only interested in helicity amplitudes of the leptons with helicities h_3 and h_5. In this case we obtain Lorentz-invariant helicity amplitudes for the leptons if we sum over the helicities of the outgoing neutralinos. This summation is always implied. Without specifying the helicities h_4 and h_6 of the neutralinos, the results (4.67, 4.68, 4.71, 4.72) become Lorentz-invariant.

Helicity asymmetry One point of phenomenological and experimental importance is that produced tau leptons decay in a self-analyzing way concerning their polarizations. By studying the energy distribution of the tau decay products, one gets information about the respective tau polarization [9]. It is therefore possible to examine helicity asymmetries of the τ^-, defined as

$$A_\tau^{hel} = \frac{d\sigma_{\tau_{-1/2}} - d\sigma_{\tau_{+1/2}}}{d\sigma_{\tau_{-1/2}} + d\sigma_{\tau_{+1/2}}}, \tag{4.73}$$

where the symbol $d\sigma_{\tau_h}$ stands either for a total or differential cross section with specific tau helicity h. It is very hard to determine the helicity of the electron experimentally, so that helicity asymmetries related to the electron are of little interest. The study of muon decays is difficult in a collider experiment due to the relative long lifetime of this lepton.

4.4 Amplitude for the whole process

With the given form of the helicity amplitudes for the production process as well as for the two sleptonic decays, the helicity-specific amplitude for the whole considered process can be obtained. The only additional factors are the propagator terms for each produced slepton. For the case of a slepton $\tilde{l}_\alpha^-$ with on-shell mass m_α, effective squared mass k^2 and total width Γ_α this scalar propagator reads

$$\pi_\alpha\left(k^2\right) = \frac{i}{k^2 - m_\alpha^2 + i m_\alpha \Gamma_\alpha}. \tag{4.74}$$

In order to obtain the desired helicity-dependent amplitude for the whole process, a summation over all possible sleptons which can be produced is necessary. Therefore the total amplitude for helicities h_1 and h_2 in the production, with a subsequent decay of $\tilde{l}_\alpha^-$ into lepton l with helicity h_3 and neutralino $\tilde{\chi}_n^0$, as well as the decay of $\tilde{l}_\beta^-$ into lepton l' with helicity h_5 accompanied by $\tilde{\chi}_{n'}^0$ reads:

$$\begin{aligned} \mathcal{M}^{tot}_{h_1,h_2,h_3,h_5} &= \sum_{\alpha=1}^{6}\sum_{\beta=1}^{6}\left(\mathcal{M}^a_{\alpha,\beta,h_1,h_2} + \mathcal{M}^b_{\alpha,\beta,h_1,h_2}\right) \\ &\quad \times \pi_\alpha\left(k_1^2\right)\mathcal{M}_{\alpha,l,n,h_3}\pi_\beta\left(k_2^2\right)\mathcal{M}_{\beta,l',n',h_5} \end{aligned} \tag{4.75}$$

Of course we need $\mathcal{M}^{tot}_{h_1,h_2,h_3,h_5}\left(\mathcal{M}^{tot}_{h_1,h_2,h_3,h_5}\right)^* = \left|\mathcal{M}^{tot}_{h_1,h_2,h_3,h_5}\right|^2$ for the calculation of physical quantities.

Calculation of scalar propagator terms As a first step let us consider the propagator terms under complex conjugation:

$$\rho_{\alpha,\alpha'}\left(k^2\right) = \quad \pi_\alpha\left(k^2\right)\pi^*_{\alpha'}\left(k^2\right) \tag{4.76}$$

$$= f_{\alpha,\alpha'} \quad \left(\frac{k^2 - m_\alpha^2 - i m_\alpha\Gamma_\alpha}{\left(k^2 - m_\alpha^2\right)^2 + m_\alpha^2\Gamma_\alpha^2} - \frac{k^2 - m_{\alpha'}^2 + i m_{\alpha'}\Gamma_{\alpha'}}{\left(k^2 - m_{\alpha'}^2\right)^2 + m_{\alpha'}^2\Gamma_{\alpha'}^2}\right) \tag{4.77}$$

$$\text{with} \quad f_{\alpha,\alpha'} = \frac{1}{m_\alpha^2 - m_{\alpha'}^2 - i\left(m_\alpha\Gamma_\alpha + m_{\alpha'}\Gamma_{\alpha'}\right)} \tag{4.78}$$

Now comes the important assumption that the terms $m_\alpha\Gamma_\alpha$ and $m_{\alpha'}\Gamma_{\alpha'}$ can be neglected compared to $(k^2 - m_\alpha^2)$: In the limit $m_\alpha\Gamma_\alpha \to 0$ and $m_{\alpha'}\Gamma_{\alpha'} \to 0$, the singular part of $\rho_{\alpha,\alpha'}(k^2)$ takes the form

$$\rho_{\alpha,\alpha'}(k^2) = f_{\alpha,\alpha'}\left(-i\pi\delta\left(k^2 - m_\alpha^2\right) - i\pi\delta\left(k^2 - m_{\alpha'}^2\right)\right) \tag{4.79}$$

$$\begin{aligned} &= \frac{\pi}{m_\alpha\Gamma_\alpha + m_{\alpha'}\Gamma_{\alpha'}}\left(1 + i\frac{m_\alpha^2 - m_{\alpha'}^2}{m_\alpha\Gamma_\alpha + m_{\alpha'}\Gamma_{\alpha'}}\right)^{-1} \\ &\quad \times\left(\delta\left(k^2 - m_\alpha^2\right) + \delta\left(k^2 - m_{\alpha'}^2\right)\right) \end{aligned} \tag{4.80}$$

$$\equiv R_{\alpha,\alpha'}\left(\delta\left(k^2 - m_\alpha^2\right) + \delta\left(k^2 - m_{\alpha'}^2\right)\right). \tag{4.81}$$

To derive this relation, the following representation of the delta function has been used [17]:

$$\delta(t) = \lim_{\epsilon\to 0}\frac{\epsilon}{\pi\left(t^2 + \epsilon^2\right)} \tag{4.82}$$

The expression (4.81) can be understood as a special kind of narrow width approximation that takes into account flavor correlations. By this approach the squared off-shell sleptonic masses are put on-shell, but there is interference between them due to the complex factor $R_{\alpha,\alpha'}$ in front of them. One can split $R_{\alpha,\alpha'}$ in a factor

$$\tilde{R}_{\alpha,\alpha'} = = \frac{1}{2}\left(1 + i\frac{m_\alpha^2 - m_{\alpha'}^2}{m_\alpha\Gamma_\alpha + m_{\alpha'}\Gamma_{\alpha'}}\right)^{-1} \tag{4.83}$$

that describes sleptonic "flavor correlations" and a factor

$$r_{\alpha,\alpha'} = \frac{2\pi}{m_\alpha\Gamma_\alpha + m_{\alpha'}\Gamma_{\alpha'}} \tag{4.84}$$

that suppresses the propagation of heavy sleptons.
It is worth noting that $R_{\alpha,\alpha'} = R^*_{\alpha',\alpha}$ which guarantees the real valuedness of

the squared total amplitude.
In [4] it has been pointed out that $\rho_{\alpha,\alpha'}(k^2)$ leads to correct cross sections in the "interference region", i.e.
$m_\alpha^2 - m_{\alpha'}^2 < m_\alpha \Gamma_\alpha + m_{\alpha'} \Gamma_{\alpha'}$ or $m_\alpha^2 - m_{\alpha'}^2 \sim m_\alpha \Gamma_\alpha + m_{\alpha'} \Gamma_{\alpha'}$
and in the "decoherent region",
$m_\alpha^2 - m_{\alpha'}^2 \gg m_\alpha \Gamma_\alpha + m_{\alpha'} \Gamma_{\alpha'}$.
In the "intermediate region" the full one-loop correction seems to be important, but shall not be applied in this work.

Exchange of outgoing neutralinos In principle we have to consider the interference terms that arise due to the crossing of outgoing neutralinos. The absolute squared amplitude that arises due to the crossing of two different outgoing neutralinos n and n' can be written as

$$|\mathcal{M}|^2 = |\mathcal{M}_{n,n'}|^2 + |\mathcal{M}_{n',n}|^2 + 2Re\left(\mathcal{M}_{n,n'}\mathcal{M}_{n',n}\right). \tag{4.85}$$

Because of the Re-term, there is interference between the two absolute squared single diagrams with exchanged neutralinos. For the case of two identical outgoing neutralinos we have to insert a statistical factor of $\frac{1}{2}$ before the terms in (4.85) and a minus sign before the interference term due to the exchange of the same (Majorana) fermions between both digrams.
Let us examine the following diagrams that take the exchange of outgoing neutralinos into account (arrows of outgoing neutralinos as on page 41):

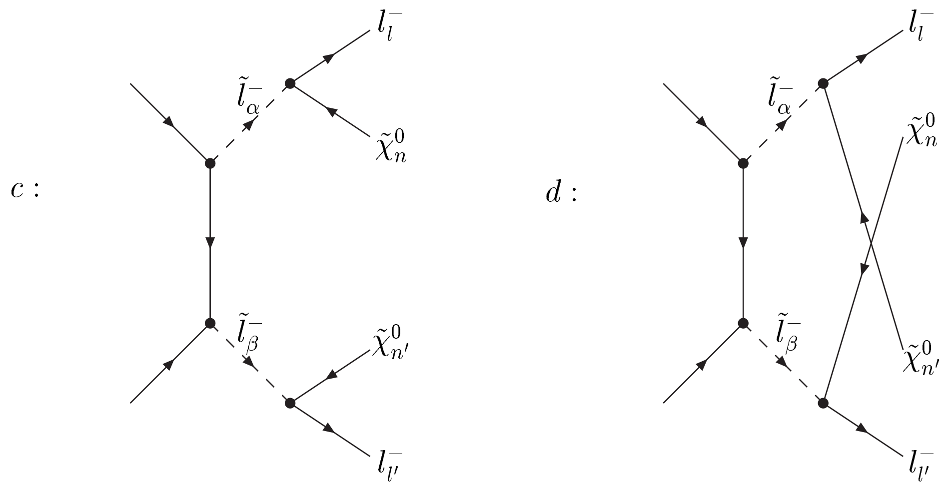

If we make use of (4.81), we obtain the following relations concerning the interference terms of the diagrams c and d:

$$k_1^2 = (p_l + p_n)^2 = m_\alpha^2 \quad k_1^2 = (p_l + p_{n'})^2 = m_\alpha^2 \tag{4.86}$$
$$k_2^2 = (p_{l'} + p_{n'})^2 = m_\beta^2 \quad k_2^2 = (p_{l'} + p_n)^2 = m_\beta^2. \tag{4.87}$$

In the interference terms for outgoing neutralinos, all these terms arise and all equations have to be fulfilled simultaneously. Due to (4.81) we could also set α' instead of α and β' instead of β. But nevertheless the squared masses in (4.86) have to be the same, because (4.81) splits the whole amplitude into sums of which each corresponds to one squared mass for k_1^2. The analogous holds for the squared masses in (4.87).
Evaluating (4.86) yields

$$p_n^2 - p_{n'}^2 = m_n^2 - m_{n'}^2 = 2p_l \cdot (p_{n'} - p_n)\,, \tag{4.88}$$

because the outgoing neutralinos are of course on-shell. In an analogous way we obtain from equations (4.87)

$$p_n^2 - p_{n'}^2 = m_n^2 - m_{n'}^2 = 2p_{l'} \cdot (p_{n'} - p_n)\,. \tag{4.89}$$

Therefore the fact that equations (4.86) and (4.87) have to be fulfilled simultaneously leads to the condition

$$(p_{n'} - p_n) \cdot (p_{l'} - p_l) = 0. \tag{4.90}$$

Of course this condition is only valid in the limit of zero width of the intermediate sleptons. For finite, but small sleptonic widths, (4.90) is no longer an exact equation, but rather an approximate result. The condition (4.90) demands that in the neutralino exchange interference terms the momenta of the final leptons and/or neutralinos have to be identical in the zero width limit or at least do not have to deviate much from being identical in the finite width case. This additional demand restricts the phase space for the final particles drastically. This is the reason why we neglect neutralino exchange interference terms in our calculation.

Squared total amplitude Neglecting the interference terms which arise from the exchange of outgoing neutralinos, one comes to the following result for the helicity-dependent squared amplitude for a fixed combination of outgoing particles $(l_l^-, \tilde{\chi}_n^0)$ and $(l_{l'}^-, \tilde{\chi}_{n'}^0)$:

$$
\begin{aligned}
\left|\mathcal{M}^{tot}_{h_1,h_2,h_3,h_5}\right|^2 &= \\
\sum_{\alpha}\sum_{\alpha'}\sum_{\beta}\sum_{\beta'} & \quad R_{\alpha,\alpha'}\left(\delta\left(k_1^2-m_\alpha^2\right)+\delta\left(k_1^2-m_{\alpha'}^2\right)\right) \\
& \times R_{\beta,\beta'}\left(\delta\left(k_2^2-m_\beta^2\right)+\delta\left(k_2^2-m_{\beta'}^2\right)\right) \\
& \times\left(\mathcal{M}^a_{\alpha,\beta}+\mathcal{M}^b_{\alpha,\beta}\right)\left(\mathcal{M}^{a\,*}_{\alpha',\beta'}+\mathcal{M}^{b\,*}_{\alpha',\beta'}\right) \\
& \times\mathcal{M}_{\alpha,l,n}\mathcal{M}^*_{\alpha',l,n}\mathcal{M}_{\beta,l',n'}\mathcal{M}^*_{\beta',l',n'} \qquad (4.91)
\end{aligned}
$$

The sum has to be taken over all sleptons that can be produced. The (formal) functional dependence of the squared total amplitude is like

$$
\left|\mathcal{M}^{tot}_{h_1,h_2,h_3,h_5}\right|^2 = \left|\mathcal{M}^{tot}_{h_1,h_2,h_3,h_5}\right|^2\left(s,k_1^2,k_2^2,\theta\right). \qquad (4.92)
$$

4.5 LFV-parameter dependence in the MSSM

In this section we will examine the MSSM with LFV in the left-handed sector or in the right-handed sector with the additional condition that left-right mixing is decoupled from flavor mixing or can be neglected. We will derive an analytical result for the basic parameter dependence for the process of $e^-e^- \to e^-l_g^- + 2\tilde{\chi}^0$ that can directly be applied to the process $e^-e^- \to e^-\mu^- + 2\tilde{\chi}^0$ (with $g:2$) or in the limit of negligible left-right mixing to the process $e^-e^- \to e^-\tau^- + 2\tilde{\chi}^0$ (with $g:3$). Let us first stick to the left-handed slepton sector with selectron-smuon mixing. The sum over intermediate slepton states $\alpha,\alpha',\beta,\beta'$ that includes the basic MSSM LFV-parameters takes the form

$$
\begin{aligned}
&\left|\mathcal{M}^{tot}_L\left(\phi_L,\Delta_L\right)\right|^2 = \\
&\qquad c_L\sum_{\alpha,\alpha',\beta,\beta'}\underbrace{U_{\alpha4}U_{\alpha'4}U_{\beta1}U_{\beta'1}}_{prod}\underbrace{U_{\alpha4}U_{\alpha'4}}_{decay\ 1}\underbrace{U_{\beta g}U_{\beta' g}}_{decay\ 2}\tilde{R}_{\alpha,\alpha'}\tilde{R}_{\beta,\beta'} \\
&\qquad +c'_L\sum_{\alpha,\alpha',\beta,\beta'}\underbrace{U_{\alpha1}U_{\alpha'1}U_{\beta1}U_{\beta'1}}_{prod}\underbrace{U_{\alpha1}U_{\alpha'1}}_{decay\ 1}\underbrace{U_{\beta g}U_{\beta' g}}_{decay\ 2}\tilde{R}_{\alpha,\alpha'}\tilde{R}_{\beta,\beta'} \qquad (4.93)
\end{aligned}
$$

with overall factors c_L and c'_L. The factors $\tilde{R}_{\alpha,\alpha'}$ and $\tilde{R}_{\beta,\beta'}$ take into account flavor correlations between the sleptons. With the only relevant, non-vanishing U-matrix elements

$$\begin{aligned} U_{11} &= \cos\phi_L \qquad U_{1g} = \sin\phi_L \\ U_{g1} &= -\sin\phi_L \qquad U_{gg} = \cos\phi_L \\ U_{44} &= 1 \end{aligned} \tag{4.94}$$

we obtain

$$\begin{aligned} \left|\mathcal{M}_L^{tot}(\phi_L,\Delta_L)\right|^2 &= \frac{1}{4}(\sin 2\phi_L)^2\left(\frac{1}{2} - Re\left(\tilde{R}_{1g}\right)\right) \\ &\times\left(c_L + c'_L(\cos\phi_L)^4 + c'_L(\sin\phi_L)^4 + c'_L(\sin 2\phi_L)^2\, Re\left(\tilde{R}_{1g}\right)\right). \end{aligned} \tag{4.95}$$

This result already shows that the squared amplitude vanishes in the limit of vanishing flavor mixing angle i.e. $\phi_L \to 0$. For small mixing angles the main contribution comes from the terms with a ϕ_L-dependence in the form $\sin^2 2\phi_L$, as long as the factors c_L and c'_L are of the same size. The superscripts on the flavor mixing angles are omitted in this section, so that $\phi_i \equiv \phi_i^{1g}$ with $i : L, R$. The same holds for the mass differences, so that $\Delta_i \equiv \Delta_i^{1g}$.
$Re\left(\tilde{R}_{1,g}\right)$ is Δ_L-dependent:

$$\begin{aligned} Re\left(\tilde{R}_{1,g}\right) &= \frac{1}{2}\frac{(m_1\Gamma_1 + m_g\Gamma_g)^2}{(m_1\Gamma_1 + m_g\Gamma_g)^2 + \left(m_1^2 - m_g^2\right)^2} \\ &= \frac{1}{2}\left(1 + \frac{4m_1^2\Delta_L^2 + 4m_1\Delta_L^3 + \Delta_L^4}{m_1^2(\Gamma_1+\Gamma_g)^2 + 2m_1\Gamma_g(\Gamma_1+\Gamma_g)\Delta_L + \Gamma_g^2\Delta_L^2}\right)^{-1} \end{aligned} \tag{4.96}$$

If we assume that m_1 is of the order of 100 GeV, Δ_L does not exceed about 10 GeV and the sleptonic widths are of the order 1 GeV or below, then the term $\Gamma_g^2\Delta_L^2$ can be neglected in a very good approximation. This approximation leads to

$$\begin{aligned} & 2Re\left(\tilde{R}_{1,g}\right) \\ &= \frac{(\Gamma_1+\Gamma_g)^2 + 2\Gamma_g(\Gamma_1+\Gamma_g)\frac{\Delta_L}{m_1}}{(\Gamma_1+\Gamma_g)^2 + 2\Gamma_g(\Gamma_1+\Gamma_g)\frac{\Delta_L}{m_1} + \Delta_L^2\left(4 + 4\frac{\Delta_L}{m_1} + \left(\frac{\Delta_L}{m_1}\right)^2\right)} \end{aligned} \tag{4.97}$$

In the limit of $\Delta_L \to 0$ one gets $Re\left(\tilde{R}_{1,g}\right) \simeq \frac{1}{2}$, so that in this case the squared amplitude becomes zero.

For finite, but small $\Delta_L \ll m_1$ we obtain the approximation

$$Re\left(\tilde{R}_{1,g}\right) \simeq \frac{1}{2}\frac{\left(\Gamma_1+\Gamma_g\right)^2}{\left(\Gamma_1+\Gamma_g\right)^2+4\Delta_L^2}. \tag{4.98}$$

If we want to examine the case of $\phi_R \neq 0$ and $\phi_L = 0$ with the further condition that left-right mixing does not affect flavor mixing, we obtain the following form of the basic MSSM LFV-parameter-dependent squared amplitude

$$\begin{aligned}
&\left|\mathcal{M}_R^{tot}\left(\phi_R,\Delta_R\right)\right|^2 = \\
&\quad c_R \sum_{\alpha,\alpha',\beta,\beta'} \underbrace{U_{\alpha 1}U_{\alpha' 1}U_{\beta 4}U_{\beta 4}}_{prod}\underbrace{U_{\alpha 1}U_{\alpha' 1}}_{decay\ 1}\underbrace{U_{\beta(g+3)}U_{\beta'(g+3)}}_{decay\ 2}\tilde{R}_{\alpha,\alpha'}\tilde{R}_{\beta,\beta'} \\
&\quad +c'_R \sum_{\alpha',\alpha,\beta,\beta'} \underbrace{U_{\alpha 4}U_{\alpha' 4}U_{\beta 4}U_{\beta' 4}}_{prod}\underbrace{U_{\alpha 4}U_{\alpha' 4}}_{decay\ 1}\underbrace{U_{\beta(g+3)}U_{\beta'(g+3)}}_{decay\ 2}\tilde{R}_{\alpha,\alpha'}\tilde{R}_{\beta,\beta'},
\end{aligned} \tag{4.99}$$

in analogy with $|\mathcal{M}_L^{tot}|^2$. One can treat $|\mathcal{M}_R^{tot}|^2$ in complete analogy with $|\mathcal{M}_L^{tot}|^2$, if one substitutes the indices $L \to R$, $1 \to 4$, $4 \to 1$ and $g \to g+3$ in the results for $|\mathcal{M}_L^{tot}|^2$.
The analytical dependence of the squared amplitudes is shown in the case of $c = c' = 1$ for realistic parameters $m_1 = 176$ GeV, $\Gamma_1 = 0.51$ GeV and $\Gamma_g = 0.53$GeV in figure 4.1.

Without left-right mixing the dependence on the flavor mixing angle ϕ has a period of $\frac{\pi}{2}$ and leads to vanishing LFV for $\phi = 0$. The greatest LFV is reached for maximal mixing, $\phi = \frac{\pi}{4}$ due to an approximated $\sin^2(2\phi)$ dependence of the squared amplitude on the respective flavor mixing angle.
The dependence of the squared total amplitude on the relevant mass difference is symmetric to the zero-value at $\Delta = 0$. In the small "interference region" around $\Delta = 0$ the squared amplitude grows very steeply, thus being very sensitive to Δ. This region of rapid growth with increasing $|\Delta|$ soon comes to a bend before the squared total amplitude turns into almost constant values for higher $|\Delta|$ in the "decoherent region".

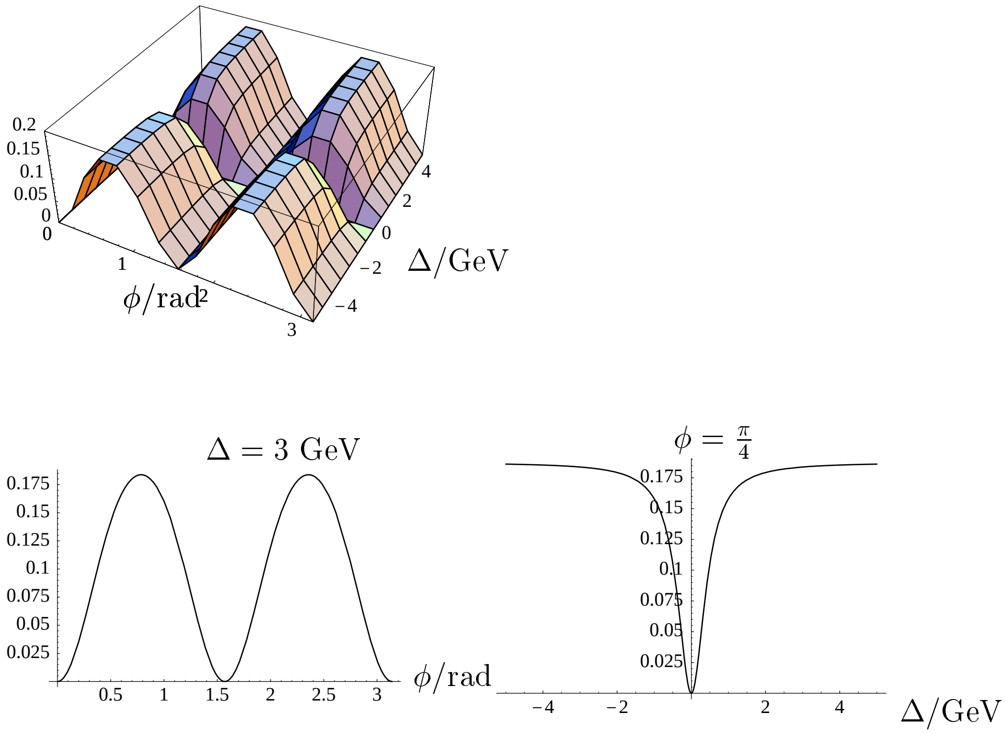

Figure 4.1: Analytical dependence of squared amplitude (in arbitrary units) on LFV-parameters in one sector without left-right mixing for typical input parameters

Chapter 5

Phase space

5.1 Introductory remarks

At first we want to illustrate the basic configuration of the momenta and angles in the cms frame of the process geometrically. For this purpose we show the (projection of the) kinematic parameters in the production plane that can be chosen to be the xz-plane:

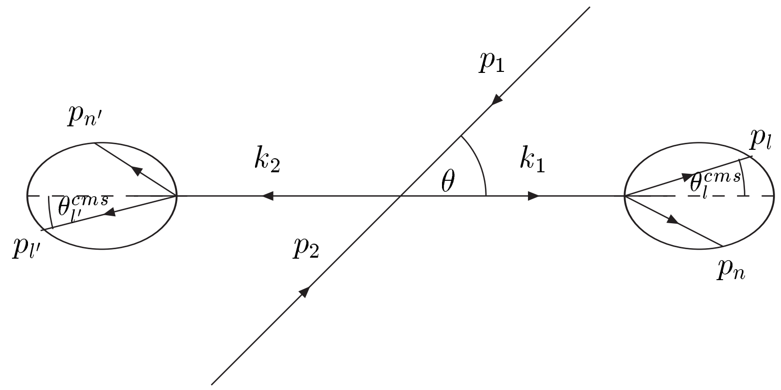

There are three important directions in this process:

- The beam axis is fixed by the direction of the incoming (massless) electrons with momenta p_1 and p_2.
- The decay pipe is formed by the produced sleptons with opposite direction and is connected to the beam axis by a rotation with the production angle θ.
- The direction of the produced leptons can either be viewed from the decay pipe or from the beam axis. The displayed angles θ_l^{cms} and $\theta_{l'}^{cms}$

are connected to the respective decay frame by a boost in $\vec{k}_1-$ or $\vec{k}_2-$ direction. But of course the angles of the final leptons are measured with respect to the beam axis, so that we need an additional rotation by an angle θ related to the beam axis to transform from angles with the cms-superscript into measurable angles (with no supersript).

The whole production process is chosen to be in the xz-plane in the laboratory frame.

5.2 Phase space decomposition

The general phase space for this process is that of a 2 to 4 reaction. With this knowledge one can write down the so-called restricted phase space which already considers the overall four-momentum conservation [8] :

$$d\Phi\left(s, p_3, p_4, p_5, p_6\right) = (2\pi)^4 \delta^{(4)} \left(p_1 + p_2 - \sum_{i=3}^{6} p_i\right) dlips\left(p_3, \ldots, p_6\right) \quad (5.1)$$

- Incoming momenta are here denoted by p_1 and p_2, whereas outgoing momenta are labeled by $p_3 \ldots p_6$.
- The symbol s stands for the square of the total cms energy, $s = (p_1 + p_2)^2$.
- The Lorentz invariant phase space element $dlips\left(p_1, \ldots, p_n\right)$ of four-momenta is in general given by

$$dlips\left(p_1, \ldots, p_n\right) = (2\pi)^{-3n} \prod_{i=1}^{n} \frac{d^3 p_i}{2E_i}. \quad (5.2)$$

Now we want to make use of the fact that there are two intermediate scalar particles which end up in four final fermions via two-body decays. Therefore it is useful to introduce the intermediate four-momenta

$$k_1 = p_3 + p_4,\ k_1^2 = s_1 \quad (5.3)$$
$$k_2 = p_5 + p_6,\ k_2^2 = s_2 \quad (5.4)$$

and to insert two delta functions that imply equation (5.3) and (5.4) for the phase space factor:

$$\begin{aligned} d\Phi\left(s, p_3, p_4, p_5, p_6\right) &= (2\pi)^4 \delta^{(4)}\left(p_1 + p_2 - k_1 - k_2\right) d^4k_1 \delta^{(4)}\left(k_1 - p_3 - p_4\right) \\ &\quad \times d^4k_2 \delta^{(4)}\left(k_2 - p_5 - p_6\right) dlips\left(p_3, \ldots, p_6\right) \end{aligned} \quad (5.5)$$

The terms d^4k_1 and d^4k_2 can be rewritten as [7]

$$d^4k_1 = d\left(k_1^2\right)\frac{d^3k_1}{2E_{k_1}} = ds_1\frac{d^3k_1}{2E_{k_1}} = (2\pi)^3 ds_1 dlips\left(k_1\right), \tag{5.6}$$

$$d^4k_2 = d\left(k_2^2\right)\frac{d^3k_2}{2E_{k_2}} = ds_2\frac{d^3k_2}{2E_{k_2}} = (2\pi)^3 ds_2 dlips\left(k_2\right), \tag{5.7}$$

so that s_1 and s_2 are now explicit integration variables.
Now the whole phase space can be conveniently written as a product of the phase space for the production $d\Phi^p$ of two scalar particles with effective masses $\sqrt{s_1}$ and $\sqrt{s_2}$ and their subsequent two-body decays into the outgoing fermions with the respective phase space factors $d\Phi_1^D$ and $d\Phi_2^D$:

$$d\Phi\left(s, p_3, p_4, p_5, p_6\right) = d\Phi^p\frac{ds_1}{2\pi}d\Phi_1^D\frac{ds_2}{2\pi}d\Phi_2^D \tag{5.8}$$

$$\begin{aligned}
d\Phi^p &= (2\pi)^4\delta^{(4)}\left(p_1+p_2-k_1-k_2\right)(2\pi)^{-3}\frac{d^3k_1}{2E_{k_1}}(2\pi)^{-3}\frac{d^3k_2}{2E_{k_2}} && (5.9)\\
d\Phi_1^D &= (2\pi)^4\delta^{(4)}\left(k_1-p_3-p_4\right)(2\pi)^{-3}\frac{d^3p_3}{2E_3}(2\pi)^{-3}\frac{d^3p_4}{2E_4} && (5.10)\\
d\Phi_2^D &= (2\pi)^4\delta^{(4)}\left(k_2-p_5-p_6\right)(2\pi)^{-3}\frac{d^3p_5}{2E_5}(2\pi)^{-3}\frac{d^3p_6}{2E_6} && (5.11)
\end{aligned}$$

From the earlier remarks concerning the process and the amplitudes it is quite obvious that in our case p_1 and p_2 are the four-momenta of the initial electrons, s_1 and s_2 are the squared effective masses of the intermediate sleptons decaying into $(l_l^-, \tilde{\chi}_n^0)$ with momenta (p_l, p_n) and $\left(l_{l'}^-, \tilde{\chi}_{n'}^0\right)$ with momenta $(p_{l'}, p_{n'})$.

5.3 Production phase space

One part of the phase space factor given above is that of a "$2 \rightarrow 2$"-process. This part of the phase space together with the "flux factor" and the squared amplitude for the production gives the differential cross section for the production part of the process [8]:

$$\begin{aligned}
d\sigma^p &= \frac{1}{2\sqrt{\lambda(s, m_1^2, m_2^2)}}\sum_{\alpha,\alpha',\beta,\beta'}\left(\mathcal{M}^a_{\alpha,\beta}+\mathcal{M}^b_{\alpha,\beta}\right)\left(\mathcal{M}^{a\,*}_{\alpha',\beta'}+\mathcal{M}^{b\,*}_{\alpha',\beta'}\right)\\
&\quad\times(2\pi)^4\delta^{(4)}\left(p_1+p_2-k_1-k_2\right)dlips\left(k_1,k_2\right) && (5.12)\\
\lambda(x,y,z) &= x^2+y^2+z^2-2xy-2xz-2yz && (5.13)\\
\lambda\left(s, m_1^2, m_2^2\right) &\equiv \lambda\left(s, m_g^2, m_g^2\right) \simeq s^2 = 16E_1^4 && (5.14)
\end{aligned}$$

The calculation of the production helicity amplitudes as well as the treatment of the production phase space is done in the cms frame of the production. For the derivation of the production phase space we concentrate on the relevant phase space factor $d\Phi^p$:

$$
\begin{aligned}
d\Phi^p &= (2\pi)^4 \delta^{(4)}\left(p_1 + p_2 - k_1 - k_2\right) (2\pi)^{-3} \frac{d^3 k_1}{2E_{k_1}} (2\pi)^{-3} \frac{d^3 k_2}{2E_{k_2}} && (5.15)\\
&= (2\pi)^4 \delta\left(2E_1 - E_{k_1} - E_{k_2}\right) \delta^{(3)}\left(-\vec{k}_1 - \vec{k}_2\right) \\
&\quad \times (2\pi)^{-3} \frac{d^3 k_1}{2E_{k_1}} (2\pi)^{-3} \frac{d^3 k_2}{2E_{k_2}} && (5.16)
\end{aligned}
$$

The three-dimensional integration over $d^3 k_2$ is done trivially using the three-dimensional delta function. This integration leads to $\vec{k}_2 = -\vec{k}_1$ which simplifies the previous expression to

$$
\begin{aligned}
d\Phi^p &= (2\pi)^{-2} \delta\left(2E_1 - \sqrt{s_1 + \left|\vec{k}_1\right|^2} - \sqrt{s_2 + \left|\vec{k}_1\right|^2}\right) \\
&\quad \times \frac{\left|\vec{k}_1\right|^2 d\left|\vec{k}_1\right| d\Omega_{k_1}}{4\sqrt{s_1 + \left|\vec{k}_1\right|^2}\sqrt{s_2 + \left|\vec{k}_1\right|^2}}. && (5.17)
\end{aligned}
$$

It should be mentioned that $d\Omega_{k_1}$ can be identified with $d\Omega = d\cos\theta d\phi$ where the four-vector k_1 is defined as in (4.46) on page (38).
Introducing [15]

$$
\epsilon^p = \sqrt{s_1 + \left|\vec{k}_1\right|^2} + \sqrt{s_2 + \left|\vec{k}_1\right|^2}, \qquad (5.18)
$$

one gets

$$
\left|\vec{k}_1\right|^2 d\left|\vec{k}_1\right| = \frac{\sqrt{s_1 + \left|\vec{k}_1\right|^2}\sqrt{s_2 + \left|\vec{k}_1\right|^2}}{\epsilon^p} \left|\vec{k}_1\right| d\epsilon^p \qquad (5.19)
$$

which leads to

$$
\begin{aligned}
d\Phi^p &= (2\pi)^{-2} \int_{\sqrt{s_1}+\sqrt{s_2}}^{\infty} d\epsilon^p \delta(2E_1 - \epsilon^p) \frac{\left|\vec{k}_1\right|}{4\epsilon^p} d\Omega \\
&= (2\pi)^{-2} \frac{1}{32E_1^2} \sqrt{\lambda\left(4E_1^2, s_1, s_2\right)} d\Omega. && (5.20)
\end{aligned}
$$

In the last step the important relation for the absolute values of the outgoing slepton momenta,

$$
\left|\vec{k}_1\right| = \left|\vec{k}_2\right| = \frac{1}{4E_1}\sqrt{\lambda\left(4E_1^2, s_1, s_2\right)} = \frac{1}{2\sqrt{s}}\sqrt{\lambda\left(s, s_1, s_2\right)} \qquad (5.21)
$$

has been used. This expression can be derived by solving the equation $\epsilon^p = \epsilon^p\left(|\vec{k}_1|, s_1, s_2\right) = 2E_1$ with respect to $|\vec{k}_1|$. Moreover the kinematical constraint

$$2E_1 = \sqrt{s} > \sqrt{s_1} + \sqrt{s_2} \tag{5.22}$$

has to be fulfilled.
The complete expression for the differential production cross section related to the production solid angle thus reads

$$\begin{aligned}\frac{d\sigma^p}{d\Omega} &= \frac{1}{2s}\sum_{\alpha,\alpha',\beta,\beta'}\left(\mathcal{M}^a_{\alpha,\beta} + \mathcal{M}^b_{\alpha,\beta}\right)\left(\mathcal{M}^{a\,*}_{\alpha',\beta'} + \mathcal{M}^{b\,*}_{\alpha',\beta'}\right)\\ &\quad\times(2\pi)^{-2}\frac{1}{8s}\sqrt{\lambda\left(s, s_1, s_2\right)}.\end{aligned} \tag{5.23}$$

5.4 Two-body decay phase space

The phase space calclations are analogous for both sleptonic two-body decays and they are done in the respective decay frame for each decay. The part of the phase space that has to be considered for the decay of the slepton with four-momentum $k_i(i:1,2)$ into a lepton with four-momentum p_l and a neutralino with four-momentum p_n then reads

$$d\Phi_i^D = (2\pi)^4\delta^{(4)}\left(k_i - p_l - p_n\right)(2\pi)^{-3}\frac{d^3p_l}{2E_l}(2\pi)^{-3}\frac{d^3p_n}{2E_n}. \tag{5.24}$$

One can start in the respective decay systems (i.e.$k_i = (\sqrt{s_i}, \vec{0})$) with the variables labeled by "$*$", when it comes to phase space calculations. These calculations can be summarized for the sleptonic decays in the following way: After integration over $\delta^{(3)}\left(-\vec{p_l}^* - \vec{p_n}^*\right)$ in the above expression for the decay phase space, one gets the condition for momentum conservation in the ($*$)-system, $\vec{p_n}^* = -\vec{p_l}^*$ leading to

$$\begin{aligned}d\Phi_i^D &= (2\pi)^{-2}\delta\left(\sqrt{s_i} - \sqrt{|\vec{p_l}^*|^2 + m_l^2} - \sqrt{|\vec{p_l}^*|^2 + m_n^2}\right)\\ &\quad\times\frac{|\vec{p_l}^*|^2\, d\,|\vec{p_l}^*|\, d\Omega_l}{4\sqrt{|\vec{p_l}^*|^2 + m_l^2}\sqrt{|\vec{p_l}^*|^2 + m_n^2}}.\end{aligned} \tag{5.25}$$

With the substitution [15]

$$\epsilon^D = \sqrt{|\vec{p_l}^*|^2 + m_l^2} + \sqrt{|\vec{p_l}^*|^2 + m_n^2}, \tag{5.26}$$

one obtains

$$\left|\vec{p_l}^*\right|^2 d\left|\vec{p_l}^*\right| = \frac{\sqrt{\left|\vec{p_l}^*\right|^2 + m_l^2}\sqrt{\left|\vec{p_l}^*\right|^2 + m_n^2}}{\epsilon^D}\left|\vec{p_l}^*\right| d\epsilon^D. \tag{5.27}$$

Now it is possible to rewrite the phase space for the decay and to integrate over ϵ^D:

$$\begin{aligned} d\Phi_i^D &= (2\pi)^{-2}\int_{m_l+m_n}^{\infty} d\epsilon^D \delta\left(\sqrt{s_i} - \epsilon^D\right)\frac{\left|\vec{p_l}^*\right|}{4\epsilon^D} d\Omega_l^* \\ &= (2\pi)^{-2}\frac{\left|\vec{p_l}^*\right|}{4\sqrt{s_i}} d\Omega_l^* \end{aligned} \tag{5.28}$$

The kinematical constraint

$$\sqrt{s_i} > m_l + m_n \tag{5.29}$$

has to be fulfilled for the last integration.
With the definition ϵ^D and $\epsilon^D\left(\left|\vec{p_l}^*\right|^2, m_l^2, m_n^2\right) = \sqrt{s_i}$, one comes to

$$\left|\vec{p_l}^*\right| = \frac{1}{2\sqrt{s_i}}\sqrt{\lambda\left(s_i, m_l^2, m_n^2\right)} \simeq \frac{1}{2\sqrt{s_i}}\sqrt{s_i^2 + m_n^4 - 2s_i m_n^2}, \tag{5.30}$$

making $\left|\vec{p_l}^*\right|$ a function of s_i.
As a result, the two-body decay phase factor factor in the decay system $(*)$ is

$$d\Phi_i^D = (2\pi)^{-2}\frac{1}{8s_i}\sqrt{\lambda\left(s_i, m_l^2, m_n^2\right)} d\Omega_l^*. \tag{5.31}$$

5.5 Total cross section

The important phase space components that are necessary for the total cross section have been derived. If we use the compact form for the phase space part, the differential cross section for the whole process takes the form

$$\begin{aligned} d\sigma &= \frac{1}{2s}\frac{ds_1}{2\pi}\frac{ds_2}{2\pi} d\Phi^p d\Phi_1^D d\Phi_2^D \left|\mathcal{M}^{tot}\right|^2 \\ &= \frac{ds_1}{2\pi}\frac{ds_2}{2\pi}\frac{(2\pi)^{-2}}{16s^2}\sqrt{\lambda\left(s, s_1, s_2\right)} d\Omega \frac{(2\pi)^{-2}}{8s_1}\sqrt{\lambda\left(s_1, m_l^2, m_n^2\right)} d\Omega_l^* \\ &\quad \times \frac{(2\pi)^{-2}}{8s_2}\sqrt{\lambda\left(s_2, m_{l'}^2, m_{n'}^2\right)} d\Omega_{l'}^* \left|\mathcal{M}^{tot}\right|^2 \left(s, s_1, s_2, \theta\right). \end{aligned} \tag{5.32}$$

For the total cross section of the process we can perform the full solid angle integrations for the decays in the respective decay frames, each time leading to factors of 4π. For a special helicity combination the total cross section reads

$$\begin{aligned}
&\sigma_{h_1,h_2,h_3,h_5}(s) = \\
&\sum_{\alpha,\alpha',\beta,\beta'} \quad (2\pi)^{-1} \int ds_1 R_{\alpha,\alpha'} \left(\delta\left(s_1 - m_\alpha^2\right) + \delta\left(s_1 - m_{\alpha'}^2\right)\right) \\
&\qquad \times (2\pi)^{-1} \int ds_2 R_{\beta,\beta'} \left(\delta\left(s_2 - m_\beta^2\right) + \delta\left(s_2 - m_{\beta'}^2\right)\right) \\
&\qquad \times (2\pi)^{-2} \frac{1}{16 s^2} \sqrt{\lambda\left(s, s_1, s_2\right)} \int_0^{2\pi} d\phi \int_0^{\pi} d\theta \sin\theta \\
&\qquad \times \left(\mathcal{M}^a_{\alpha,\beta,h_1 1,h_2}\left(s, s_1, s_2, \theta\right) + \mathcal{M}^b_{\alpha,\beta,h_1,h_2}\left(s, s_1, s_2, \theta\right)\right) \\
&\qquad \times \left(\mathcal{M}^{a\,*}_{\alpha',\beta',h_1,h_2}\left(s, s_1, s_2, \theta\right) + \mathcal{M}^{b\,*}_{\alpha',\beta',h_1,h_2}\left(s, s_1, s_2, \theta\right)\right) \\
&\qquad \times \frac{1}{8\pi s_1} \sqrt{\lambda\left(s_1, m_l^2, m_n^2\right)} \mathcal{M}_{\alpha,l,n,h_3}\left(s_1\right) \mathcal{M}^*_{\alpha',l,n,h_3}\left(s_1\right) \\
&\qquad \times \frac{1}{8\pi s_2} \sqrt{\lambda\left(s_2, m_{l'}^2, m_{n'}^2\right)} \mathcal{M}_{\beta,l',n',h_5}\left(s_2\right) \mathcal{M}^*_{\beta',l',n',h_5}\left(s_2\right). \quad (5.33)
\end{aligned}$$

Integrating over $d\phi$ gives a factor of 2π and the integration over $d\theta$ can be done numerically or analytically using the integration formulas of Appendix A.
But for the distributions we cannot simply integrate over the whole phase space. For the later expressions of distributions it is useful to introduce a function $g(s,\theta)$ that collects all parts of the cross section that are not affected by differential distributions of the outgoing leptons:

$$\begin{aligned}
g(s,\theta) \;&=\; \int ds_1 \int ds_2 \frac{1}{2^{18}\pi^8} \frac{1}{s^2 s_1 s_2} \sqrt{\lambda\left(s, s_1, s_2\right)} \sqrt{\lambda\left(s_1, m_l^2, m_n^2\right)} \\
&\quad \times \sqrt{\left(s_2, m_{l'}^2, m_{n'}^2\right)} \left|\mathcal{M}^{tot}\right|^2 \left(s, s_1, s_2, \theta\right) \qquad (5.34)
\end{aligned}$$

With the help of $g(s,\theta)$, expressions for the distributions can be derived from the differential cross section in the compact form

$$d\sigma = g(s,\theta) d\Omega d\Omega_l^* d\Omega_{l'}^*. \qquad (5.35)$$

The total cross section can formally be written in a factorized form [4]

$$
\begin{aligned}
&\sigma_{h_1,h_2,h_3,h_5}(s) = \\
&\textstyle\sum_{\alpha,\alpha',\beta,\beta'} \quad \int ds_1 \tilde{R}_{\alpha,\alpha'} \left(\delta\left(s_1 - m_\alpha^2\right) + \delta\left(s_1 - m_{\alpha'}^2\right)\right) \\
&\qquad\qquad \times \int ds_2 \tilde{R}_{\beta,\beta'} \left(\delta\left(s_2 - m_\beta^2\right) + \delta\left(s_2 - m_{\beta'}^2\right)\right) \\
&\qquad\qquad \times \sigma^p_{\alpha,\alpha',\beta,\beta' h_1,h_2}\left(s, s_1, s_2\right) \\
&\qquad\qquad \times \overline{BR}_{\alpha,\alpha',l,n,h_3}\left(s_1\right) \overline{BR}_{\beta,\beta',l',n',h_5}\left(s_2\right). \qquad (5.36)
\end{aligned}
$$

Here the slepton pair production cross section $\sigma^p_{\alpha,\alpha',\beta,\beta',h_1,h_2}\left(s, s_1, s_2\right)$ and the modified branching ratios for the slepton decays are

$$
\begin{aligned}
\sigma^p_{\alpha,\alpha',\beta,\beta',h_1,h_2}\left(s, s_1, s_2\right) &= \frac{1}{2\sqrt{\lambda\left(s, s_1, s_2\right)}} \int \left(\mathcal{M}^a_{\alpha,\beta,h_1,h_2} + \mathcal{M}^b_{\alpha,\beta,h_1,h_2}\right) \\
&\quad \times \left(\mathcal{M}^{a\,*}_{\alpha',\beta',h_1,h_2} + \mathcal{M}^{b\,*}_{\alpha',\beta',h_1,h_2}\right) d\Omega_{two-body} \qquad (5.37) \\
\overline{BR}_{\alpha,\alpha' l,n,h_3}\left(s_1\right) &= \frac{1}{m_\alpha \Gamma_\alpha + m_{\alpha'} \Gamma_{\alpha'}} \int \mathcal{M}_{\alpha,l,n,h_3} \mathcal{M}^*_{\alpha',l,n,h_3} \\
&\quad \times d\Omega_{two-body} \qquad (5.38) \\
\overline{BR}_{\beta,\beta',l',n',h_5}(s_2) &= \frac{1}{m_\beta \Gamma_\beta + m_{\beta'} \Gamma_{\beta'}} \int \mathcal{M}_{\beta,l',n',h_5} \mathcal{M}^*_{\beta',l',n',h_5} \\
&\quad \times d\Omega_{two-body}. \qquad (5.39)
\end{aligned}
$$

The integrals have to be done over the two-body phase space with four-momentum conservation.

Polarized cross sections From an experimental point of view it is impossible to work with incoming particle beams of one definite helicity. In a realistic situation there will always be mixtures of the helicities for the incoming particles. In our case of two incoming "massless" electrons one can treat this problem by introducing the probability p for an electron having helicity $+\frac{1}{2}$. Then the probability for an electron having the switched helicity $-\frac{1}{2}$, is of course $1-p$. Now any kind of cross section related to the helicity mixture of incoming electrons can be written as

$$
\begin{aligned}
d\sigma^{p_1,p_2}_{h_3,h_5} &= p_1 p_2 d\sigma_{+\frac{1}{2},+\frac{1}{2},h_3,h_5} + \left(1-p_1\right)\left(1-p_2\right) d\sigma_{-\frac{1}{2},-\frac{1}{2},h_3,h_5} \\
&\quad + p_1\left(1-p_2\right) d\sigma_{+\frac{1}{2},-\frac{1}{2},h_3,h_5} + \left(1-p_1\right) p_2 d\sigma_{-\frac{1}{2},+\frac{1}{2},h_3,h_5}. \qquad (5.40)
\end{aligned}
$$

The introduced positive helicity degree p for each incoming electron is easily connected to the definition of the polarizations,

$$\begin{aligned} P &= \frac{p-(1-p)}{p+(1-p)} = 2p-1, \quad -1 \leq P \leq 1 && (5.41) \\ p &= \frac{1}{2}(1+P), \ 0 \leq p \leq 1 && (5.42) \\ 1-p &= \frac{1}{2}(1-P). && (5.43) \end{aligned}$$

Therefore cross sections which include the polarizations of the incoming electrons that have helicities h_1 and h_2 are written as

$$d\sigma_{h_3,h_5}^{P_1,P_2} = \frac{1}{4}\sum_{h_1,h_2} (1+2h_1P_1)\,(1+2h_2P_2)\,d\sigma_{h_1,h_2,h_3,h_5}. \tag{5.44}$$

This type of cross sections is still dependent on the helicities of the outgoing leptons. Apart from the results on the helicity asymmetry of a final tau lepton, we typically do not want to specify the helicities of the outgoing particles which means that we have to sum over their helicities. This summation over final helicities in (5.44) leads to cross sections that still depend on the beam polarizations, but which are no longer sensitive to the final helicites,

$$d\sigma^{P_1,P_2} = \sum_{h_3}\sum_{h_5} d\sigma_{h_3,h_5}^{P_1,P_2}. \tag{5.45}$$

In the case of cross sections for unpolarized beams i.e. $P_1 = 0$ and $P_2 = 0$ without specified final helicities we obtain

$$d\sigma^{P=0} = \frac{1}{4}\sum_{h_1,h_2}\sum_{h_3}\sum_{h_5} d\sigma_{h_1,h_2,h_3,h_5}. \tag{5.46}$$

5.6 Energy distributions

For the energy distribution of an outgoing lepton, one can consider the final expression for the two-body decay phase space (5.31). We will derive the relevant energy distribution expression $\frac{d\sigma}{dE_l}$ for a kinematic massless lepton l, using the notations given before. Integrating over the azimuthal angle in the respective decay frame yields a factor of 2π, a factor that arises in the integration over the azimuthal angle of production, too. We can integrate over the full solid angle element of the other lepton l', yielding 4π. Therefore the relevant differential cross section for the energy distribution of a single outgoing lepton l can be written as:

$$\begin{aligned} d\sigma &= 16\pi^3 g(s,\theta) d\cos\theta_l^* d\cos\theta \\ &= 16\pi^3 \int g(s,\theta) dE_l^* \delta\left(E_l^* - \left|\vec{p_l}^*\left(s_1\right)\right|\right) d\cos\theta_l^* d\cos\theta. \end{aligned} \tag{5.47}$$

In order to keep expressions shorter, we define

$$\epsilon_l = \left|\vec{p_l}^*\left(s_1\right)\right|, \quad \epsilon_{l'} = \left|\vec{p_{l'}}^*\left(s_2\right)\right|. \tag{5.48}$$

The absolute value of the cms velocity (5.67) of the slepton with momentum $k_i(i:1,2)$ and the corresponding boost factor depend on s_i, too. Therefore we introduce

$$v_i = |v(s_i)| \text{ and } \gamma_i = \gamma\left(s_i\right) = \frac{1}{\sqrt{1-v_i^2}}. \tag{5.49}$$

The introduced lepton energy variable E_l^* in the decay frame can now be connected to the measurable lepton energy E_l in the cms frame of the process:

$$E_l^* = \frac{E_l}{\gamma_1\left(1+v_1\cos\theta_l^*\right)} \tag{5.50}$$

$$dE_l^* = \frac{dE_l}{\gamma_1\left(1+v_1\cos\theta_l^*\right)} \tag{5.51}$$

The derivation of the relation (5.50) can be found in the context of "Angular distributions" (5.71). Now we can write the differential cross section related to E_l:

$$\begin{aligned} \frac{d\sigma}{dE_l} &= 16\pi^3 \int d\cos\theta d\cos\theta_l^* \frac{g(s,\theta)}{\gamma_1\left(1+v_1\cos\theta_l^*\right)} \\ &\times\delta\left(\frac{E_l}{\gamma_1\left(1+v_1\cos\theta_l^*\right)} - \epsilon_l\right) \end{aligned} \tag{5.52}$$

One can integrate concerning $d\cos\theta_l^*$ using [18]

$$\delta\left(f\left(\cos\theta_l^*\right)\right) = \sum_{\left(\cos\theta_l^*\right)_{0i}} \frac{\delta\left(\cos\theta_l^* - (\cos\theta_l^*)_{0i}\right)}{\left|f'\left(\cos\theta_l^*\right)\right|_{\left(\cos\theta_l^*\right)_{0i}}}\Bigg|_{\left(f\left(\cos\theta_l^*\right)_0=0\wedge f'\left(\cos\theta_l^*\right)_0\neq 0\right)} \tag{5.53}$$

$$\text{with } f(\cos\theta_l^*) = \frac{E_l}{\gamma_1\left(1+v_1\cos\theta_l^*\right)} - \epsilon_l \tag{5.54}$$

which leads to

$$\begin{aligned} \frac{d\sigma}{dE_l} &= 16\pi^3 \int d\cos\theta d\cos\theta_l^* \delta\left(\cos\theta_l^* - (\cos\theta_l^*)_0\right) \\ &\times \frac{g(s,\theta)}{\gamma_1\left(1+v_1\cos\theta_l^*\right)} \frac{\gamma_1\left(1+v_1(\cos\theta_l^*)_0\right)^2}{v_1 E_l}. \end{aligned} \tag{5.55}$$

Integration over the Delta function implies that

$$\cos\theta_l^* \;=\; (\cos\theta_l^*)_0 = \frac{E_l - \epsilon_l\gamma_1}{\epsilon_l\gamma_1 v_1} \tag{5.56}$$

which can be fullfilled if

$$-1 \le \frac{E_l - \epsilon_l\gamma_1}{\epsilon_l\gamma_1 v_1} \le 1. \tag{5.57}$$

The single energy distribution of lepton l reads

$$\begin{aligned} \frac{d\sigma}{dE_l} &= 16\pi^3 \int_0^\pi d\theta \sin\theta \frac{g(s,\theta)}{\epsilon_l\gamma_1 v_1}\ , \text{ for } -1 \le \frac{E_l - \epsilon_l\gamma_1}{\epsilon_l\gamma_1 v_1} \le 1 \\ &\text{and} \quad 0 \qquad \text{otherwise.} \end{aligned} \tag{5.58}$$

The necessary condition (5.57) for a non-vanishing energy distribution can directly be written as a kinematical constraint for E_l,

$$\epsilon_l\gamma_1\,(1 - v_1) \le E_l \le \epsilon_l\gamma_1\,(1 + v_1)\,. \tag{5.59}$$

The analogous expression for the energy distribution of the other outgoing lepton l' is obtained by substituting the indices $1 \to 2$ and $l \to l'$ in (5.58). In order to get the double differential energy distributions related to the outgoing leptons, we start with (5.35), integrated over the three azimuthal components:

$$d\sigma \;=\; 8\pi^3 g(s,\theta) d\cos\theta_l^* d\cos\theta_{l'}^* d\cos\theta. \tag{5.60}$$

Now we can introduce differential lepton energies twice and use the aforementioned results. This yields the following result for the double differential lepton energy distribution:

$$\begin{aligned} \frac{d\sigma}{dE_l dE_{l'}} &= 8\pi^3 \int_0^\pi d\theta \sin\theta \frac{g(s,\theta)}{\epsilon_l\gamma_1 v_1 \epsilon_{l'}\gamma_2 v_2} \\ \text{for} \quad & -1 \le \frac{E_l - \epsilon_l\gamma_1}{\epsilon_l\gamma_1 v_1} \le 1 \ \wedge\ -1 \le \frac{E_{l'} - \epsilon_{l'}\gamma_2}{\epsilon_{l'}\gamma_2 v_2} \le 1 \\ \text{and} \quad & 0 \qquad \text{otherwise.} \end{aligned} \tag{5.61}$$

Missing energy distribution For later distributions it is useful to introduce the missing energy $\not{E}$ as

$$\not{E} = \sqrt{s} - E_l - E_{l'}, \tag{5.62}$$

so that it is equal to the total energy of the outgoing neutralinos. If we integrate over the double differential lepton energy distribution provided that (5.62) is fulfilled, the missing energy distribution can be calculated:

$$\frac{d\sigma}{d\not{E}} = \int \delta\left(\not{E} - \sqrt{s} + E_l + E_{l'}\right) \frac{d^2\sigma}{dE_l dE_{l'}} \left(E_l, E_{l'}\right) dE_l dE_{l'} \tag{5.63}$$

$$= \int_0^{\sqrt{s}-m_n-m_{n'}} dE_{l'} \frac{d^2\sigma}{dE_l dE_{l'}} \left(\sqrt{s} - \not{E} - E_{l'}, E_{l'}\right) \tag{5.64}$$

5.7 Angular distributions

The next task is to write down the expressions for the measurable angular distribution $\frac{d\sigma}{d\cos\theta_l}$ of lepton l; the measurable angular distribution $\frac{d\sigma}{d\cos\theta_{l'}}$ of the other lepton l' is then easily obtained.
For that purpose we start with (5.35), integrated over the solid angle of lepton l':

$$d\sigma = 4\pi g(s,\theta) d\Omega_l^* d\Omega \tag{5.65}$$

At first one must boost the decay frame of the decaying slepton into the cms reference frame. Under this boost the solid angle $d\Omega_l^*$ transforms like

$$d\Omega_l^* = d\phi_l^* d\cos\theta_l^* = d\phi_l^{cms} \frac{d\cos\theta_l^*}{d\cos\theta_l^{cms}} d\cos\theta_l^{cms}. \tag{5.66}$$

The azimuthal component is not affected for a boost along the z-axis in the cms reference frame, because this coordinate is perpendicular to the boost direction. But of course the distribution in the decay angle $\cos\theta_l^{cms}$ is no longer isotropic in the cms. The boost in z-direction of this system is done for the absolute value of the relative velocity

$$v_1 = \frac{\left|\vec{k}_1\right|}{\sqrt{s_1 + \left|\vec{k}_1\right|^2}} \tag{5.67}$$

of the decaying slepton in the cms, with $\left|\vec{k}_1\right|$ given by (5.21). The necessary transformation $\frac{d\cos\theta_l^*}{d\cos\theta_l^{cms}}$ in the massless limit $m_l \to 0$ [7] is

$$\frac{d\cos\theta_l^*}{d\cos\theta_l^{cms}} = \frac{1 - v_1^2}{\left(1 - v_1\cos\theta_l^{cms}\right)^2}. \tag{5.68}$$

This relativistic transformation factor is large for small angles of θ_l^{cms} and soon decreases as the outgoing lepton moves into more and more deviating

directions compared to the decaying slepton.
In order to obtain this relativistic angular transformation relation, one can examine the general case of a boost along the z-direction for two systems, with the second frame of reference characterized by "$'$":

$$E' = \gamma\left(E + vp_z\right) = \gamma\left(E + vp\cos\theta\right) \tag{5.69}$$
$$p'_z = \gamma\left(p_z + vE\right) = \gamma\left(p\cos\theta + vE\right) \tag{5.70}$$

Now in the limit of negligible mass $m \to 0$, these relations can be combined:

$$p' = E' = \gamma p\left(1 + v\cos\theta\right) \tag{5.71}$$
$$p'\cos\theta' = \gamma\left(p\cos\theta + vp\right) \tag{5.72}$$

Thus we arrive at

$$\cos\theta = \frac{\cos\theta' - v}{1 - v\cos\theta'}, \tag{5.73}$$

as the connection between the angles related to the boost direction. In our case the variables without "$'$" can be identified with the respective variables in the decay frame of the decaying slepton, whereas the variables assigned with "$'$" refer to the quantities in the cms reference frame. In this way we arrive at the relativistic transformation rule (5.68) concerning angles that are measured in boost direction in the massless limit case.
Now we first have to integrate over the "inner angles" θ and ϕ in order to get the angular distribution of an outgoing lepton.
Spherical trigonometry (see Appendix B) yields

$$\cos\theta_l^{cms} = \cos\theta_l\cos\theta + \sin\theta_l\sin\theta\cos\left(\phi_l - \phi\right), \tag{5.74}$$

so that a non-trivial integration over the azimuthal angle of production is necessary. Substituting (5.74) into the angular boost factor (5.68) yields

$$\frac{d\cos\theta_l^*}{d\cos_l^{cms}} = \frac{1 - v_1^2}{\left(1 - v_1\cos\theta\cos\theta_l - v_1\sin\theta\sin\theta_l\cos\left(\phi_l - \phi\right)\right)^2}. \tag{5.75}$$

The integration over the azimuthal angle of the production is done using formula (A.17) of Appendix A:

$$\int_0^{2\pi} d\phi \frac{d\cos\theta_l^*}{d\cos_l^{cms}} = \frac{2\pi\left(1 - v_1^2\right)\left(1 - v_1\cos\theta_l\cos\theta\right)}{\left(1 - v_1\cos(\theta_l - \theta)\right)^{3/2}\left(1 - v_1\cos(\theta_l + \theta)\right)^{3/2}} \tag{5.76}$$

If we rotate from the cms-angles to the measurable ones, the respective solid angles transform identically into each other:

$$d\Omega_l^{cms} = d\Omega_l \tag{5.77}$$
$$d\cos\theta_l^{cms} d\phi_l^{cms} = d\cos\theta_l d\phi_l \tag{5.78}$$

Now we can integrate over the production angle θ:

$$\begin{aligned} d\sigma &= 8\pi^2 d\phi_l d\cos\theta_l \int_0^\pi d\theta \sin\theta g(s,\theta) \\ &\quad \times \frac{\left(1-v_1^2\right)\left(1-v_1\cos\theta_l\cos\theta\right)}{\left(1-v_1\cos(\theta_l-\theta)\right)^{3/2}\left(1-v_1\cos(\theta_l+\theta)\right)^{3/2}} \end{aligned} \tag{5.79}$$

The integration over the azimuthal angle $d\phi_l$ can be done trivially,

$$\int_0^{2\pi} d\phi_l = 2\pi. \tag{5.80}$$

This implies that the angular distribution is azimuthally isotropic. The measurable angular distribution of lepton l finally reads

$$\begin{aligned} \frac{d\sigma}{d\cos\theta_l} &= 16\pi^3 \int_0^\pi d\theta \sin\theta g(s,\theta) \\ &\quad \times \frac{\left(1-v_1^2\right)\left(1-v_1\cos\theta_l\cos\theta\right)}{\left(1-v_1\cos(\theta_l-\theta)\right)^{\frac{3}{2}}\left(1-v_1\cos(\theta_l+\theta)\right)^{3/2}}. \end{aligned} \tag{5.81}$$

In order to obtain the analogous distribution for the outgoing lepton l' connected to the other slepton, one has to keep in mind that the two decaying sleptons move in opposite directions. One can take this into account by setting the production angle $\theta \to \pi - \theta$ in the respective decay phase space factors of (5.79). The measurable angular distribution of lepton l' then takes the form

$$\begin{aligned} &\frac{d\sigma}{d\cos\theta_{l'}} = 16\pi^3 \int_0^\pi d\theta \sin\theta g(s,\theta) \\ &\times \frac{\left(1-v_2^2\right)\left(1-v_2\cos\theta_l\cos(\pi-\theta)\right)}{\left(1-v_2\cos(\theta_{l'}-\pi+\theta)\right)^{3/2}\left(1-v_2\cos(\theta_{l'}+\pi-\theta)\right)^{3/2}}. \end{aligned} \tag{5.82}$$

In order to illustrate the differences between the two outgoing leptons geometrically, one can consider the following diagrams in the production plane:

For the case of an angular distribution of lepton l:

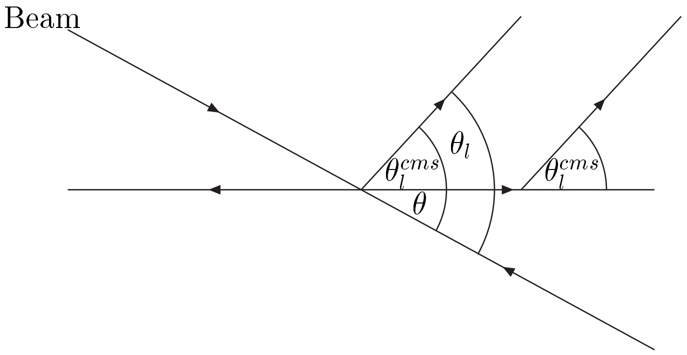

For the case of an angular distribution of lepton l':

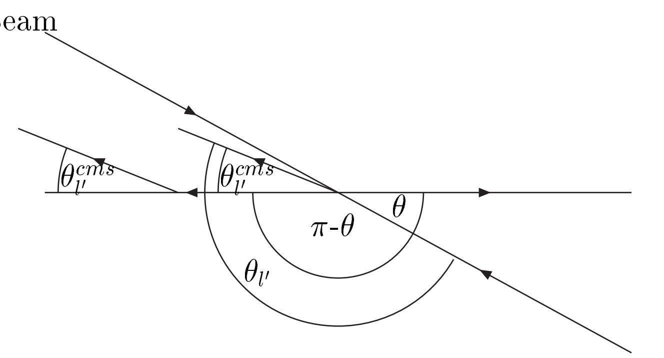

5.8 Energy-angle distributions

At first we want to derive the energy-angle distribution of lepton l. Therefore we start with (5.35), integrated over the solid angle of the other lepton l' and introduce the lepton energy E_l^* in the decay frame as a new integration variable:

$$d\sigma = 4\pi \int g(s,\theta)\delta\left(E_l^* - \epsilon_l\right) dE_l^* d\cos\theta_l^* d\phi_l^* d\Omega \tag{5.83}$$

For the necessary boost of the sleptonic decay frame to the cms reference system rotated into slepton direction, the azimuthal component is not affected, $d\phi_l^* \to d\phi_l^{cms}$. In order to get the energy-angle distribution in the cms frame of reference, we have to transform the variables $E_l^*, \cos\theta_l^*$ connected to the decay frame into the cms-variables $E_l, \cos_l^{cms}$:

$$dE_l^* d\cos_l^* = \frac{\partial\left(E_l^*, \cos\theta_l^*\right)}{\partial\left(E_l, \cos\theta_l^{cms}\right)} dE_l d\cos\theta_l^{cms}, \tag{5.84}$$

with the Jacobi determinant

$$\frac{\partial\left(E_l^*, \cos\theta_l^*\right)}{\partial\left(E_l, \cos\theta_l^{cms}\right)} = \begin{vmatrix} \frac{\partial E_l^*}{\partial E_l} & \frac{\partial E_l^*}{\partial \cos\theta_l^{cms}} \\ \frac{\partial \cos\theta_l^*}{\partial E_l} & \frac{\partial \cos\theta_l^*}{\partial \cos\theta_l^{cms}} \end{vmatrix} \text{ and } E_l^{cms} \equiv E_l. \tag{5.85}$$

With the help of the relativistic transformation formulas (5.73), (5.71)

$$\begin{aligned} \cos\theta_l^* &= \frac{\cos\theta_l^{cms} - v_1}{1 - v_1 \cos_l^{cms}} \\ E_l^* &= \gamma_1 E_l \left(1 - v_1 \cos\theta_l^{cms}\right) \end{aligned} \tag{5.86}$$

the necessary determinant (5.85) can be obtained,

$$\frac{\partial\left(E_l^*, \cos\theta_l^*\right)}{\partial\left(E_l, \cos\theta_l^{cms}\right)} = \left(\gamma_1 \left(1 - v_1 \cos\theta_l^{cms}\right)\right)^{-1}. \tag{5.87}$$

Now the energy-angle distribution in the cms reference frame reads

$$\begin{aligned} \frac{d\sigma}{dE_l d\cos\theta_l^{cms}} &= 4\pi \int d\phi d\cos\theta d\phi_l^{cms} \delta\left(\gamma_1 E_l \left(1 - v_1 \cos\theta_l^{cms}\right) - \epsilon_l\right) \\ &\quad \times g(s,\theta) \left(\gamma\left(1 - v_1 \cos\theta_l^{cms}\right)\right)^{-1}. \end{aligned} \tag{5.88}$$

But of course we must again rotate the differential solid angle labeled with "cms" into the measurable differential solid angle. For that purpose we have to make use of (5.74) and (5.78) again, resulting in

$$\begin{aligned} \frac{d\sigma}{dE_l d\cos\theta_l} &= 4\pi \int d\phi d\cos\theta d\phi_l g(s,\theta) \\ &\times \frac{\delta\left(\gamma_1 E_l \left(1 - v_1 \left(\cos\theta_l \cos\theta + \sin\theta_l \sin\theta \cos\left(\phi_l - \phi\right)\right)\right) - \epsilon_l\right)}{\gamma_1 \left(1 - v_1 \left(\cos\theta_l \cos\theta + \sin\theta_l \sin\theta \cos\left(\phi_l - \phi\right)\right)\right)} \end{aligned} \tag{5.89}$$

In order to integrate over the azimuthal angle of production analytically, we can use the identity [18]

$$\delta\left(f\left(\phi\right)\right) = \sum_{(\phi)_{0,i}} \frac{\delta\left(\phi - (\phi)_{0,i}\right)}{\left|f'\left(\phi\right)\right|_{(\phi)_{0,i}}} \Bigg|_{\left(f(\phi)_0 = 0 \wedge f'(\phi)_0 \neq 0\right)}. \tag{5.90}$$

The argument of the delta function becomes zero for

$$
\begin{aligned}
(\phi)_{0,1} &= \phi_l - \arccos(arg) \qquad\quad \text{for } 0 \leq \arccos(arg) \leq \pi && (5.91)\\
(\phi)_{0,2} &= \phi_l - 2\pi + \arccos(arg) \ \text{for } \pi < \arccos(arg) < 2\pi && (5.92)\\
\text{with } arg &= \frac{1 - v_1 \cos\theta_l \cos\theta - \epsilon_l \left(\gamma_1 E_l\right)^{-1}}{v_1 \sin\theta_l \sin\theta}. && (5.93)
\end{aligned}
$$

The necessary derivatives are

$$
\begin{aligned}
\frac{1}{\left|f'(\phi)\right|_{(\phi)_{0,1}}} &= \left(\gamma_1 v_1 E_l \sin\theta_l \sin\theta \left|\sin(\arccos(arg))\right|\right)^{-1}, && (5.94)\\
\frac{1}{\left|f'(\phi)\right|_{(\phi)_{0,2}}} &= \left(\gamma_1 v_1 E_l \sin\theta_l \sin\theta \left|\sin(-2\pi + \arccos(arg))\right|\right)^{-1}\\
&= \frac{1}{\left|f'(\phi)\right|_{(\phi)_{0,1}}}. && (5.95)
\end{aligned}
$$

Now the analytical integration over $d\phi$ can be done and one gets two times the contribution for the first zero $(\phi)_{0,1}$ of $f(\phi)$,

$$
\frac{d\sigma}{dE_l d\cos\theta_l} = 8\pi \int d\cos\theta d\phi_l \frac{g(s,\theta)}{\left|f'(\phi)\right|_{(\phi)_{0,1}}} \frac{E_l}{\epsilon_l}. \tag{5.96}
$$

The integration over $d\phi_l$ is now rendered trivially, because the whole integrand is independent of ϕ_l. The desired energy-angle distribution now reads

$$
\begin{aligned}
\frac{d\sigma}{dE_l d\cos\theta_l} &= 16\pi^2 \int d\theta \sin\theta g(s,\theta)\\
\times &\left(\gamma_1 \epsilon_l \sqrt{\left(v_1 \sin\theta_l \sin\theta\right)^2 - \left(1 - v_1 \cos\theta_l \cos\theta - \epsilon_l \left(\gamma_1 E_l\right)^{-1}\right)^2}\right)^{-1}. && (5.97)
\end{aligned}
$$

One can give kinematic limits for this distribution, because the argument $arg\,(E_l, \theta_l, \theta)$ (5.93) of arccosine must lie within the intervall of [-1,1]. This demand is equivalent to

$$
-1 \leq \frac{1 - v_1 \cos\theta_l \cos\theta - \epsilon_l \left(\gamma_1 E_l\right)^{-1}}{v_1 \sin\theta_l \sin\theta} \leq 1 \tag{5.98}
$$

as a kinematical constraint for the range of the two dimensional energy-angle distribution.

The energy-angle distribution of the other lepton l' is now obtained easily: As in the case of angular distributions, we have to substitute $l \to l'$, $1 \to 2$ in the respective indices and $\theta \to \pi - \theta$ in the respective decay phase space factors of (5.97). This yields

$$\frac{d\sigma}{dE_{l'}\,d\cos\theta_{l'}} = 16\pi^2 \int d\theta \sin\theta g(s,\theta)$$
$$\times \left(\gamma_2 \epsilon_{l'} \sqrt{(v_2 \sin\theta_{l'} \sin\theta)^2 - \left(1 + v_1 \cos\theta_{l'} \cos\theta - \epsilon_l \left(\gamma_1 E_l\right)^{-1}\right)^2}\right)^{-1}. \quad (5.99)$$

Transverse momentum distribution The transverse momentum $p_l^\perp$ of a massless lepton l,

$$p_l^\perp = E_l \sin\theta_l \quad (5.100)$$

measures the momentum perpendicular to the beam direction. In order to calculate the transverse momentum distribution of one outgoing lepton l, we just have to integrate over the energy-angle distribution and include an additional delta function that guarantees (5.100):

$$\frac{d\sigma}{dp_l^\perp} = \int \delta\left(p_l^\perp - E_l \sin\theta_l\right) \frac{d^2\sigma}{dE_l d\cos\theta_l}\left(E_l, \cos\theta_l\right) dE_l d\cos\theta_l \quad (5.101)$$
$$= \int_{-1}^{1} d\cos\theta_l \frac{1}{\sin\theta_l} \frac{d^2\sigma}{dE_l d\cos\theta_l}\left(\frac{p_l^\perp}{\sin\theta_l}, \cos\theta_l\right) \quad (5.102)$$

Chapter 6

Numerical values for the scenarios

In this part three different scenarios [10], [11], [12] corresponding to special input parameter points in MSSM parameter space will be examined. We took the numerical values of the parameters at the electroweak scale in the reference scenarios as appropriate input parameters for further computation in the MSSM case. In models with right-handed neutrinos, this EW-input was modified with the corrections of sections 3.4 and 3.5, respectively. Masses of neutralinos and sleptons were obtained by diagonalization of the mass matrices with Mathematica, whereas all of the widths given below were obtained by using the Comphep code.

6.1 Survey of the scenario input

All of the parameters given in this section were taken from [10], [11], [12]. At first we want to mention the SM input at the electroweak (EW) scale:
$M_Z = 91.187$ GeV, $m_t = 175$ GeV, $m_\tau = 1.777$ GeV, $\alpha_{EM} = 7.76 \cdot 10^{-3}$, $\sin^2 \theta_W = 0.2315$
Furthermore the scale of unification of the gauge couplings is given as
$M_{GUT} = 2.14 * 10^{16}$ GeV.

The five basic mSUGRA parameters are fixed by the following input values:

Parameter	Explanation	Input values in		
		I	II	III
m_0/GeV	Common scalar mass at M_{GUT}	100	160	100
$m_{1/2}$/GeV	Common gaugino mass at M_{GUT}	200	200	200
A_0/GeV	Common tri-linear coupling at M_{GUT}	0	600	-715
$\tan\beta$	Ratio of Higgs VEV's at EW scale	3	30	3
sign(μ)	Sign of SUSY Higgs mixing term	+	+	+

Already at this stage one can see some basic features of the three mSUGRA scenarios:
The first scenario has vanishing tri-linear coupling at M_{GUT} and small $\tan\beta$, so that we expect that left-right mixing effects in the slepton sector should be rather suppressed, even at the EW scale. In scenario II the left-right mixing effects are quite enhanced, because of large input values of A_0 and $\tan\beta$. Moreover the second scenario has a larger input value for scalar particles, so that most of the scalar particles are heavier than in the other scenarios. In the third scenario, $\tan\beta$ is small, but the tri-linear coupling is large and negative which leads us to the expectation that the effects of left-right mixing should assume medium values in comparison to the first two scenarios. Due to the same m_0 input value at M_{GUT}, the masses of the sleptons should be similar in scenario I and III. These input parameters serve as boundary conditions to evolve the RGEs of the MSSM from the M_{GUT} scale down to the EW scale.
This procedure yields the following numerical values at the electroweak scale that serve as input parameters for our further calculations:

Parameter	Explanation	Numerical value in		
		I	II	III
M_1/GeV	U(1) gaugino mass	78.7	78.0	79.5
M_2/GeV	SU(2) gaugino mass	152	150	153
μ/GeV	SUSY Higgs-mixing term	316	263	435
$\tan\beta$	Ratio of Higgs VEV's	3.00	30.0	3.00
$\left(m_{\tilde{l}_L}\right)_e$/GeV, $\left(m_{\tilde{l}_L}\right)_\mu$/GeV	Left slepton SSB mass for 1st 2 generations	171	212	171
$\left(m_{\tilde{l}_R}\right)_e$/GeV, $\left(m_{\tilde{l}_R}\right)_\mu$/GeV	Right slepton SSB mass for 1st 2 generations	127	179	127
$\left(m_{\tilde{l}_L}\right)_\tau$/GeV	Left stau SSB mass	171	189	171
$\left(m_{\tilde{l}_R}\right)_\tau$/GeV	Right stau SSB mass	126	115	125
A_τ/GeV	τ tri-linear SSB cplg.	-133	384	-847

6.2 Scenario I

The given set of basic input parameters implies the observation of the lighter neutral Higgs boson h^0 with mass $m_{h^0} = 97.7$ GeV. The four neutralinos are described in the following way:

Particle	Mass/ GeV	Width/ GeV	N_{1j}	N_{2j}	N_{3j}	N_{4j}
$\tilde{\chi}_1^0$	71.9	0	0.78	-0.60	0.19	-0.097
$\tilde{\chi}_2^0$	130	$2.40 \cdot 10^{-5}$	0.63	0.71	-0.27	0.17
$\tilde{\chi}_3^0$	320	2.15	-0.0068i	0.092i	0.70i	0.71 i
$\tilde{\chi}_4^0$	348	3.03	-0.045	-0.37	-0.64	0.67

The neutralinos are written in the $\tilde{\psi}^0$ basis (see 3.4) with the diagonalization matrix elements N_{ij} according to (3.10) and $j : 1, \ldots, 4$.
The mixing of the gaugino states shows that there is large mixing between the photino-zino-states and between the two neutral Higgsino-states, respectively. Therefore the two lightest neutralinos are primarily composed of the photino-zino-components, whereas the two heavy neutralinos consist mainly of Higgsino-states. The photino-Higgsino-mixing is quite small.
The significant ($> 5\%$) neutralino decay channels and branching ratios are [10]:

Particle	Decay channel	BR
$\tilde{\chi}_1^0$		
$\tilde{\chi}_2^0$	$\tilde{\chi}_1^0 \tau^+ \tau^-$	0.24
	$\tilde{\chi}_1^0 e^+ e^-$	0.20
	$\tilde{\chi}_1^0 \mu^+ \mu^-$	0.20
	$\tilde{\chi}_1^0 \nu_e \bar{\nu}_e$	0.10
	$\tilde{\chi}_1^0 \nu_\mu \bar{\nu}_\mu$	0.10
	$\tilde{\chi}_1^0 \nu_\tau \bar{\nu}_\tau$	0.10
$\tilde{\chi}_3^0$	$\tilde{\chi}_1^+ W^-, \tilde{\chi}_1^- W^+$	0.31
	$\tilde{\chi}_2^0 Z^0$	0.20
	$\tilde{\chi}_1^0 Z^0$	0.14
$\tilde{\chi}_4^0$	$\tilde{\chi}_1^+ W^-, \tilde{\chi}_1^- W^+$	0.26
	$\tilde{\chi}_2^0 h^0$	0.11
	$\tilde{\chi}_1^0 h^0$	0.07

In this scenario the second lightest neutralino has a relative small width and equivalently a greater lifetime in comparison to the heavier neutralinos. The second lightest neutralino mainly decays into the LSP and two leptons. Two-body decays of $\tilde{\chi}_2^0$ into slepton and lepton are kinematically forbidden, because $\tilde{\chi}_2^0$ is lighter than the sleptons.

6.2.1 MSSM

The sleptons are described as follows:

Particle	Mass/GeV	Width/GeV
$\tilde{e}_L^-$	176	0.507
$\tilde{\mu}_L^-$	176	0.507
$\tilde{\tau}_2^-$	177	0.517
$\tilde{e}_R^-$	133	0.314
$\tilde{\mu}_R^-$	133	0.314
$\tilde{\tau}_1^-$	131	0.298

In this scenario (referred to as $MSSMI$) the mass differences as well as the stau left-right mixing angle resulting from the given electroweak parameters are:

$$\Delta_L^{13} = 0.009 \text{ GeV} \qquad \Delta_R^{13} = -0.943 \text{ GeV} \qquad \theta_{\tilde{\tau}} = -0.138$$

As already mentioned before, left-right mixing effects are rather suppressed in the first scenario (see $\theta_{\tilde{\tau}}$), so that the heavier stau is predominantly composed of the left-handed stau, whereas the lighter stau consists practically of the right-handed stau component. This results in almost mass-degenerate left-handed sleptons of the first two generations and $\tilde{\tau}_2^-$ on the one side and right-handed sleptons of the first two generations that are nearly degenerate in mass with $\tilde{\tau}_1^-$ on the other side.

6.2.2 MSSM with right-handed neutrinos

The sleptons are characterized by:

Particle	Mass/GeV	Width/GeV	U_{1j}	U_{2j}	U_{3j}	U_{4j}	U_{5j}	U_{6j}
$\tilde{l}_1^-$	176	0.507	1.00	-0.04	-0.06	0	0	0.01
$\tilde{l}_2^-$	175	0.492	0.07	0.86	0.51	0	0	-0.07
$\tilde{l}_3^-$	177	0.506	0.03	-0.51	0.85	0	0	-0.12
$\tilde{l}_4^-$	133	0.314	0	0	0	1	0	0
$\tilde{l}_5^-$	133	0.314	0	0	0	0	1	0
$\tilde{l}_6^-$	131	0.297	0	0	0.14	0	0	0.99

The slepton diagonalization matrix elements U_{ij} correspond to their definition in (3.21) with $j : 1, \ldots, 6$. It should be mentioned that we have chosen the form of U in the models with right-handed neutrinos so that the resulting

mass eigenstates are as close as possible to the gauge eigenstates in the basis $(\tilde{e}_L^-, \tilde{\mu}_L^-, \tilde{\tau}_L^-, \tilde{e}_R^-, \tilde{\mu}_R^-, \tilde{\tau}_R^-)$. This has the consequence that the largest elements of U in each row are the diagonal ones. In order to have a notion about the relative magnitude of the lepton flavor violating effects for different leptons, we use the term "direct" mixing i.e. mixing due to the single U-matrix element $U_{ij} \simeq |U_{ji}|$.
For further reference, this model is characterized as $\nu_R I$. It should be mentioned that in the $\nu_R I$, $\nu_R II$, $\nu_R III$ models the zero entries in rows and columns 4 and 5 for slepton mixing are exact, whereas the other "vanishing" (i.e.$<$ 0.005) slepton mixing elements can only be shown in their rounded form here.
As was expected, the matrix elements in the left-right mixing sector are rather small compared to the other scenarios. This is due to the fact that in the left-right sector the corrections from right-handed neutrinos actually vanish, so that the relative small left-right mixing of $MSSMI$ is not enhanced. The direct mixing U_{23} between $\tilde{\mu}_L^-$ and $\tilde{\tau}_L^-$ is much larger than the $\tilde{e}_L^-$-$\tilde{\mu}_L^-$-mixing or the $\tilde{e}_L^-$-$\tilde{\tau}_L^-$-mixing which are rougly of the same size.
The mass spectrum is very similar to the case of $MSSMI$.

6.2.3 SU(5) SUSY GUT with right-handed neutrinos

The charged sleptons are described in the following way:

	Mass/GeV	Width/GeV	U_{1j}	U_{2j}	U_{3j}	U_{4j}	U_{5j}	U_{6j}
$\tilde{l}_1^-$	176	0.507	0.99	0.05	-0.15	0	0	0.01
$\tilde{l}_2^-$	174	0.472	0.06	0.77	0.63	0	0	-0.06
$\tilde{l}_3^-$	176	0.493	0.15	-0.63	0.76	0	0	-0.07
$\tilde{l}_4^-$	133	0.314	0	0	0	0.99	0.14	0
$\tilde{l}_5^-$	133	0.314	0	0	0.01	-0.14	0.99	0.04
$\tilde{l}_6^-$	105	0.142	0	0	0.10	0.01	-0.04	0.99

We refer to this kind of model as $\nu_{R,GUT}I$. In this case there are no slepton mixing elements that exactly vanish, the zero values are only due to rounding. As in the previous model of scenario I, U-matrix elements of the left-right mixing sector are still quite suppressed compared to the other scenarios. Now we have a tiny direct mixing between $\tilde{e}_R^-$ and $\tilde{\tau}_R^-$ and the direct $\tilde{e}_R^-$-$\tilde{\mu}_R^-$ mixing is even larger than the respective one in the left-handed sector. The direct mixing between $\tilde{e}_L^-$ and $\tilde{\tau}_L^-$ is significantly larger than in the previous model and larger than the direct mixing of selectrons and smuons in the left-handed sector, too. The resulting slepton masses are comparable to the masses of the $MSSMI$ case with the exception of the lighter stau that has

more possibilities for mixing here.
For a model of SUSY SU(5) GUT with right-handed neutrinos only scenario 1 is considered, because in the other two scenarios a negative mass squared slepton would arise. This is a consequence of large left-right mixing terms in the respective slepton mass squared matrix [3].

6.3 Scenario II

The second scenario refers to supergravity parameters that cannot be checked at LEP2 [11], because most of the scalar particles are rather massive.
For the mentioned values of the SUSY parameters at the EW scale, the neutralinos are described as:

Particle	Mass/GeV	Width/GeV	N_{1j}	N_{2j}	N_{3j}	N_{4j}
$\tilde{\chi}_1^0$	74.8	0	0.82	-0.53	0.20	-0.064
$\tilde{\chi}_2^0$	133	0.0522	0.57	0.72	-0.34	0.18
$\tilde{\chi}_3^0$	273	1.26	-0.013i	0.16i	0.68i	0.71i
$\tilde{\chi}_4^0$	293	1.77	-0.063	-0.41	-0.61	0.68

In comparison to scenario I the zino-Higgsino-mixing is enlarged and the photino-zino-mixing is a bit reduced.
In this case the significant decay channels and their branching ratios are given as [11]:

Particle	Decay channel	BR
$\tilde{\chi}_1^0$		
$\tilde{\chi}_2^0$	$\tilde{\tau}_1^+\tau^-, \tilde{\tau}_1^-\tau^+$	0.50
$\tilde{\chi}_3^0$	$\tilde{\chi}_1^+W^-, \tilde{\chi}_1^-W^+$	0.27
	$\tilde{\chi}_2^0Z^0$	0.15
	$\tilde{\chi}_1^0Z^0$	0.28
	$\tilde{\tau}_1^+\tau^-, \tilde{\tau}_1^-\tau^+$	0.05
$\tilde{\chi}_4^0$	$\tilde{\chi}_1^+W^-, \tilde{\chi}_1^-W^+,$	0.26
	$\tilde{\chi}_2^0h^0$	0.09
	$\tilde{\chi}_1^0h^0$	0.06

Here the second lightest neutralino can decay via two-body decays into light stau and tau, other leptonic two-body decay modes are forbidden kinematically, because $\tilde{\chi}_2^0$ is lighter than the other sleptons.

6.3.1 MSSM

The charged sleptons have the following properties:

Particle	Mass/GeV	Width/GeV
$\tilde{e}_L^-$	216	1.02
$\tilde{\mu}_L^-$	216	1.02
$\tilde{\tau}_2^-$	209	0.839
$\tilde{e}_R^-$	183	0.614
$\tilde{\mu}_R^-$	183	0.615
$\tilde{\tau}_1^-$	92.8	0.0607

In this scenario (referred to as $MSSMII$), the mass differences as well as the stau left-right mixing angle resulting from the given electroweak parameters are:

$$\Delta_L^{13} = -22.5 \text{ GeV} \qquad \Delta_R^{13} = -61.7 \text{ GeV} \qquad \theta_{\tilde{\tau}} = -0.433$$

There are large mass differences between the staus and other sleptons due to the enhanced left-right mixing effects in the second scenario.

6.3.2 MSSM with right-handed neutrinos

The sleptons are described in the following way:

Particle	Mass/GeV	Width/GeV	U_{1j}	U_{2j}	U_{3j}	U_{4j}	U_{5j}	U_{6j}
$\tilde{l}_1^-$	217	1.03	0.99	-0.15	0.05	0	0	-0.02
$\tilde{l}_2^-$	214	0.984	0.16	0.82	-0.51	0	0	0.22
$\tilde{l}_3^-$	198	0.736	0.04	0.55	0.73	0	0	-0.40
$\tilde{l}_4^-$	184	0.621	0	0	0	1	0	0
$\tilde{l}_5^-$	184	0.621	0	0	0	0	1	0
$\tilde{l}_6^-$	90.9	0.0430	0	0.04	0.46	0	0	0.89

We refer to this model as $\nu_R II$.

In this case the right-handed staus are strongly coupled to the left-handed staus, because of the large U-elements U_{36} and U_{63}. But the direct $\tilde{e}_L^-$-$\tilde{\tau}_L^-$-mixing is rather small, comparable to $\nu_R I$. The direct $\tilde{e}_L^-$-$\tilde{\mu}_L^-$-mixing is of the same size as the direct mixing between $\tilde{e}_L^-$ and $\tilde{\tau}_L^-$ in the $\nu_{R,GUT}$ model. The masses are not very close to the mass spectrum in the $MSSMII$ case, especially $\tilde{l}_3^-$ becomes significantly lighter than $\tilde{\tau}_2^-$.

6.4 Scenario III

The mSUGRA parameters in this scenario lead to a light stop particle [12] with mass $m_{\tilde{t}_1} = 133$ GeV at the electroweak scale.
The neutralinos have the following properties:

Particle	Mass/GeV	Width/GeV	N_{1j}	N_{2j}	N_{3j}	N_{4j}
$\tilde{\chi}_1^0$	75.3	0	0.82	-0.56	0.12	-0.058
$\tilde{\chi}_2^0$	139	0.00137	0.57	0.79	-0.19	0.11
$\tilde{\chi}_3^0$	438	7.12	-0.0042i	0.072i	0.70i	0.71i
$\tilde{\chi}_4^0$	456	19.4	-0.022	-0.25	-0.68	0.69

In scenario 3 the mixing of both photino-Higgsino as well as the mixing of zino-Higgsino are reduced compared to the second scenario. The significant decay channels and the respective branching ratios read in the third scenario [12]:

Particle	Decay channel	BR
$\tilde{\chi}_1^0$		
$\tilde{\chi}_2^0$	$\tilde{\tau}_1^+\tau^-, \tilde{\tau}_1^-\tau^+$	0.42
$\tilde{\chi}_3^0$	$\tilde{t}_1\bar{t}, \bar{\tilde{t}}_1 t$	0.25
	$\tilde{\chi}_1^+W^-, \tilde{\chi}_1^-W^+$	0.16
	$\tilde{\chi}_2^0 Z^0$	0.12
	$\tilde{\chi}_1^0 Z^0$	0.05
$\tilde{\chi}_4^0$	$\tilde{t}_1\bar{t}, \bar{\tilde{t}}_1 t$	0.40
	$\tilde{\chi}_1^+W^-, \tilde{\chi}_1^-W^+$	0.06

In this scenario the two-body decays of $\tilde{\chi}_2^0$ into stau and tau are still predominant, but other leptonic deacy modes of the type slepton plus lepton are possible for the second lightest neutralino, too.

6.4.1 MSSM

In this case the sleptons have the following masses and widths:

Particle	Mass/GeV	Width/GeV
$\tilde{e}_L^-$	176	0.409
$\tilde{\mu}_L^-$	176	0.409
$\tilde{\tau}_2^-$	179	0.455
$\tilde{e}_R^-$	133	0.301
$\tilde{\mu}_R^-$	133	0.301
$\tilde{\tau}_1^-$	127	0.251

In this scenario (referred to as $MSSMIII$) the mass differences as well as the stau left-right mixing angle resulting from the given electroweak parameters are:

$\Delta_L^{13} = 0.009$ GeV $\qquad \Delta_R^{13} = -1.90$ GeV $\qquad \theta_{\tilde{\tau}} = -0.252$

The mass spectrum is similar to $MSSMI$, only the mass difference between the staus is a bit enlarged due to greater left-right mixing.

6.4.2 MSSM with right-handed neutrinos

The sleptons have the following properties:

Particle	Mass/GeV	Width/GeV	U_{1j}	U_{2j}	U_{3j}	U_{4j}	U_{5j}	U_{6j}
$\tilde{l}_1^-$	175	0.400	0.96	0.14	-0.24	0	0	0.07
$\tilde{l}_2^-$	151	0.115	0.06	0.74	0.56	0	0	-0.38
$\tilde{l}_3^-$	177	0.299	0.28	-0.64	0.69	0	0	-0.19
$\tilde{l}_4^-$	133	0.301	0	0	0	1	0	0
$\tilde{l}_5^-$	133	0.301	0	0	0	0	1	0
$\tilde{l}_6^-$	125	0.230	0.01	0.17	0.39	0	0	0.90

This model is called $\nu_R III$ for further reference. In this framework the direct mixing between $\tilde{e}_L^-$ and $\tilde{\tau}_L^-$ is enhanced compared to the other scenarios/models with right-handed neutrinos. Together with the facts that we have considerable left-right mixing here and that sleptons are typically lighter than in the second scenario, this leads us to the expectation of the largest cross sections for $e^-\tau^-$ as final leptons in $\nu_R III$. The direct $\tilde{e}_L^-$-$\tilde{\mu}_L^-$ mixing is not of the same size as the selectron-stau mixing in the left-handed slepton sector. In this model $\tilde{l}_2^-$ becomes significantly lighter than $\tilde{\mu}_L^-$ in the $MSSMIII$ case.
It should not be forgotten to mention that in all models with right-handed neutrinos the direct mixing between $\tilde{\mu}_L^-$ and $\tilde{\tau}_L^-$ is the largest one and could be tested at a future linear collider experiment with muons.

Chapter 7

Cross sections

All types of total cross sections or distributions presented in this chapter were computed numerically with Mathematica.

7.1 Total cross sections

7.1.1 Right-handed neutrino models

Helicity-specific total cross sections At first we want to give a survey of initial-helicity specific cross sections at a beam energy of 500 GeV. Of course the respective results of the initial helicity combination $\left(+\frac{1}{2},-\frac{1}{2}\right)$ equal those of the shown combination $\left(-\frac{1}{2},+\frac{1}{2}\right)$. In the column with σ_{max} we display results for the maximal cross sections that are obtained for polarized initial beams with $P_1 = P_2 = -0.80$.

The two tables (7.1, 7.2) show some general features concerning the cross sections of different models for each process:
As is expected from the remarks on the structure of the slepton diagonalization matrix U in the previous chapter, the smallest cross sections are obtained in the $\nu_R I$ model, whereas the $\nu_R III$ model delivers the largest cross sections. The cross sections in the $\nu_R II$ model are somewhere between these two extremes. Moreover the cross sections for the $\nu_{R,GUT} I$ model are larger in comparison to the $\nu_R I$ kind of model which has less possibilities for slepton mixing than the previous one. In the modes with opposite electron helicities the cross sections with two second lightest neutralinos outgoing are highly suppressed for all models.
Now we would like to compare the size of cross sections in different models for the processes $e^-e^- \to e^-\tau^- + 2\tilde{\chi}^0$ and $e^-e^- \to e^-\mu^- + 2\tilde{\chi}^0$, in each case with the same outgoing neutralinos and for beam energies sufficiently above

Products	Model	$\sigma_{-\frac{1}{2},-\frac{1}{2}}$/fb	$\sigma_{-\frac{1}{2},+\frac{1}{2}}$/fb	$\sigma_{+\frac{1}{2},+\frac{1}{2}}$/fb	σ_{max}/fb
$e^-\tau^-\tilde{\chi}_1^0\tilde{\chi}_1^0$	$\nu_R I$	0.34	0.28	0	0.32
	$\nu_R II$	1.19	0.75	0	1.10
	$\nu_R III$	34.08	19.36	0	31.09
	$\nu_{R,GUT} I$	1.19	1.00	0.19	1.15
$e^-\tau^-\tilde{\chi}_1^0\tilde{\chi}_2^0$	$\nu_R I$	1.40	0.54	0	1.23
	$\nu_R II$	4.08	0.82	0	3.46
	$\nu_R III$	64.02	14.50	0	54.46
	$\nu_{R,GUT} I$	5.14	2.09	$< 10^{-4}$	4.54
$e^-\tau^-\tilde{\chi}_2^0\tilde{\chi}_2^0$	$\nu_R I$	1.45	$< 10^{-4}$	0	1.18
	$\nu_R II$	3.05	0.01	0	2.48
	$\nu_R III$	28.87	0	0	23.39
	$\nu_{R,GUT} I$	5.52	$< 10^{-3}$	$< 10^{-6}$	4.47

Table 7.1: Helicity-specific total cross sections for $e^-e^- \rightarrow e^- + \tau^- + 2\tilde{\chi}^0$ at $\sqrt{s} = 500$ GeV

Products	Model	$\sigma_{-\frac{1}{2},-\frac{1}{2}}$/fb	$\sigma_{-\frac{1}{2},+\frac{1}{2}}$/fb	$\sigma_{+\frac{1}{2},+\frac{1}{2}}$/fb	σ_{max}/fb
$e^-\mu^-\tilde{\chi}_1^0\tilde{\chi}_1^0$	$\nu_R I$	0.49	0.41	0	0.47
	$\nu_R II$	2.21	1.37	0	2.04
	$\nu_R III$	14.37	8.16	0	13.11
	$\nu_{R,GUT} I$	0.64	0.53	$< 10^{-3}$	0.61
$e^-\mu^-\tilde{\chi}_1^0\tilde{\chi}_2^0$	$\nu_R I$	2.18	0.90	0	1.93
	$\nu_R II$	10.30	3.19	0	8.92
	$\nu_R III$	32.08	8.99	0	27.60
	$\nu_{R,GUT} I$	2.82	1.18	$< 10^{-6}$	2.50
$e^-\mu^-\tilde{\chi}_2^0\tilde{\chi}_2^0$	$\nu_R I$	2.42	$< 10^{-3}$	0	1.96
	$\nu_R II$	12.00	0.03	0	9.72
	$\nu_R III$	17.90	0	0	14.50
	$\nu_{R,GUT} I$	3.12	$< 10^{-3}$	0	2.53

Table 7.2: Helicity-specific total cross sections for $e^-e^- \rightarrow e^- + \mu^- + 2\tilde{\chi}^0$ at $\sqrt{s} = 500$ GeV

the threshold region:
For the $\nu_R I$ model we see that the cross section for $e^-e^- \rightarrow e^-\mu^- + 2\tilde{\chi}^0$ is larger than that for $e^-e^- \rightarrow e^-\tau^- + 2\tilde{\chi}^0$. This relation is mainly due to the

fact that the direct mixing between $\tilde{e}_L^-$ and $\tilde{\mu}_L^-$ is a bit greater than the direct $\tilde{e}_L^- - \tilde{\tau}_L^-$- mixing. In this model the left-right mixing is almost negligible and thus cannot enlarge the cross section in the case of $e^-\tau^-2\tilde{\chi}^0$ considerably.
For the $\nu_R II$ model the direct mixing of $\tilde{e}_L^-$ and $\tilde{\mu}_L^-$ is enlarged, so that we expect that the ratio of cross sections of the processes $e^-\tau^- + 2\tilde{\chi}^0$ and $e^-\mu^- + 2\tilde{\chi}^0$ is reduced in comparison to the $\nu_R I$ case. But without the considerable left-right mixing in the second scenario, the rate for $e^-\tau^- + 2\tilde{\chi}^0$ would be even smaller. The suppression of the propagation of heavy sleptons (see 4.84) reduces the size of the cross sections.
For the $\nu_R III$ model the situation is reversed: Here the direct mixing between $\tilde{e}_L^-$ and $\tilde{\tau}_L^-$ is considerably greater than that of $\tilde{e}_L^-$ and $\tilde{\mu}_L^-$. In this model there is smuon and stau left-right mixing of comparable size that does not alter the fact that the cross sections for $e^-\tau^- + 2\tilde{\chi}^0$ are about a factor of two larger than that for $e^-\mu^- + 2\tilde{\chi}^0$.
In case of the $\nu_{R,GUT} I$ model we see that, differently from the $\nu_R I$ model, the cross section for $e^-\tau^- + 2\tilde{\chi}^0$ is greater than for the process $e^-\mu^- + 2\tilde{\chi}^0$. The main reason for this relation is that now the direct mixing between $\tilde{e}_L^-$ and $\tilde{\tau}_L^-$ is considerably larger than that for $\tilde{e}_L^-$ and $\tilde{\mu}_L^-$. The $\nu_{R,GUT} I$ model is the only one with non-vanishing, but relative small cross sections for incoming electrons of positive helicity, because in this model there is a tiny mixing of sleptons in the right-handed sector.

Beam energy-dependent total cross sections Now we want to make some remarks about the form of the unpolarized total cross sections in figures 7.2 and 7.1:
The threshold of the total cross section is determined by the kinematical constraint (5.22) for production and (5.29) for every decay. Before $\sigma(\sqrt{s})$ steeply ascends to its maximum value, there is typically a kind of more or less marked bend. This bend is the result of the propagation and the decay of relative light sleptons predominantly composed of right-handed states. These lighter sleptons can already be produced for beam energies that do not suffice to produce sleptons that mainly consist of left-handed states. However the signal of those lighter sleptons is considerably smaller than that from the heavier ones, because the greatest slepton mixing elements are typically in the left-handed sector. The position of the maximum value of the total cross section is basically determined by the conditions that the beam energy suffices to produce sleptons that consist mainly of left-handed states and that the denominator of the production propagator is as small as possible. The descent of $\sigma(\sqrt{s})$ for high energies in the $\nu_R II$ model is more gradually than in the other models, because in $\nu_R II$ there are heavier sleptons which are

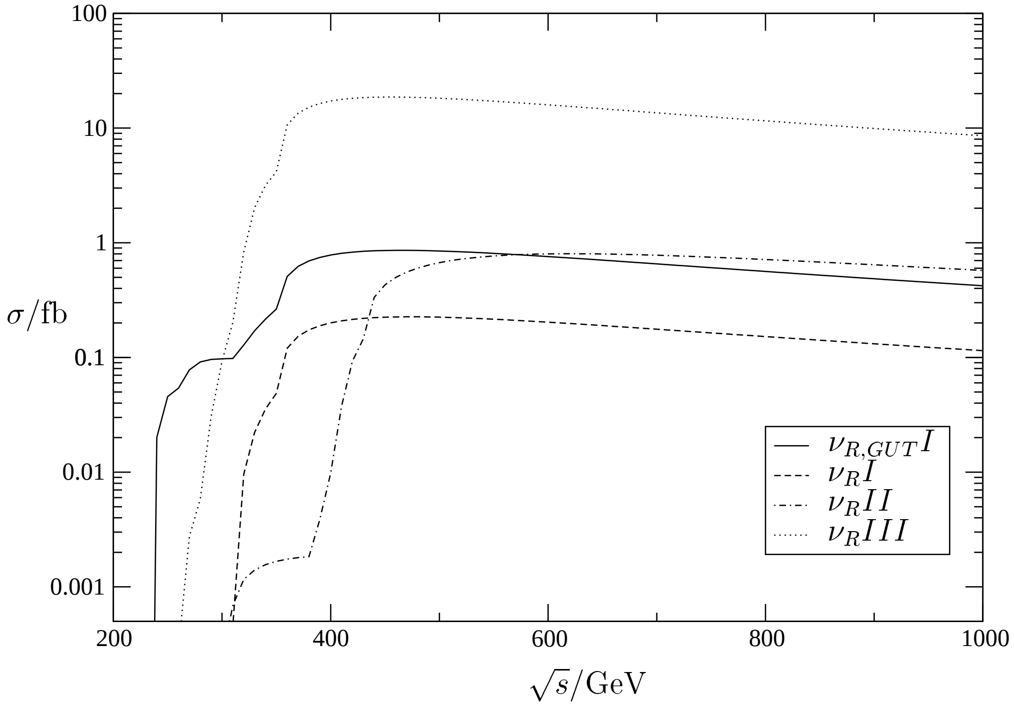

Figure 7.1: Total cross sections (unpolarized) as a function of the beam energy for the process $e^- e^- \to e^- \tau^- \tilde{\chi}_1^0 \tilde{\chi}_1^0$

preferrably produced for high beam energies.
For the cases of outgoing $\tilde{\chi}_1^0 \tilde{\chi}_2^0$ or $\tilde{\chi}_2^0 \tilde{\chi}_2^0$, the form of the curves is similar as in the production of two LSPs, only the kinematical constraints (5.22) and (5.29) result in a shift of the threshold to higher energies. This shift is more marked for $\tilde{\chi}_2^0 \tilde{\chi}_2^0$ than for $\tilde{\chi}_1^0 \tilde{\chi}_2^0$.

τ^--helicity asymmetry We can connect the τ^--helicity asymmetry A_τ^{hel}, defined on page 45, to the ratio of cross sections with τ^- of negative or positive helicity:

$$\frac{\sigma_{\tau_{-1/2}}}{\sigma_{\tau_{+1/2}}} = \frac{1 + A_\tau^{hel}}{1 - A_\tau^{hel}}$$

From the earlier discussion concerning the form of $\sigma(\sqrt{s})$ we know that for lower beam energies the propagating sleptons are relative light and are mainly composed of right-handed states. These lighter sleptons are responsible for the region of τ^--helicity asymmetry around -1 for small $\sqrt{s}$-values, because then LFV is mainly induced by the coupling of right-handed staus to left-handed sleptons through left-right mixing and lepton flavor mixing. As soon

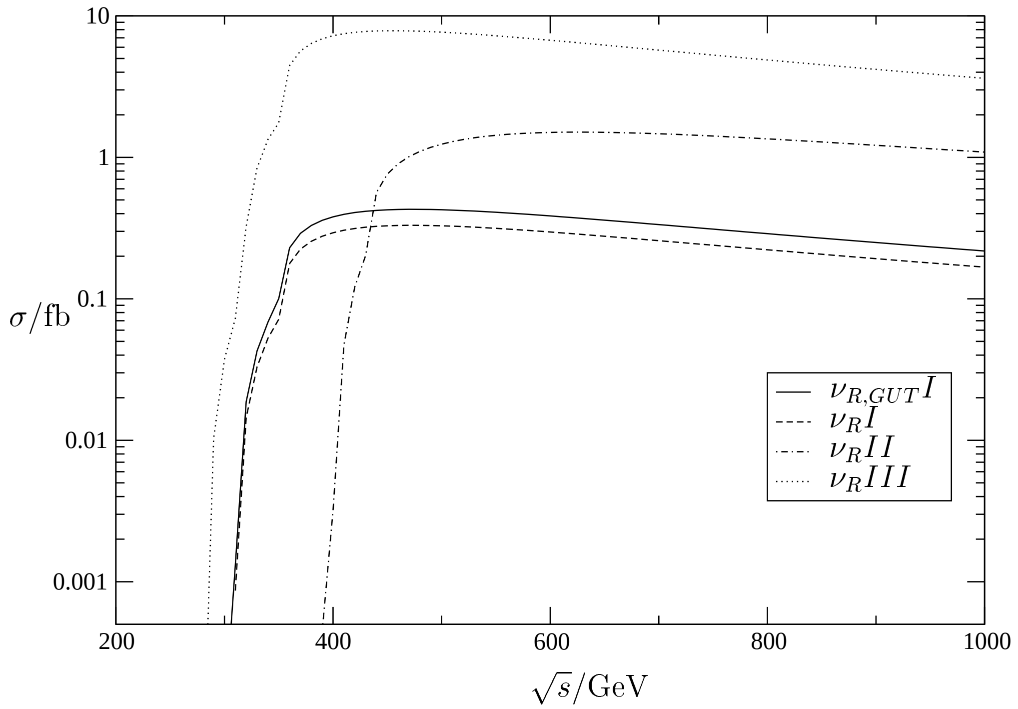

Figure 7.2: Total cross sections (unpolarized) as a function of the beam energy for the process $e^-e^- \to e^-\mu^-\tilde{\chi}_1^0\tilde{\chi}_1^0$

as the beam energy suffices to produce heavier sleptons consisting predominantly of left-handed states, the sign of A_τ^{hel} switches its sign. This is due to the fact that the greatest contribution to LFV comes from the left-handed slepton sector in all models. However left-right mixing results in an admixture of right-handed sleptons whose propagation is less suppressed than that of heavier sleptons. The splitting of the values of A_τ^{hel} can be understood as a consequence of the strength of the respective left-right mixing. The stronger the left-right mixing contributions, the greater is the admixture of left-handed sleptons for low energies, and the greater is the admixture of propagation-wise preferred right-handed sleptons for high energies. It should however be mentioned that the cross sections for low beam energies are considerably smaller than that for higher beam energies so that one can only expect to measure τ^--helicity asymmetries in the latter case.
In the $\nu_{R,GUT}I$ model there is LFV in the pure right-handed slepton sector. For this model the contribution to LFV through left-handed slepton states grows gradually for increasing $\sqrt{s}$, because the heavier sleptons are kinematically more suppressed for smaller beam energy compared to lighter sleptons mainly composed of right-handed states.

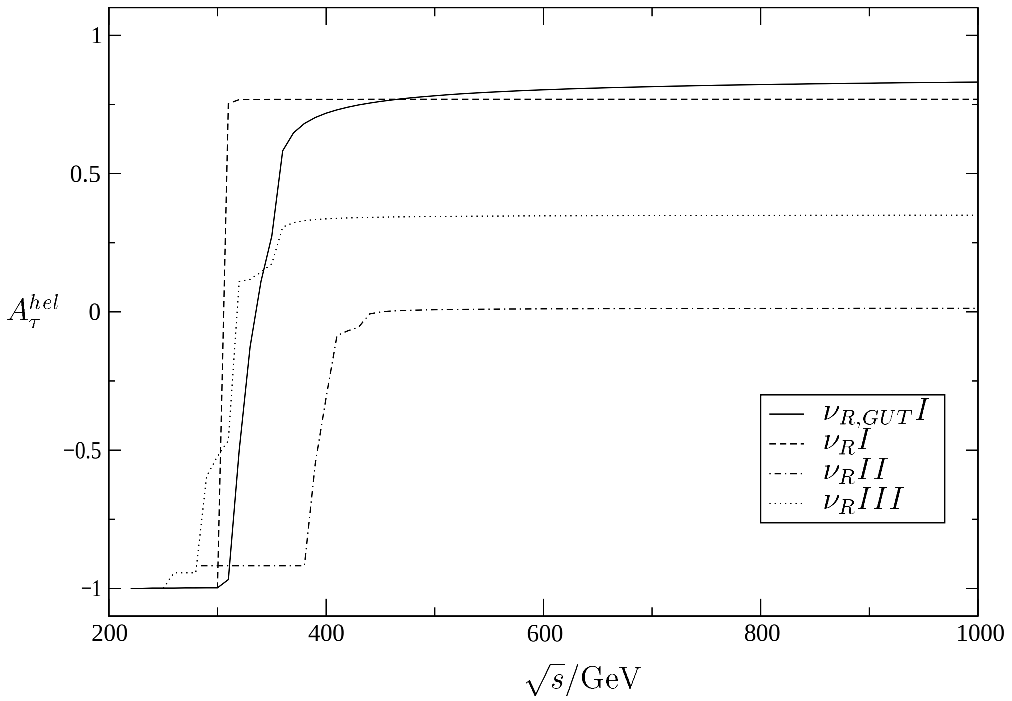

Figure 7.3: τ^- helicity asymmetry as a function of the beam energy for unpolarized beams in the process $e^-e^- \to e^-\tau^-\tilde{\chi}_1^0\tilde{\chi}_1^0$

7.1.2 MSSM

In this section we want to examine the parameter dependence of the total cross section at $\sqrt{s} = 500$ GeV on the flavor mixing angle ϕ and on the relevant mass difference in the MSSM models. For each of the three scenarios we separately consider LFV in the left- or right-handed slepton sector and the possible mixing between selectrons and smuons or selectrons and staus. The flavor mixing angle runs through the values from 0 to $\frac{\pi}{2}$, whereas the respective mass difference runs between $\Delta - 5$ GeV, $\ldots, \Delta + 5$ GeV, with the values for Δ given in the sections with MSSM scenario parameters. We use the sleptonic widths of the MSSM sections in chapter 6 for this relative small mass intervall for the sleptons.

Selectron-smuon mixing At first we consider selectron-smuon mixing in the process $e^-e^- \to e^-\mu^-\tilde{\chi}_1^0\tilde{\chi}_1^0$:
The given numbers of contours in figures (7.4, 7.5) are easily transferred to the other contour lines, because the cross sections are approximately symmetric with respect to $\Delta^{12} = 0$ for the examined relative small mass interval.

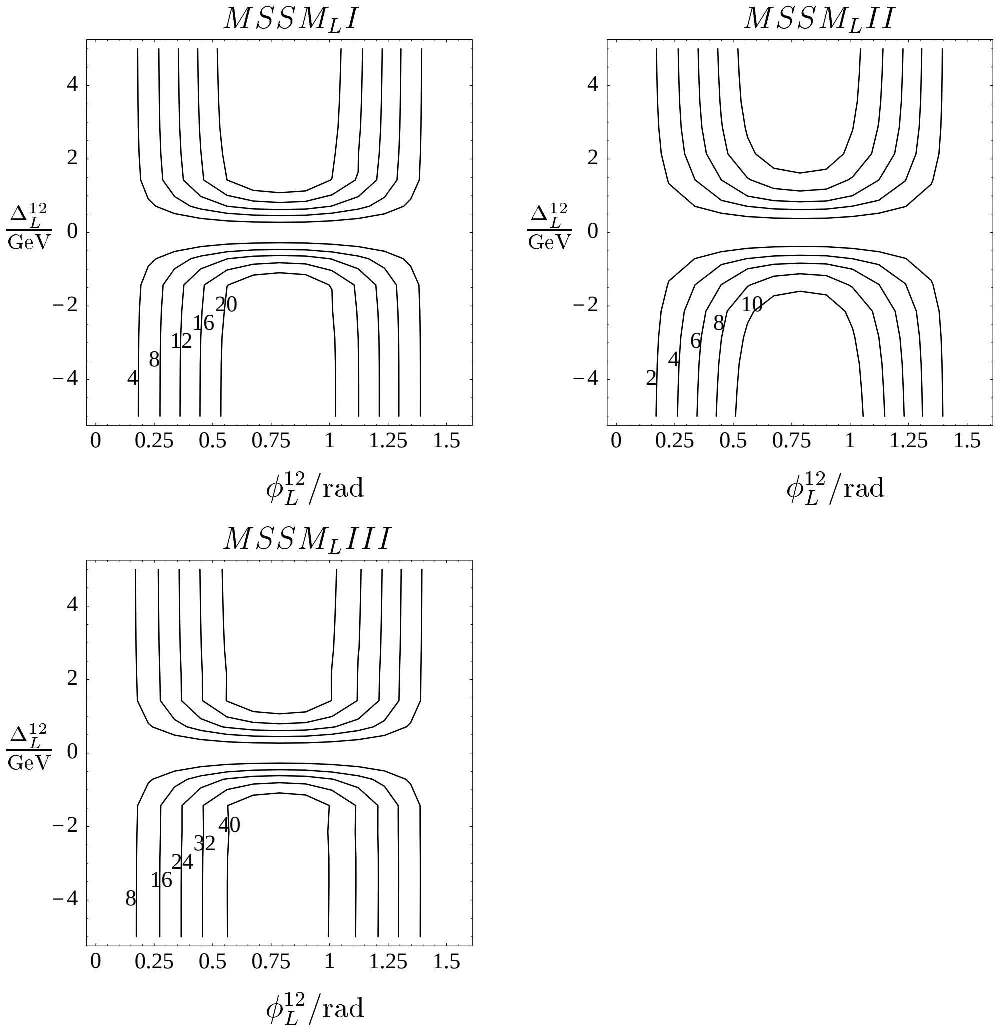

Figure 7.4: Contours of unpolarized total cross sections in fb for the process $e^-e^- \to e^-\mu^-\tilde{\chi}_1^0\tilde{\chi}_1^0$ with LFV in the left-handed slepton sector ($\sqrt{s} = 500$ GeV)

In this case left-right mixing is decoupled from selectron-smuon mixing, so that the dependence on the mixing parameters of section 3.5 for the total squared amplitude is applied to the total cross section in a good approximation. The relative sizes of cross sections for fixed ϕ^{12} and Δ^{12} in different scenarios are (for this kinematical parameters) predominantly determined by the suppression factors (4.84) in the slepton propagators: Looking at the respective MSSM parameters, one sees that the products of mass and total width for the sleptons of the first two generations are smallest for the

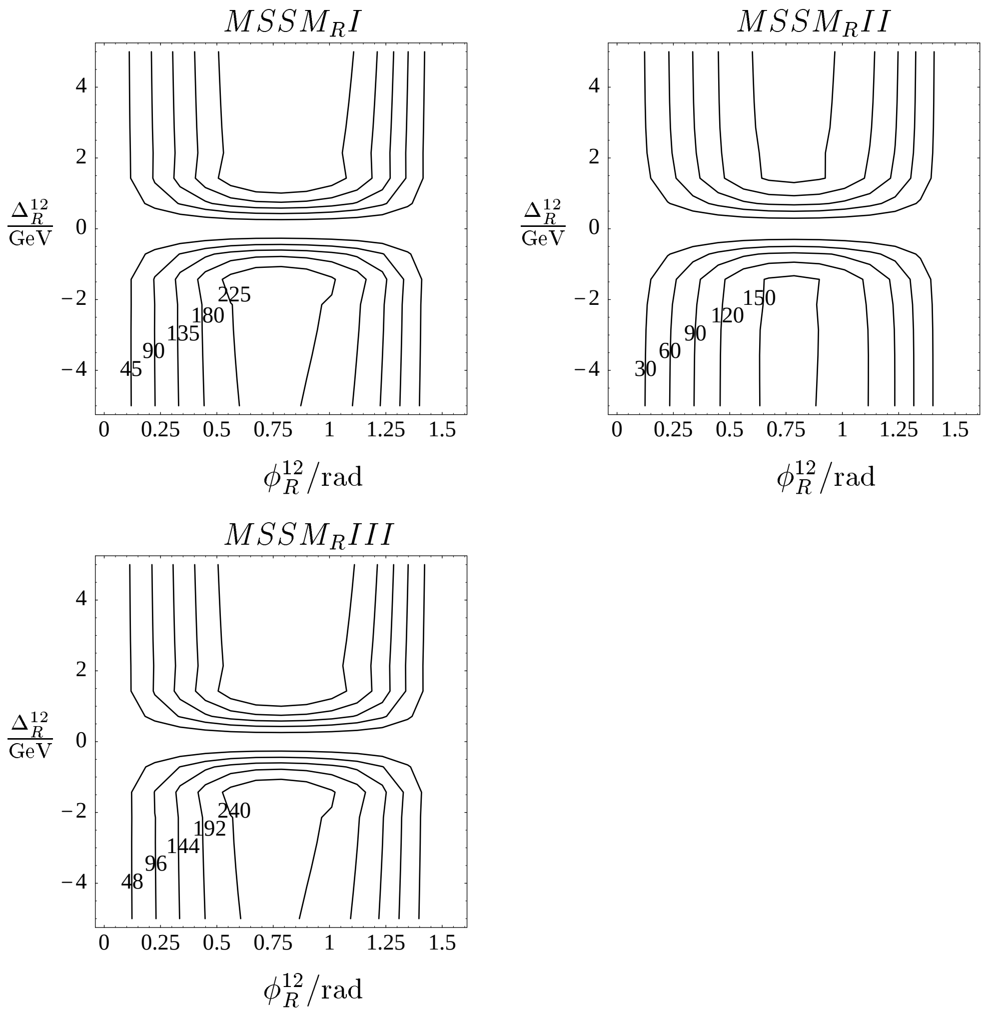

Figure 7.5: Contours of unpolarized total cross sections in fb for the process $e^-e^- \to e^-\mu^-\tilde{\chi}_1^0\tilde{\chi}_1^0$ with LFV in the right-handed slepton sector ($\sqrt{s} = 500$ GeV)

third scenario and greatest for the second scenario. Therefore one expects the largest cross sections for $MSSMIII$ and the smallest cross sections for $MSSMII$.
The fact that the cross sections are more suppressed for LFV in the left-handed slepton sector than for LFV in the right-handed sector is in accordance with the stronger suppression of the propagation of heavier sleptons.

Selectron-stau mixing Now we want to consider selectron-stau mixing where left-right mixing of different strength modifies the contour lines in figures 7.6 and 7.7 for the three scenarios in comparison to the cases of selectron-smuon mixing. The symmetry of the contour lines with respect to $\frac{\pi}{2}$ is basically maintained in the case of selectron-stau mixing.

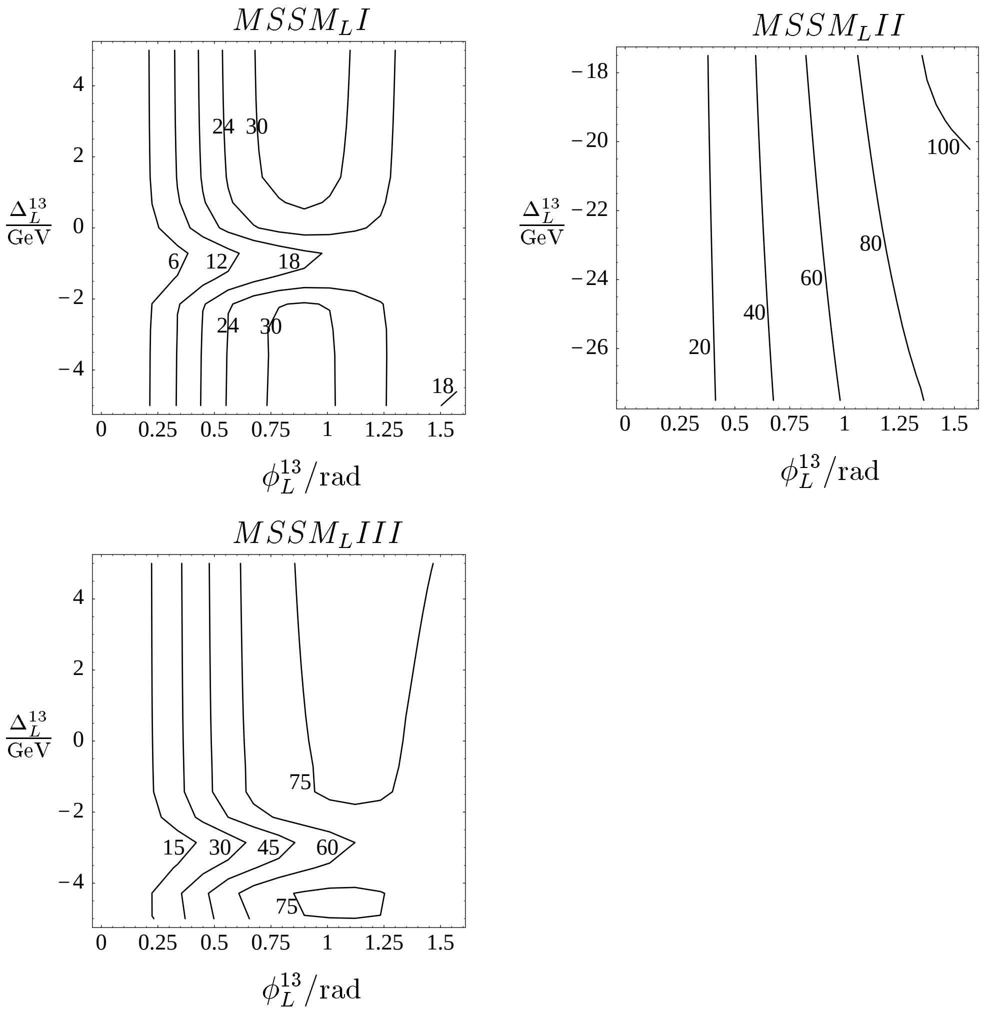

Figure 7.6: Contours of unpolarized total cross sections in fb for the process $e^-e^- \to e^-\tau^-\tilde{\chi}_1^0\tilde{\chi}_1^0$ with LFV in the left-handed slepton sector ($\sqrt{s}$ = 500 GeV)

In the $MSSM_L I$ model the respective contours of selectron-smuon mixing are not so strongly deformed as in the other scenarios due to the weak left-right mixing here. Nevertheless the cross section does not vanish in

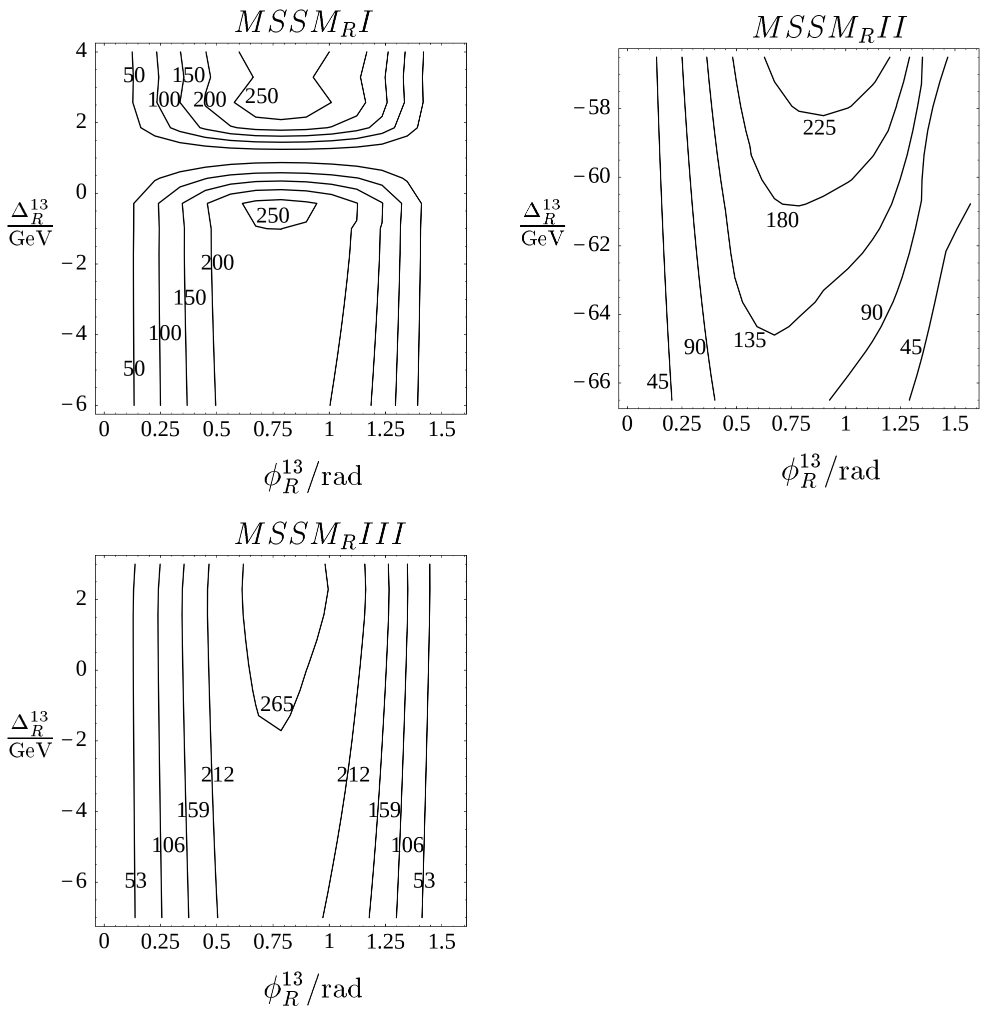

Figure 7.7: Contours of unpolarized total cross sections in fb for the process $e^-e^- \to e^-\tau^-\tilde{\chi}_1^0\tilde{\chi}_1^0$ with LFV in the right-handed slepton sector ($\sqrt{s} = 500$ GeV)

the limit $\Delta_L^{13} \to 0$, we can see a relative weak "indentation" of σ around $\Delta_L^{13} \sim -1$ GeV. In this region of Δ_L^{13} the cross section assumes its smallest value for arbitrary ϕ_L^{13} i.e. roughly $\frac{1}{2}$ of the maximal cross section over the whole parameter space.

In the $MSSM_R I$ model the contribution of the left-handed sleptons is more suppressed kinematically, so that the left-right mixing effects should be even smaller than in the $MSSM_L I$ model. The "indentation" is thus stronger as in the latter case: The cross section for $\Delta_R^{13} \sim 1$ GeV is only a factor of about $\frac{1}{25}$ of the maximal cross section over the whole parameter space.

Examining selectron-stau mixing in the second scenario, we realize that the similarity to $\tilde{e}^-$-$\tilde{\mu}^-$-mixing is lost due to large left-right mixing effects and very large mass differences.
In the case of $MSSM_LII$ the strong left-right mixing leads to a dominant contribution of the kinematically preferred right-handed sleptons, so that the $\sin^2(2\phi_L^{13})$-behavior concerning the slepton mixing angle gets totally smeared out.
In the $MSSM_RII$ model the cross section decreases again for $\phi_R^{13} \to \frac{\pi}{2}$, but left-right mixing contributions and the huge mass difference distort the well-known behavior of $\sigma \to 0$ for $\phi_R^{13} \to \frac{\pi}{2}$.

The $MSSM_LIII$ model is similar to the $MSSM_LI$ case, but the ratio of the maximal cross section in the "indentation" around $\Delta_L^{13} \sim -3$ GeV to the maximal cross section of the whole parameter space is around 0.8. This relative large ratio is basically due to stronger left-right mixing contributions, also in the "indentation" region.
In the $MSSM_RIII$ model we see roughly a similar behavior concerning the ϕ_R^{13} dependence as in $MSSM_RI$. However the "indentation" region for specific Δ_R^{13} is shifted out of the considered parameter region.

7.2 Distributions

We study distributions for the process $e^-e^- \to e^-\tau^-\tilde{\chi}_1^0\tilde{\chi}_1^0$ at a beam energy of $\sqrt{s} = 500$ GeV with unpolarized beams. This process has the basic signature $e^-\tau^- + \not{E}$, because the lightest neutralino $\tilde{\chi}_1^0$ is the stable LSP in all our scenarios. In the actual collider experiment, the τ^--lepton is typically identified via its decay products and the properties of the final electron can be measured accurately.
In order to compare the specific forms of the distributions in different models and scenarios, we normalize the distributions with respect to the respective total and unpolarized cross section. The beam helicity-dependent cross sections for the process have already been given in table 7.1 and the unpolarized total cross sections for $\sqrt{s} = 500$ GeV can easily be obtained:

Model	ν_RI	ν_RII	ν_RIII	$\nu_{R,GUT}I$
σ/fb	0.22	0.67	18.20	0.85

Angular distributions At first we consider the form of the forward-backward symmetric angular distributions of the electron in figure (7.8):

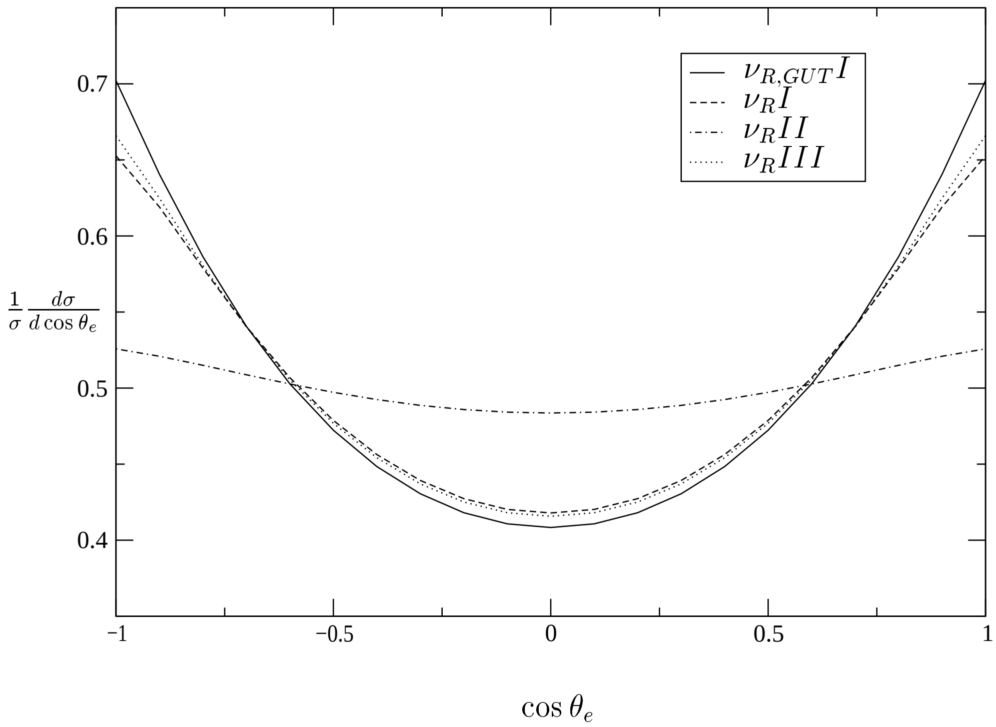

Figure 7.8: Normalized electron angle distributions for $\sqrt{s} = 500$ GeV, unpolarized beams

This symmetry is the result of the overlap of the contributions of the forward peaked t-channel (for $e = l$ in (5.81)), the inverted backward peaked u-channel, the forward-backward symmetric production interference channel and the boost of the produced slepton in its forward direction. The greater the boost factor, the steeper are the angular distributions. Therefore the resulting angular distributions are "sharper peaked" for large beam energies and light sleptons, whereas the angular distributions are "flatter" for small beam energy and heavy sleptons. For a fixed beam energy of 500 GeV the decisive factor is the mass of the boosted sleptons. For this reason the $\nu_R II$ model has a flatter normalized angular distribution than the other models. The latter have nearly the same sleptonic mass spectrum with the exception of the lightest slepton that is predominantly composed of the right-handed stau state and thus does not contribute very much to the cross sections. However the $\nu_{R,GUT}I$ is the right-handed neutrino model with the steepest angular electron distribution what we can trace back to the small slepton mixing in the right-handed sector in the case of $\nu_{R,GUT}I$ absent in the other

models.
The τ^-- angular distributions have been examined, too. These are almost identical to the angular electron distributions for the respective model. There is only a slight tendency that the τ^-- angular distributions are a little "flatter" than that of the electron. For the outgoing electrons this implies that there are a bit more contributions from lighter sleptons of the right-handed sector that couple to right-handed electrons (incoming and outgoing).

Energy distributions The step form of the electron energy distributions in figure (7.9) is a result of the fact that the E_e-distribution (5.58) assumes constant values as long as the relevant kinematical parameters fulfill (5.59). The basic reason for this behavior is that we boost the constant electron energy values in the respective decay frame of an on-shell slepton. Without this narrow-width approximation for the sleptons the electron energy distributions would be more continously. The interval of possible electron energy values (5.59) is strongly dependent on the velocity of the intermediate sleptons: The greater the velocity of the sleptons, the broader is the possible energy interval.

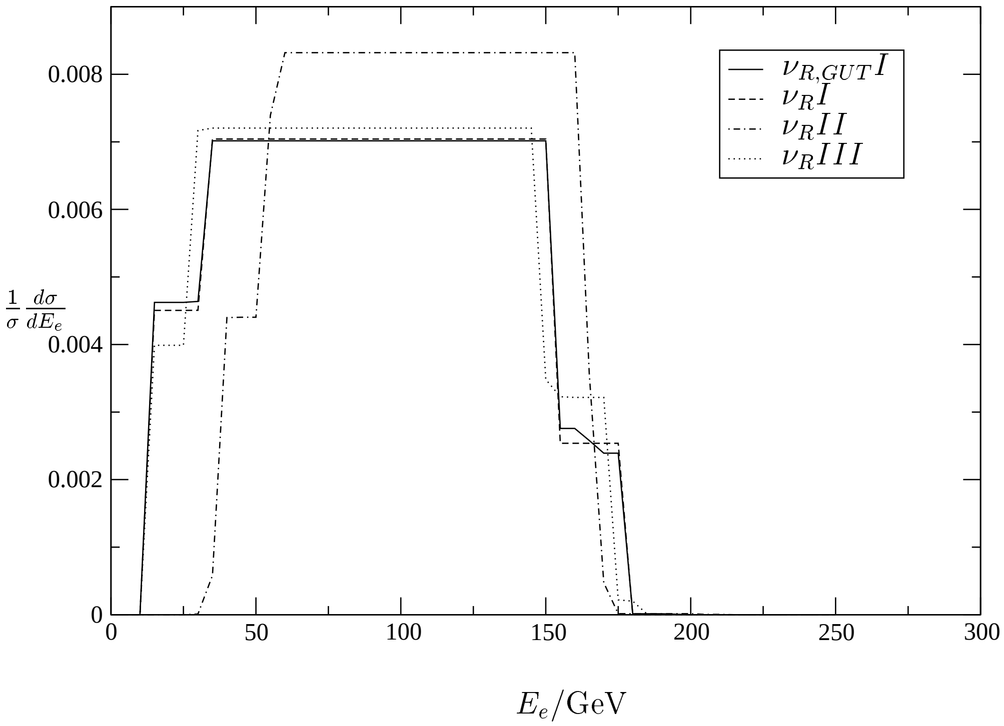

Figure 7.9: Normalized electron energy distributions in units of $(\mathrm{GeV})^{-1}$ for $\sqrt{s} = 500$ GeV, unpolarized beams

This is the reason why the normalized electron energy distribution in the $\nu_R II$ model is concentrated in a more narrow energy interval in comparison to the other models where the contributing sleptons are lighter. The extension of the electron energy distribution to the double differential lepton energy distributions of figure (7.10) is straightforward, because the relevant phase space factor is a product of the single lepton energy distributions. Due

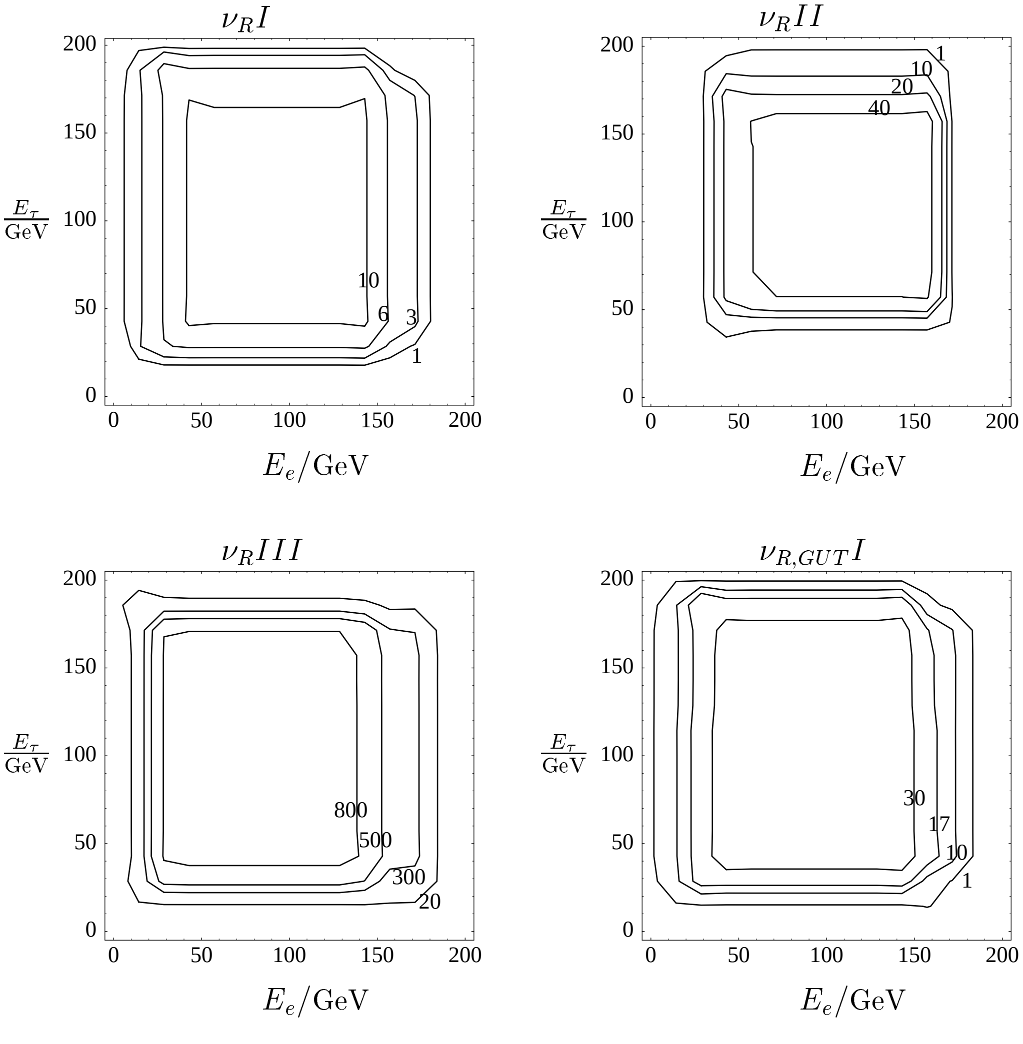

Figure 7.10: Contours for double energy differential cross sections in units of $\frac{10^{-6}\mathrm{fb}}{(\mathrm{GeV})^2}$ for $\sqrt{s} = 500$ GeV, unpolarized beams

to the higher masses of contributing sleptons in the $\nu_R II$ scenario, the range of the double lepton energy distribution is more narrow in both energy directions than in the case of the other models. The start point of the tau energy distribution is shifted to higher energies than in the electron case. This is a result of the fact that the rest energies i.e. masses of the contributing sleptons in (5.59) are a little higher than in the case of an outgoing electron where we have a greater contribution from lighter, right-handed selectron states. To obtain the missing energy distributions of figure (7.11) we have to integrate over the cuboid-like double differential energy distribution: As

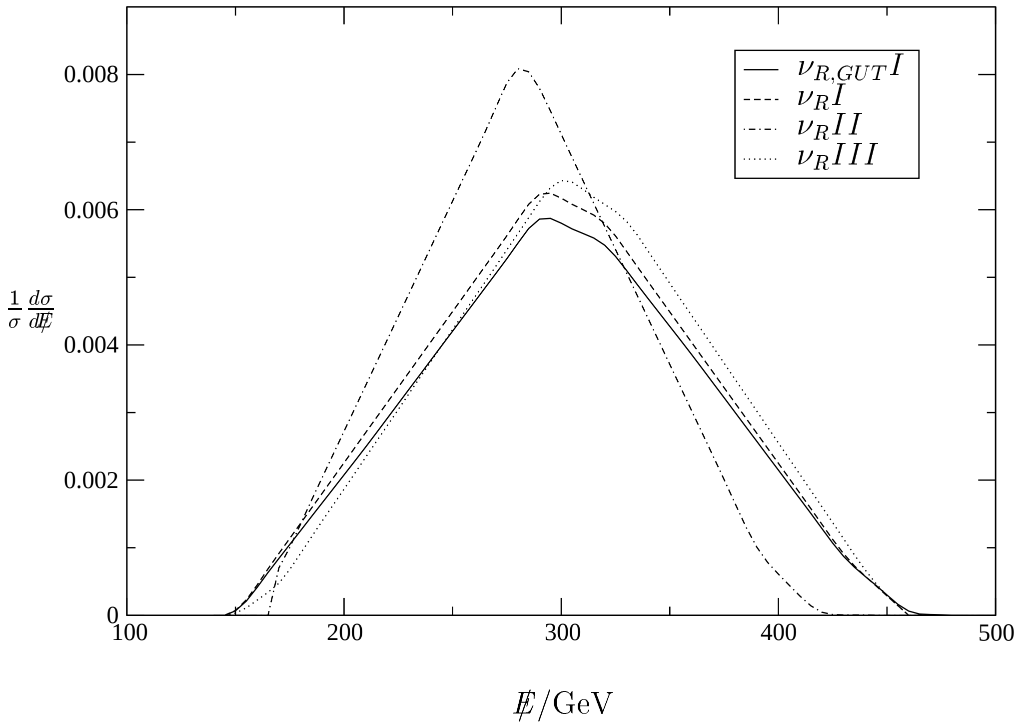

Figure 7.11: Normalized missing energy distributions in units of $(\mathrm{GeV})^{-1}$ for $\sqrt{s} = 500$ GeV, unpolarized beams

indicated by (5.64), we integrate for each value of the missing energy over the decreasing energy variable $\sqrt{s} - \not{E} - E_{l'}$ in the first "direction" of the energy in $\frac{d^2\sigma}{dE_l dE_{l'}}$ and, at the same time over the increasing energy variable $E_{l'}$ in the other energy "direction". The size of the "volume" one integrated over determines the magnitude of the missing energy distribution. With this idea in mind it is clear that the necessary integration for small or large values of $\not{E}$ only passes through the double differential energy distribution at its rim regions, whereas for some medium $\not{E}$-value the integration passes through the greatest area of the middle region of the "cuboid" with the largest differential cross sections, thus yielding a maximum value for the missing energy distribution. The missing energy distributions are nearly symmetric around their maxima, because the contours of the double differential energy distribution are almost symmetric, too. As the energy range of the double differential energy distribution is smaller in the $\nu_R II$ model than in the other models, the resulting normalized missing energy distribution is more compressed in the former model.

Energy-angle distributions The possible regions of $(\cos\theta_e, E_e)$-values in the energy-angle distributions of figure (7.12) are determined by (5.98).

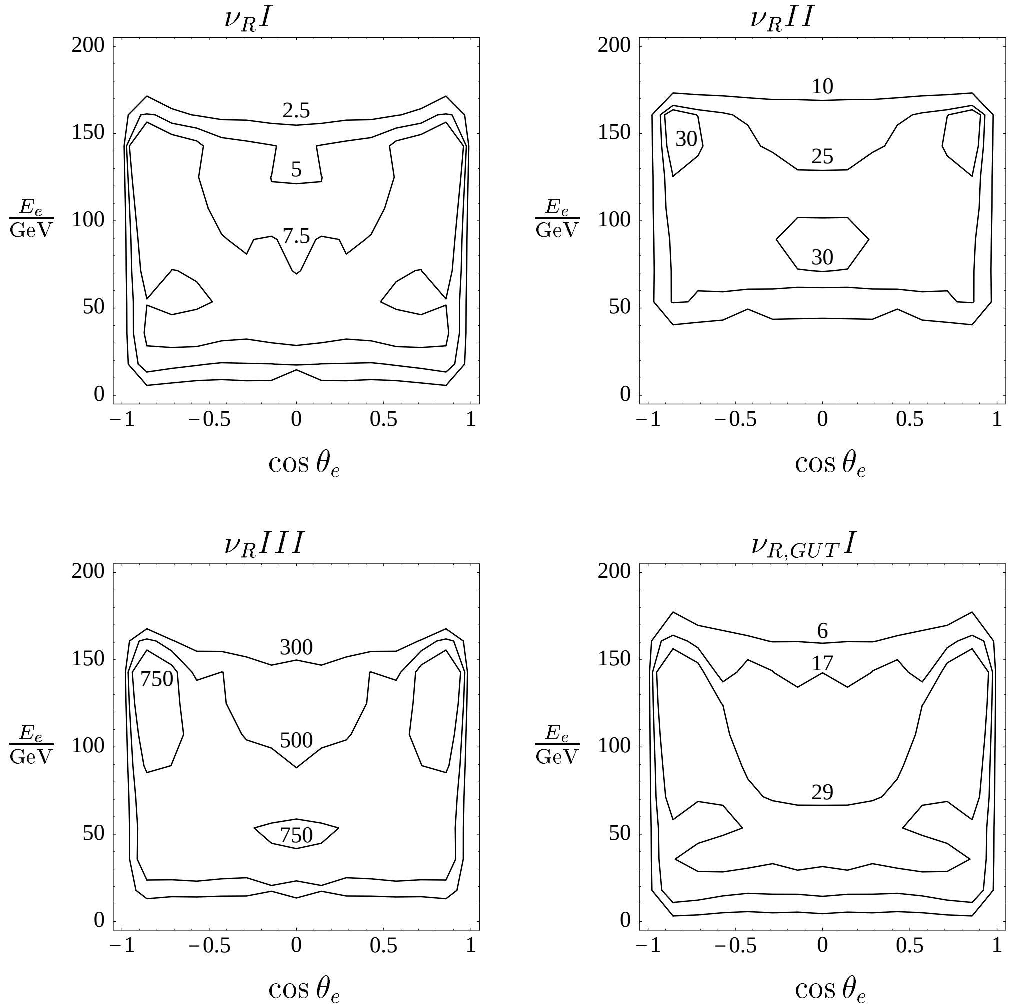

Figure 7.12: Contours for energy-angle differential cross sections in units of $\frac{10^{-4}\mathrm{fb}}{(\mathrm{GeV})}$ at $\sqrt{s} = 500$ GeV, unpolarized beams

The region of high transverse momentum values lies near $\cos\theta_e = \pm 1$ and relative high energy values. The $\frac{1}{\sin\theta_e}$-factor in (5.102) even stresses the contribution of the region near $\cos\theta_e = \pm 1$ for the $p_e^{\perp}$-distribution. The kinematical region for $\frac{d^2\sigma}{dE_e d\cos\theta_e}$ is shifted to higher electron energy values in $\nu_R II$ in comparison to the other models. This leads to an electron transverse momentum distribution that is shifted to higher $p_e^{\perp}$-values in the case of $\nu_R II$, see (7.13).

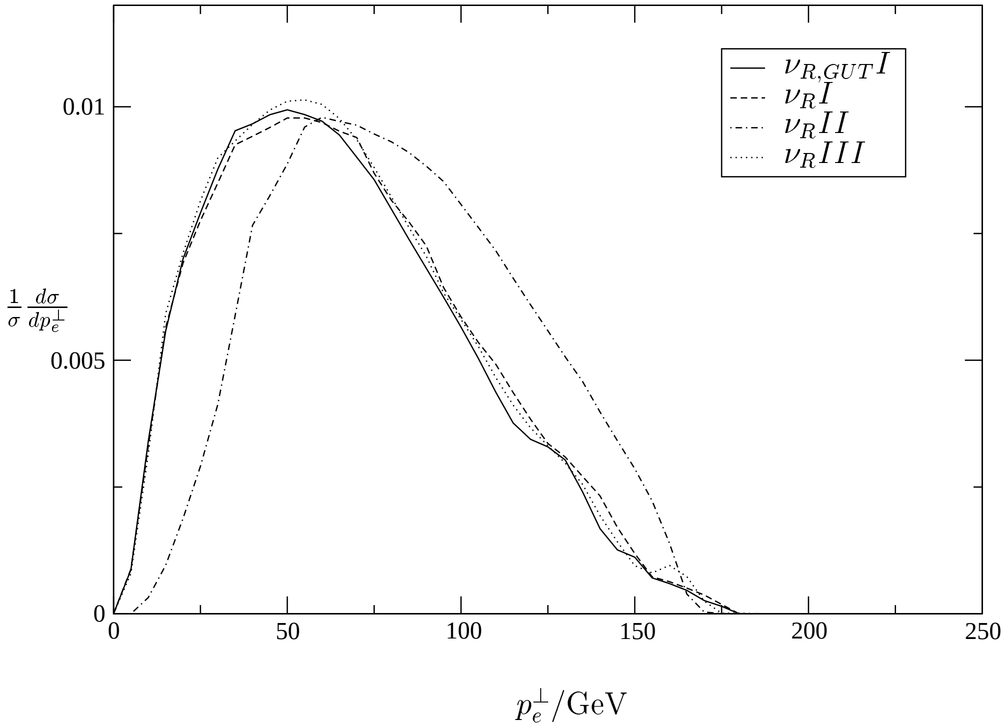

Figure 7.13: Normalized electron transverse momentum distributions in units of $(\mathrm{GeV})^{-1}$ for $\sqrt{s} = 500$ GeV, unpolarized beams

Chapter 8

Background processes

There are two Standard Model background processes fitting for $e^-e^- \to e^-\tau^- + 2$ fermions that have to be taken into account:

1. $e^-e^- \to e^-\nu_e\tau^-\overline{\nu}_\tau$

2. $e^-e^- \to e^-e^-\tau^-\tau^+$

For a real background study however one has to be precise about what really would be measured in either case. For example, the LFV signal $e^-\tau^-\chi_1^0\chi_1^0$ with the lightest neutralinos as LSP can only be detected as $e^-\tau^-$ plus missing energy and has the first mentioned SM background process as a real background from an experimental point of view. The second process given above can however be distinguished from $e^-\tau^- + \not{E}$. But things become more complicated if heavier neutralinos are produced that can decay in various ways, even into leptons. In order to compare such kind of signals to the respective SM background, one really has to go into detail concerning the particle phenomenology of the models.
For a cms energy of about 500 GeV one can have five additional background processes without LFV in the MSSM without R-parity violation:

1. $e^-e^- \to e^-\tau^-\tilde{\nu}_e\overline{\tilde{\nu}_\tau}$

2. $e^-e^- \to e^-\tau^-\tilde{e}_2^-\tilde{\tau}_2^+$

3. $e^-e^- \to e^-\tau^-\tilde{e}_1^-\tilde{\tau}_2^+$

4. $e^-e^- \to e^-\tau^-\tilde{e}_2^-\tilde{\tau}_1^+$

5. $e^-e^- \to e^-\tau^-\tilde{e}_1^-\tilde{\tau}_1^+$

But all of these additional background reactions produce short-lived sleptons, so that these processes do not contribute to the signal $e^- \tau^- + \not{E}$.
For our background calculations we consider the SM background process $e^- e^- \rightarrow e^- \nu_e \tau^- \overline{\nu}_\tau$ that has the same basic signal $e^- \tau^- + \not{E}$ as our "main process".
This background reaction is characterized by the following lowest-order diagrams:

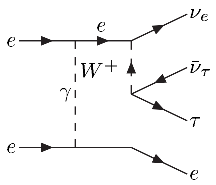

diagr.1

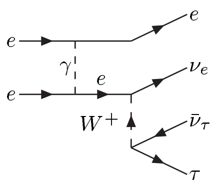

diagr.2

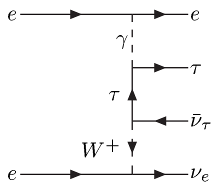

diagr.3

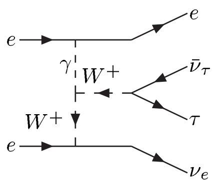

diagr.4

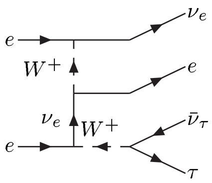

diagr.5

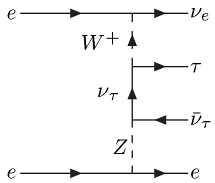

diagr.6

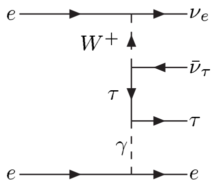

diagr.7

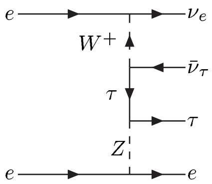

diagr.8

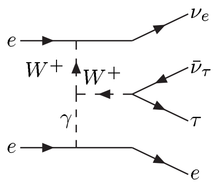

diagr.9

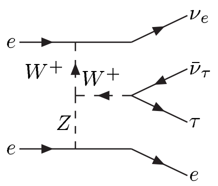

diagr.10

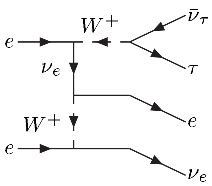

diagr.11

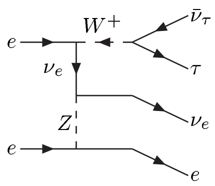

diagr.12

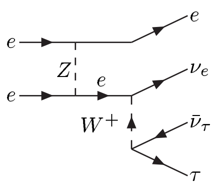

diagr.13

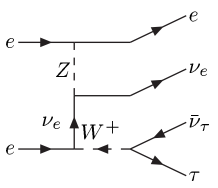

diagr.14

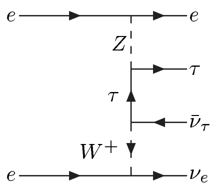

diagr.15

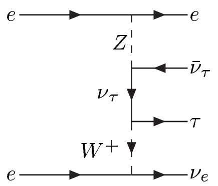

diagr.16

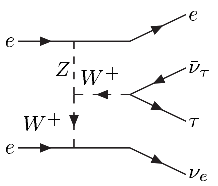

diagr.17

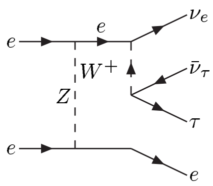

diagr.18

Due to the geometry of the collider any signal that is nearer to the beam pipe than $|\cos\theta| \leq 0.98$, cannot be detected [20]. This fact imposes a kind of minimal angle cut in beam direction: $|\cos\theta| \leq 0.98$
For any SM background consideration we have to incorporate this cut into the phase space. A cut in $|\cos\theta_e|$ is even necessary to render the background diagrams 1, 2, 3, 4, 7 and 9 finite. These diagrams connect one incoming and outgoing electron via photon exchange. For the limit of $|\cos\theta_e| \to 0$ or no momentum transfer to the photon, the corresponding photon propagator terms would become singular.
The distributions and the total cross section for the background process were computed using the Comphep code for the lowest-order diagrams shown above. For the results on lepton flavor violating signals we used Mathematica. At first we want to give the results for the total cross sections for unpolarized beams at $\sqrt{s} = 500$ GeV with the angle cut $|\cos\theta_e| \leq 0.98$:

	$\nu_R I$	$\nu_R II$	$\nu_R III$	$\nu_{R,GUT} I$	Background
σ/ fb	0.22	0.66	17.72	0.82	91.13

As for the signal distributions we again use the normalized distributions to compare the peculiar form of the background distributions with that of the signal.

Angular electron distributions The normalized angular electron distribution of the background in figure (8.1) is a lot steeper, i.e. more peaked in forward-backward direction than the angular distributions of the signal. This is a consequence of the fact that there is less momentum transfer to virtual

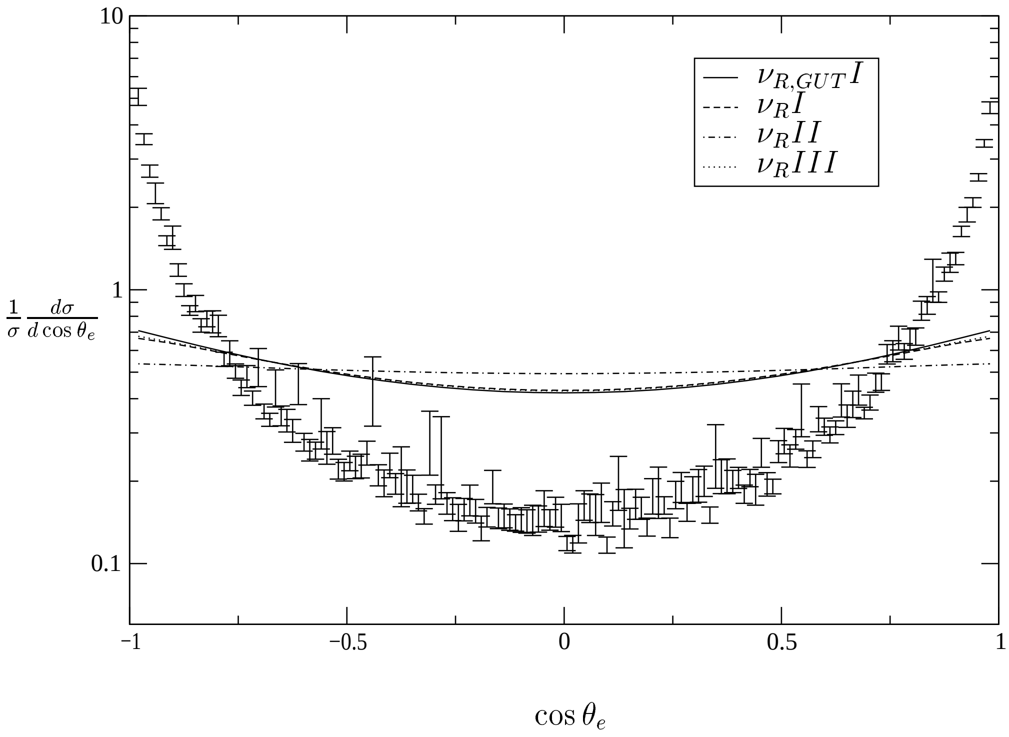

Figure 8.1: Normalized electron angle distributions for $\sqrt{s} = 500$ GeV, unpolarized beams; background with error bars

and intermediate particles for the background than for the signal. The heaviest particles in an intermediate state are the W-bosons, the heavier Z-bosons appear as virtual particles. But the virtual/intermediate particles do not have to be on their mass shells, so that the momentum transfer to intermediate particles can be much smaller for the background than for the signal. For the latter the intermediate sleptons are, with the possible exception of the lightest slepton, considerably heavier than the Z-bosons. In our calculation the sleptons are explicitly put on-shell, so that the momentum transfer to the intermediate particles is much greater than for the background. The tendency that the angular distributions are flatter for more massive particles in the intermediate state can also be seen in the signal distributions, where the angular distribution in the $\nu_R II$ model is considerably flatter than those of the other models.
These considerations suggest an angular cut for large angles in the form $|\cos\theta_e| \leq 0.75$ to us, so that the background to signal ratio is reduced.

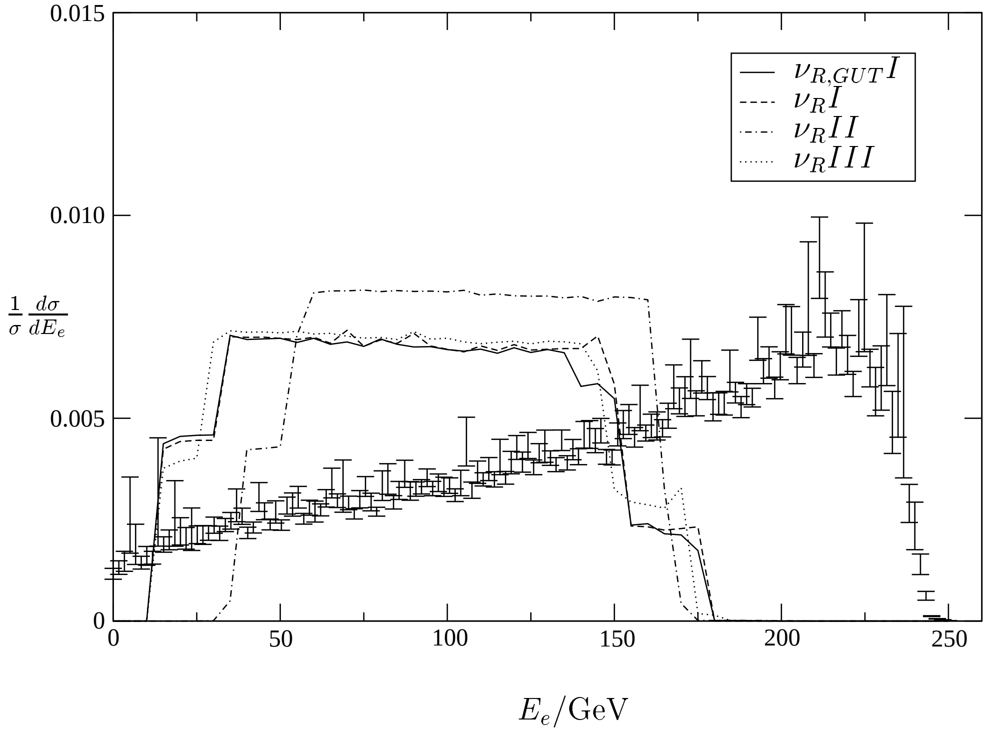

Figure 8.2: Normalized electron energy distributions in units of $(\mathrm{GeV})^{-1}$ for $\sqrt{s} = 500$ GeV, unpolarized beams; background with error bars

Electron energy distributions Concerning the normalized electron energy distribution (see figure 8.2) of the background one should keep in mind that all of the final particles are practically massless in this case. Therefore almost the whole beam energy is used for the energies of the outgoing particles. But for the signal around 140 GeV up to 150 GeV of the beam energy are “lost” for the energies of the outgoing particles, because this amount of energy is necessary to put the outgoing LSPs on their mass shells. This is the reason for $\frac{d\sigma}{dE_e}$ of the signal ending at a considerably smaller energy value than the electron energy distribution of the background. This behavior suggests a cut in the background electron energy distribution at $E_e = 180$ GeV that does not affect the signal.

The background electron energy distribution is maximal for E_e-values around 220 GeV. There are large contributions of the diagrams with photon exchange between incoming and outgoing electron to this maximum of $\frac{d\sigma}{dE_e}$, because there is typically only a small momentum transfer to the photon in these processes, so that the outgoing electron obtains almost the whole energy of the photon-scattered incoming electron.

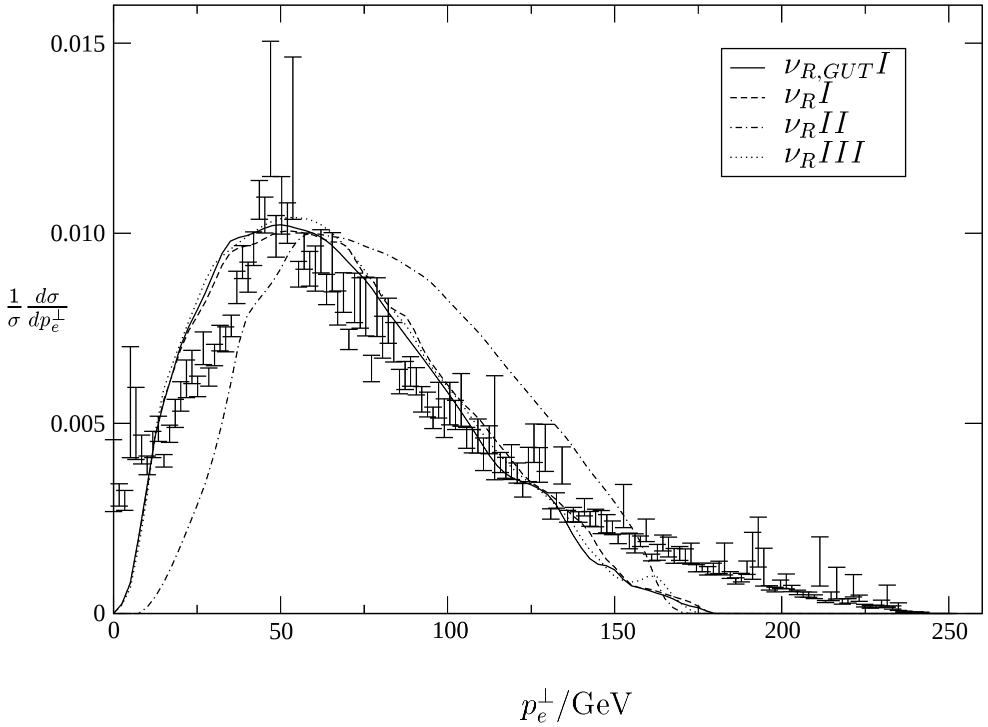

Figure 8.3: Normalized electron transverse momentum distributions in units of $(\mathrm{GeV})^{-1}$ for $\sqrt{s} = 500$ GeV, unpolarized beams; background with error bars

Electron transverse momentum distributions A similar argument as for the range of the electron energy distribution of the background holds for the background electron transverse momentum distribution: Almost the whole beam energy is distributed among the energies of outgoing particles, so that higher $p_e^\perp$-values can be reached than for the signal. But the $\frac{d\sigma}{dp_e^\perp}$-distribution is rather reduced for high $p_e^\perp$-values, as are the processes with large momentum transfer that lead to high $p_e^\perp$-values.

Realizing a greater cut As already mentioned, we expect to reduce the background to signal ratio by imposing a reasonable angular cut in the form of $|\cos\theta_e| \leq 0.75$ that also affects the signal. A energy cut of $E_e \leq 180$ GeV and a transverse momentum cut $p_e^\perp \leq 180$ GeV do not reduce our signal rate at all and thus are very suitable for a further reduction of the background to signal ratio.

With these three cuts, we obtained the following total cross sections for unpolarized beams at $\sqrt{s} = 500$ GeV:

	$\nu_R I$	$\nu_R II$	$\nu_R III$	$\nu_{R,GUT} I$	Background
σ fb	0.16	0.50	12.62	0.58	26.25

With these cuts, the possible signals are reduced by a factor of about 1.4 compared to the possible signal events by applying a minimal cut of $|\cos\theta_e| \leq 0.98$, whereas the background events are reduced by a factor of 3.5. There seems a good opportunity that signals of the $\nu_R III$ model could be discovered, whereas the possible signals of the other models with right-handed neutrinos are rather suppressed compared to the SM-background.
It should not be forgotten that the cross sections of a lepton flavor violating signal can be enlarged by a factor of about 1.5, when one uses initial electron beams with polarization -0.80, as shown in table 7.1.

Chapter 9

Summary

As long as the supersymmetric particle spectrum remains undiscovered, there is a great number of free parameters in supersymmetric models. In this work we have considered different supersymmetric models in a mSUGRA framework. The discussion of cross sections for lepton flavor violating processes has shown that the expected signals are highly model-dependent.
For the case of the MSSM we want to emphasize the following: Lepton flavor violating entries in the slepton mass matrix are not fixed a priori. Therefore one cannot even roughly estimate the expected cross sections at highest energies right now. One expects to measure SUSY processes without LFV before such events with LFV, because the latter ones are more suppressed. If the supersymmetric particle spectrum is actually measured in non-lepton flavor violating reactions, one can use the spectrum to clear up lepton flavor conserving MSSM mass matrix entries at the electroweak scale. With a later observation of LFV, off-diagonal elements in these matrices or equivalently flavor mixing angles can be derived gradually. Of course one has to measure different transitions between lepton generations to reveal the possible flavor mixing angles. A possible non-observation of lepton flavor violating processes would lead to upper limits on flavor mixing angles or off-diagonal elements in the slepton mass matrix.
Concerning the framework of supersymmetric models with right-handed neutrinos we want to stress the following general results: Once we fix the necessary new parameters in these models, we obtain specific values for cross sections and distributions. But these new parameters include the parameters of the neutrino mixing phenomena and very high energy scales, namely the mass scale of the right-handed neutrinos, the scale of unification of the gauge coupling constants and the Planck scale. Therefore we are very sensitive to neutrino mixing phenomena and very high energy scales in these models. But especially the absolute masses of the neutrinos, the solution of

the solar neutrino anomaly and the theoretical mass scale of right-handed neutrinos are uncertain, so that predictions of the supersymmetric models with right-handed neutrinos have to be considered carefully. All of the examined models with right-handed neutrinos have in common that a beam energy of about 500 GeV would suffice to produce lepton flavor violating signals above the kinematical threshold for slepton pair production. For the process $e^-e^- \to e^-\tau^-\tilde{\chi}_1^0\tilde{\chi}_1^0$ the right-handed neutrino model $\nu_R III$ yields the largest cross sections. These relative large cross sections are within the same order of magnitude as the SM background reaction $e^-e^- \to e^-\tau^-\nu_e\bar{\nu}_\tau$. Due to large mixing between smuons and staus we expect relative great cross sections for processes like $\mu^-\mu^- \to \mu^-\tau^-\tilde{\chi}_1^0\tilde{\chi}_1^0$ that could be measured in muon-muon scattering. Moreover it has been shown that a signal can be studied in a much more extensive way if one exhausts the possibilities of initial beam polarization and if one is able to measure helicity asymmetries of an outgoing τ^--lepton: By gradually varying the polarization of the initial electron beams one is able to enhance or weaken the contributions of the different electron helicity combinations. When one studies the coupling of the initial helicity modes to the slepton sectors, one gets a clue from which slepton sector the main contribution to a lepton flavor violating signal comes. By examining the τ^--helicity asymmetry for different beam energies one can get information which slepton sector is predominant for varying beam energy. The Standard Model background of the discussed "main process" $e^-e^- \to e^-\tau^-\tilde{\chi}_1^0\tilde{\chi}_1^0$ can be considerably reduced by reasonable cuts. Moreover it has been shown that a lepton flavor violating signal produced with unpolarized electron beams can be enlarged by highly polarized beams.
Finally there seems to be a good possibility to measure events at a beam energy of 500 GeV in the case of large or medium lepton flavor violating mixing. An identification of very rare events due to small lepton flavor violating mixing might be possible with enough effort. A combination of theoretical, phenomenological and experimental studies of lepton flavor violating processes will remain a very attractive field for physics beyond the Standard Model.

Acknowledgements

Here I want to express my gratitude towards the following people for help throughout the last year:
Dr. Shimizu was always a helpful and competent address for theoretical problems concerning supersymmetric theories. The continous discussions with Frank Deppisch were constructive and helped to clear up many details. These two collaborators deserve an extra thanks for proofreading my script. Professor Rückl always tried to ensure that this Diploma thesis did not go in the wrong direction.
Last but not least I do not want to forget useful discussions with other people of this working group.

Appendix A

Integration formulas

Here we want to give analytical results for the integration over the production angle that can be applied for the calculation of total cross sections or energy-distributions. In these cases, the only θ-dependent factor comes from the absolute squared production amplitude that has to be integrated over $\sin\theta d\theta$. Every squared production helicity amplitude has an explicit θ-dependence that arises through the propagator terms (4.56, 4.57). When we square the production amplitude, we can get the following types of propagators:

$$\frac{1}{(t-m_j)(t-m_{j'})} \tag{A.1}$$

$$\frac{1}{(t-m_j)(u-m_{j'})} \tag{A.2}$$

$$\frac{1}{(u-m_j)(u-m_{j'})} \tag{A.3}$$

These propagators correspond to t-, interference- and u-channel production, respectively. Inserting the explicit form of the mandelstam variables t and u in the cms frame of reference (4.56, 4.57) shows that we can write the propagator terms in the squared production amplitudes in the following form:

$$\frac{1}{a \pm b\cos\theta + c\cos^2\theta} \tag{A.4}$$

The coefficients a, b and c each depend on $\sqrt{s}$, s_1, s_2 and a also depends on the masses of the exchanged neutralinos. If one has a close look at the propagator terms of t- and u-channel (A.1), (A.3), it is clear that their only differences are the exchanged effective squared masses s_1, s_2 and the sign before the b-coefficient. For production helicities $(+\frac{1}{2},+\frac{1}{2})$ and $(-\frac{1}{2},-\frac{1}{2})$, one has to solve an integral of the form I_1 or I_1'.

$$I_1 = \int_0^\pi \frac{\sin\theta d\theta}{a + b\cos\theta + c\cos^2\theta} = \int_{-1}^1 \frac{du}{a+bu+cu^2}. \tag{A.5}$$

$$I_1 = \frac{2}{\sqrt{4ac-b^2}}\left(\arctan\frac{2c+b}{\sqrt{4ac-b^2}} - \arctan\frac{-2c+b}{\sqrt{4ac-b^2}}\right)$$
$$\text{for } 4ac - b^2 \geq 0, \tag{A.6}$$

$$I_1 = -\frac{2}{\sqrt{b^2-4ac}}\left(Artanh\frac{2c+b}{\sqrt{b^2-4ac}} - Artanh\frac{-2c+b}{\sqrt{b^2-4ac}}\right)$$
$$\text{for } 4ac - b^2 < 0. \tag{A.7}$$

$$I_1' = \int_0^\pi \frac{\sin\theta d\theta}{a - b\cos\theta + c\cos^2\theta} = \int_{-1}^1 \frac{du}{a-bu+cu^2}. \tag{A.8}$$

$$I_1' = \frac{2}{\sqrt{4ac-b^2}}\left(-\arctan\frac{-2c+b}{\sqrt{4ac-b^2}} + \arctan\frac{2c+b}{\sqrt{4ac-b^2}}\right)$$
$$\text{for } 4ac - b^2 \geq 0, \tag{A.9}$$

$$I_1' = -\frac{2}{\sqrt{b^2-4ac}}\left(-Artanh\frac{-2c+b}{\sqrt{b^2-4ac}} + Artanh\frac{2c+b}{\sqrt{b^2-4ac}}\right)$$
$$\text{for } 4ac - b^2 < 0, \tag{A.10}$$

so that $I_1 = I_1'$.
In the case of $(-\frac{1}{2}, +\frac{1}{2})$ and $(+\frac{1}{2}, -\frac{1}{2})$ production helicities, there is an additional factor of $\sin^2\theta$ for the production amplitudes. Here the integral over the production angle can be written in the form I_2 or I_2':

$$I_2 = \int_0^\pi \frac{\sin^3\theta d\theta}{a + b\cos\theta + c\cos^2\theta} = \int_{-1}^1 \frac{(1-u^2)\,du}{a+bu+cu^2} \tag{A.11}$$

$$= I_1 + \int_1^{-1} \frac{u^2 du}{a+bu+cu^2} \tag{A.12}$$

$$= I_1 + \left[\frac{u}{c}\right]_1^{-1} - \frac{b}{2c^2}\left[\ln(a+bu+cu^2)\right]_1^{-1}$$
$$-\frac{b^2-2ac}{2c^2}\underbrace{\int_{-1}^1 \frac{du}{a+bu+cu^2}}_{I_1}$$

$$= I_1\left(1 - \frac{b^2-2ac}{2c^2}\right) - \frac{2}{c} - \frac{b}{2c^2}\ln\left(\frac{a-b+c}{a+b+c}\right) \tag{A.13}$$

$$
\begin{aligned}
I_2' &= \int_0^{\pi} \frac{\sin^3\theta d\theta}{a - b\cos\theta + c\cos\theta} = \int_{-1}^{1} \frac{(1-u^2)\,du}{a - bu + cu^2} && \text{(A.14)}\\
&= I_1 + \int_1^{-1} \frac{u^2 du}{a - bu + cu^2} && \text{(A.15)}\\
&= I_1\left(1 - \frac{b^2 - 2ac}{2c^2}\right) - \frac{2}{c} + \frac{b}{2c^2}\ln\left(\frac{a+b+c}{a-b+c}\right), && \text{(A.16)}
\end{aligned}
$$

so that $I_2 = I_2'$. The integrals I_1, I_1', I_2 and I_2' have been solved with the help of [16]

Integral over azimuthal angle of production In order to integrate over the azimuthal angle of production for the angular distributions, the following integration formula was used [19]:

$$
I_3 = \int_0^{2\pi} \frac{d\phi}{\left(a + b\cos\left(\phi_l - \phi\right)\right)^2} = \frac{2\pi a}{(a+b)^{3/2}(a-b)^{3/2}} \qquad \text{(A.17)}
$$

Appendix B

Spherical Trigonometry

For the description of the angular distribution of the outgoing leptons we have to consider the angles from a spherical trigonometry point of view. The derivation of the mathematical results can be found in [7]. We consider a general spherical triangle with sides a, b, c and angles α, β, γ:

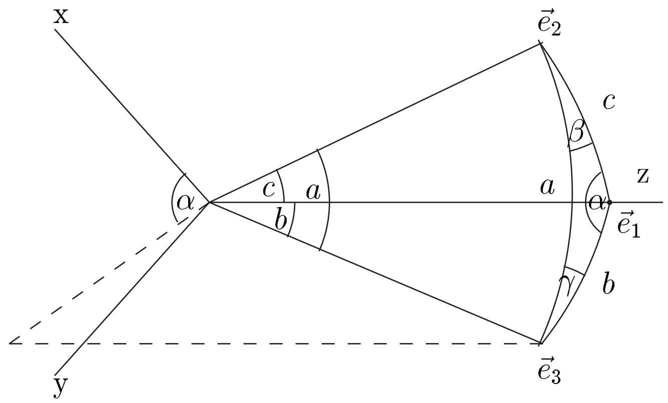

The unit vectors to the corners of the triangle are

$$\begin{aligned} \vec{e}_1 &= (0, 0, 1) \\ \vec{e}_2 &= (\sin c, 0, \cos c) \\ \vec{e}_3 &= (\sin b \cos \alpha, \sin b \sin \alpha, \cos b). \end{aligned} \tag{B.1}$$

One can derive the law of the sines by evaluating the volume of the parallelepiped spanned by the unitvectors:

$$\vec{e}_1 \cdot \vec{e}_2 \times \vec{e}_3 = \sin b \sin c \sin \alpha \tag{B.2}$$

Because of the cyclic symmetry of the parallelepipedal product, the last expression obviously equals $\sin c \sin a \sin \beta$ or $\sin a \sin b \sin \gamma$. This can be expressed as the law of sines

$$\frac{\sin a}{\sin \alpha} = \frac{\sin b}{\sin \beta} = \frac{\sin c}{\sin \gamma}. \tag{B.3}$$

The law of cosines for sides or the cosine theorem can be derived by computing the scalar products between different unit vectors:

$$\vec{e}_1 \cdot \vec{e}_2 = \cos c = \cos a \cos b + \sin a \sin b \cos \gamma \tag{B.4}$$

$$\vec{e}_1 \cdot \vec{e}_3 = \cos b = \cos a \cos c + \sin a \sin c \cos \beta \tag{B.5}$$

$$\vec{e}_2 \cdot \vec{e}_3 = \cos a = \cos b \cos c + \sin b \sin c \cos \alpha \tag{B.6}$$

The directions of the unit vectors can be connected to the following directions in the cms:

- $\vec{e}_1$: Direction of slepton
- $\vec{e}_2$: Beam axis
- $\vec{e}_3$: Direction of lepton l_l^-

This choice is consistent with the production plane i.e. the plane spanned by $\vec{e}_1$ and $\vec{e}_2$ being the xz-plane. Now the cms angles that we have to take into account for the angular distribution of lepton l_l^- can be identified as follows:

$$\begin{aligned} a \equiv \theta_l \quad & b \equiv \theta_l^{cms} \\ c \equiv \theta \quad & \beta \equiv \phi_l - \phi \end{aligned} \tag{B.7}$$

The angle β is measured with respect to the beam axis and can be identified with the difference of the azimuthal angles of the final lepton and the slepton. With (B.5) these relations lead to

$$\cos \theta_l^{cms} = \cos \theta_l \cos \theta + \sin \theta_l \sin \theta \cos (\phi_l - \phi)\,. \tag{B.8}$$

We obtain the analogous equation for the angular distribution of lepton $l_{l'}^-$ with l→l' and $\theta \to \pi - \theta$.

Bibliography

[1] H. E. Haber, G. L. Kane, *Phys. Rep. 117* (1985) 75.

[2] H. E. Haber, J. F. Gunion, *Nucl. Phys. B272* (1986) 1.

[3] S. P. Martin, *A Supersymmetry Primer*, hep-ph/9709356.

[4] J. Hisano, M. Nojiri, Y. Shimizu, M. Tanaka, *Lepton-Flavor Violation in the Left-handed Slepton Production at Future Lepton Colliders,* KEK-TH-586.

[5] C. Caso et al., *The European Physics Journal C3,* 1 (1998) and 1999 off-year partial update for the 2000 edition.

[6] K. Kolodziej, M. Zralek, *Phys. Rev. D43* (1991) 3620.

[7] E. Byckling, K. Kajantie, *Particle Kinematics,* John Wiley & Sons, London 1973.

[8] H. Pilkuhn, *The Interactions of Hadrons,* North Holland Publishing Company, Amsterdam 1967.

[9] H. E. Haber, *Spin Formalism and Applications to New Physics Searches,* SCIPP 93/49 (1994).

[10] S. Ambrosanio, G. A. Blair, P. M. Zerwas, *A Study of mSUGRA for the Linear Collider (tanβ=3),* (1998).

[11] S. Ambrosanio, G. A. Blair, P. M. Zerwas, *A Study of mSUGRA for the Linear Collider (tanβ=30),* (1998).

[12] S. Ambrosanio, G. A. Blair, P. M. Zerwas, *A Study of mSUGRA for the Linear Collider, Light Stop,* (1998).

[13] Y. Shimizu, *Note on Lepton Flavor Violation in Supersymmetric Models,* unpuplished (2000) and further discussions.

[14] E. K. Akhmedov, *Neutrino Physics,* hep-ph/0001264.

[15] D. Griffiths, *Introduction to Elementary Particles,* John Wiley & Sons, 1987.

[16] I. N. Bronstein, K. A. Semendjajew, G. Musiol, H. Mühlig, *Taschenbuch der Mathematik,* Verlag Harri Deutsch, Thun, Frankfurt am Main, second edition 1995.

[17] W. Hackbusch, H. R. Schwarz, E. Zeidler, *Teubner-Taschenbuch der Mathematik,* Teubner Verlagsgesellschaft, Leipzig 1996.

[18] Wong, C. W., *Mathematische Physik: Konzepte, Methoden, Übungen,* Spektrum Akademischer Verlag, Heidelberg 1994.

[19] Gradshteyn I. S., Ryzhik I. M., *Table of Integrals, Series, and Products,* Academic Press, San Diego, fifth edition.

[20] KEK Report 92-16.

[21] F. J. Gilman, K. Kleinknecht, *Phys. Rev. D50,* (1994) 1315.

[22] W. Greiner, B. Müller, *Eichtheorie der schwachen Wechselwirkung,* Verlag Harri Deutsch, Thun, Frankfurt am Main, second edition 1994.

[23] H.P. Nilles, *Supersymmetry, Supergravity and Particle Physics,* Phys. Rep. 110 (1984) 1.

[24] J. Sato, K.Tobe, T. Yanagida, *A Constraint on Yukawa-Coupling Unification from Lepton-Flavor Violating Processes,* CERN-TH/2000-323.

[25] D. Bowser-Chao and W.-Y. Keung, *CP Violation and Scalar Lepton Flavor Oscillation,* hep-ph/9704219.

[26] The SuperKamiokande Collaboration, *Phys. Rev. Lett. 81* (1998) 1562.

[27] K. S. Hirata et al., *Phys. Rev. Lett. 63* (1989); ibid 65 (1990) 1297.

Erklärung

Hiermit versichere ich, daß ich die vorliegende Arbeit selbständig verfaßt und keine anderen als die angegebenen Hilfsmittel verwendet habe.

Würzburg, den 15. Dezember 2000

Andreas Redelbach